

UNCLASSIFIED

UKINDC(80)P96
NEANDC(E)212 VOL.8
INDC(UK)-32/LH

U.K. NUCLEAR DATA PROGRESS REPORT FOR THE PERIOD
JANUARY - DECEMBER 1979

Editor: E.W. Lees.

Nuclear Physics Division,
AERE Harwell,
Oxon OX11 0RA.

March 1980

CONTENTS

	<u>Accelerator*</u>	<u>Page No.</u>
CONTENTS		2
PREFACE		6
NUCLEAR DATA FORUM LECTURES		7
Integral data studies for fast reactor operation		8
CINDA TYPE INDEX		18
1. <u>NUCLEAR PHYSICS DIVISION, AERE, HARWELL</u>		20
Introduction		20
1.1 The new machine for the electron linac laboratory	E	21
1.2 Capture cross sections of structural materials	E	21
1.2.1 Detector efficiency		22
1.2.2 Resonance parameters of iron		23
1.3 Neutron transmission measurements on the structural materials	H	29
1.4 Background evaluation in synchrocyclotron transmission data	H	31
1.5 Monte Carlo simulation of the synchrocyclotron source	H	32
1.6 An assessment of the accuracy requirements on higher actinide nuclear data for fast reactors		34
1.7 An evaluation of the prompt gamma-ray spectrum of natural Ti produced by thermal neutrons		37
1.8 Evaluation of differential nuclear data for ^{243}Am		38
1.9 Nuclear data files		38
1.10 (α, n) yields from light elements	D	38
1.11 Safeguards Research		42
1.11.1 Theoretical analysis of the Variable Dead Time Counter (VDC)		42
1.11.2 A model for studying coincidence systems used in plutonium assay		45
1.11.3 N.M.A.C.T. Portable Neutron Coincidence Counter (PNCC)		47
1.11.4 Calculations of neutron multiplication and its effect on the response of neutron coincidence counters		49
1.12 (n, α) cross-sections	A	52
1.13 Verification of tritium activation measurements by $^6\text{Li}(n, \alpha t)$ cross section determination		52
1.14 Measurements of the $^{60}\text{Ni}(n, p)^{60}\text{Co}$ and $^{62}\text{Ni}(n, \alpha)^{59}\text{Fe}$ cross sections at 14.7 MeV neutron energy	E	54

*For a key, see the Introduction to Chapter 1 on page

	<u>Page No.</u>
1.15 The response of solid state track recorders to fast neutrons.	57
1.16 Studies of parallel plate avalanche detectors.	59
1.17 A fission chamber for the intercomparison of fast neutron flux density measurements	60
1.18 Neutron Monte Carlo studies.	60
1.19 The status of the Harwell version of FISFIN.	62
1.20 Neutron sensitivity of two neutron capture detectors	B 63
2. <u>CHEMICAL NUCLEAR DATA</u>	64
2.1 <u>Report from the Chemical Nuclear Data Committee</u>	64
2.2 <u>Fission measurements</u>	64
2.2.1 ZEBRA-BIZET experiments to study the effects of change of reactor neutron spectrum on fission yields.	64
2.2.2 Mass and kinetic energy distributions of fragments formed in the heavy ion induced fission of ^{208}Po .	64
2.2.3 The competition between fission and neutron emission in Po compound nuclei.	66
2.2.4 A study of some of the neutron deficient isotopes of Po.	67
2.2.5 The effect of angular momentum and excitation energy on mass, kinetic energy and prompt neutron distributions of highly fissionable nuclei.	67
2.2.6 The competition between fission, spallation and deep inelastic transfer in heavy ion induced reactions.	67
2.2.7 The role of angular momentum in nuclear reactions.	68
2.2.8 Fission-spallation competition in the $A = 200$ mass region	68
2.2.9 Angular momentum studies in heavy ion induced fission	68
2.2.10 Tritium yields in thermal and fast fission.	68
2.3 <u>Cross section measurements</u>	70
2.3.1 Integral experiments to measure the partial capture cross section for the production of ^{242}Cm and ^{244}Cm .	70
2.3.2 Measurement of neutron cross sections in PFR.	72
2.4 <u>Half-life measurements</u>	72
2.4.1 ^{242}Cm half-life	72
2.4.2 ^{237}Np decay data	72

	<u>Page No.</u>
2.5 <u>Data file sub-committee</u>	73
2.5.1 Fission product decay data	73
2.5.2 Heavy element and actinide decay data	74
2.6 <u>Fission product yields: assessments and consistent sets</u>	75
2.7 <u>Computer code development</u>	76
2.7.1 Development of CASCADE; a computer code to convert evaluated decay scheme data into radiation data sets.	76
2.7.2 Improvements to the GAMANAL γ -ray analysis code.	77
2.7.3 Improvements to PDP11 pulse height analyser software.	77
3. <u>REA-TOR PHYSICS DIVISION, AEE WINFRITH</u>	78
3.1 The U.K. Nuclear Data Library	78
3.2 Libraries of fission product decay data and yields	78
3.3 Measurement of the $^{93}\text{Nb}(n,n')^{93\text{m}}\text{Nb}$ excitation function.	79
4. <u>CEGB RESEARCH DIVISION, BERKELEY NUCLEAR LABORATORIES</u>	81
4.1 ^{235}U fission product gamma spectra: a comparison between experiment and calculation	81
4.2 Decay heat	81
5. <u>PHYSICS DEPARTMENT, NATIONAL RADIOLOGICAL PROTECTION BOARD</u>	83
5.1 Neutron facility	83
5.2 Neutron detection	83
5.3 Iron shielding benchmark experiment	84
5.4 Neutron cross section and kerma calculations	84
6. <u>DIVISION OF RADIATION SCIENCE AND ACOUSTICS, NATIONAL PHYSICAL LABORATORY</u>	86
6.1 Neutron source calibrations	86
6.2 International comparison of neutron source emission rate	86
6.3 Neutrons in the 1-1000 eV energy range	86
6.4 Intermediate energy neutrons	87
6.5 The cross section for the $^{56}\text{Fe}(n,p)$ reaction for 14.73 MeV neutrons	87
6.6 Neutron cross sections at 14.68 MeV	87
6.7 The decay scheme of $^{180\text{m}}\text{Ta}$	88
6.8 International comparison of neutron fluence rate	89
6.9 Photoneutron production in high energy electron and X-ray beams used for radiotherapy	89

	<u>Page No.</u>
6.10 Fast neutron energies	90
6.11 Reference standard for fast neutron absorbed dose	90
6.12 Nuclear decay scheme measurements	90
6.13 W-value measurements	91
7. <u>UNIVERSITY OF EDINBURGH, DEPARTMENT OF PHYSICS</u>	92
7.1 ${}^6\text{He}$ emission accompanying the spontaneous fission of ${}^{252}\text{Cf}$	92
7.2 Light emission accompanying fission	93
7.3 The polarisation and differential cross section for the elastic scattering of 16 MeV neutrons	94
7.4 The polarisation of 14 MeV neutrons due to elastic scattering	95
7.5 The polarisation and differential cross section for the elastic scattering of 2.9 MeV neutrons	95
7.6 Neutron polarisation in the ${}^7\text{Li}(d,n){}^8\text{Be}$ reaction	96
7.7 The polarisation of neutrons from the ${}^2\text{H}(d,n){}^3\text{He}$ reaction	96
8. <u>BIRMINGHAM RADIATION CENTRE, UNIVERSITY OF BIRMINGHAM</u>	97
8.1 Delayed neutron energy spectra	97
8.2 The neutron spectrum from an Am/Li source	100
9. <u>UNIVERSITY OF LONDON REACTOR CENTRE</u>	103
9.1 Decay scheme studies	103

PREFACE

This report is prepared at the request of the United Kingdom Nuclear Data Committee and covers the period from January to December, 1979.

Nuclear data are presented by laboratory. There are contributions this year from the Harwell and Winfrith laboratories of the UKAEA, the National Physical Laboratory, the CEBG Berkeley Nuclear Laboratories, the National Radiological Protection Board, the Birmingham Radiation Centre, the University of London Reactor Centre and the University of Edinburgh.

This report includes work from various collaborations between laboratories of Harwell, Dounreay, Winfrith, Windscale, Berkeley (CEGB), MOD Aldermaston, Imperial College, Glasgow University, Manchester University and Universities Reactor, Risley. Contributions on "Chemical Nuclear Data" are gathered by the Chemical Nuclear Data Committee and grouped under that heading.

Contributions to the report on nuclear data topics are welcome from all sources and we extend an invitation to researchers in other laboratories of industry, government, the universities and polytechnics to use this channel of communication.

Where the work is clearly relevant to requests in WRENDA 79/80 (INDC(SEC)-73/URSF) request numbers are given after the title of the contribution.

NUCLEAR DATA FORUM LECTURES

The thirteenth Nuclear Data Forum was held on December 4th at AEE Winfrith. The themes this year were differential and integral data. The meeting was well supported, there being 82 registrations and 12 contributed papers. The aspects of integral data studies were covered in an invited talk by Dr. J. Sanders which is reproduced below. The aspects of differential data with respect to the new 136 MeV electron linac at Harwell were dealt with by Dr. M.S. Coates but details are not reproduced here since a more comprehensive description was published in the October issue (No. 276) of Atom.

INTEGRAL DATA STUDIES FOR FAST REACTOR OPERATION

J.E. Sanders

UKAEA, Reactor Physics Division, AEE Winfrith

Lecture given at the Nuclear Data Forum, AEE Winfrith, on 4 December 1979.

Despite the continuing development of the facilities for measurement of differential cross sections - as exemplified by the new Harwell Linac - integral measurements still constitute an important and complementary source of fast reactor data. Among the reasons for this are:-

- (a) direct activation measurements with mono-energetic sources are difficult below ~ 30 keV, although many of the neutron interactions in sodium-cooled fast reactors take place in this energy region;
- (b) integral measurements can often be made with very small samples, an important consideration, particularly in the case of actinides and other radioactive nuclides;
- (c) integral measurements can provide an independent cross-check on the absolute normalisation of differential results.

For meaningful experiments it is essential that the spectrum and the absolute flux (or fluence) are accurately defined. If the spectrum is close to that of the eventual application of the data, bias factors (E/C) may be acceptable. Preferably, measurements in a range of well-characterised spectra can be used as a basis for a few-group adjustment of the differential data, as in the production of the FGL5 library and, more recently, in the fission-product studies with the STEK facility. The flux is best determined via the ^{239}Pu fission-rate in view of its rather flat (and well-known) cross section over the range of interest for fast reactors. Moreover, since this reaction is also the source of 60% of the reactor power, it provides an operationally relevant normalisation.

The measurement techniques used in integral experiments comprise:-

- (a) direct detection of reaction products by gas and semi-conductor counters, solid-state track recorders. Generally limited to (n, fission) and (n, alpha);
- (b) activation, followed by non-destructive β or γ -counting;
- (c) activation, followed by radiochemistry and α , β or γ -counting;

(d) mass spectrometry of irradiated samples;

(e) reactivity perturbation ("oscillation") techniques. Note that relatively larger samples (~ few gms) are needed than for the previous techniques. Also that interpretation may be complicated since the worth is a function of neutron elastic and inelastic scattering as well as capture and fission.

Fast reactor integral data measurements are made in three types of facility, viz. benchmark fields (e.g. NISUS, $\phi \sim 10^8$); zero-power criticals (e.g. ZEBRA, $\phi \sim 10^{10}$); and full-power reactors (e.g. PFR, $\phi \sim 5 \times 10^{15}$). The obvious merit of the power reactor is the high flux intensity which leads to readily measurable changes in the isotopic composition of irradiated samples, as well as the possibility of experiments in regions outside the core. On the other hand, considerable problems may arise in the provision of samples able to withstand the stringent thermal and radiation environment, and post-irradiation retrieval may take several months. In most other respects the zero-power reactor provides a good solution since the neutronic conditions of the power reactor can be closely simulated, introduction and removal of samples is straightforward, and extensive flux monitoring is available.

This paper describes briefly four examples of integral experiments made in large plutonium-fuelled assemblies in Zebra, simulating PFR or CFR conditions.

1. Component Activation

The build-up of long-lived γ -emitters in the sodium coolant as a result of corrosion of the fuel cladding, and their subsequent distribution and deposition in other parts of the primary circuit, such as pumps and intermediate heat exchangers, is a matter of concern for fast reactor design and operation. Although there are many uncertainties in the mechanisms of corrosion and deposition, it was considered important to confirm the predicted activation rates of key materials in some well-defined fast reactor spectra.

Two main experiments have been made. In the first, metallic samples of various elements were exposed for 5 days to the core-centre and upper-axial-breeder flux of the PFR mock-up assembly. In the second, various alloys were exposed for a similar period to the core centre flux of Core 16, with a spectrum characteristic of that of a commercial reactor. Following irradiation, the samples were dissolved and liquid sources prepared for γ -counting on a calibrated Ge-Li spectrometer.

In most cases the core-centre activations were predicted using the cross sections

in the 37-group FD5 data set (taken from the UK Nuclear Data Library) and fluxes obtained from a MURAL collision-probability treatment of the plate-cell. For stellite (60% Co) the calculations were made in fine groups (with FGL5) in order to take better account of the strong resonance self-shielding of the 132 eV resonance in the ^{59}Co (n, γ) cross section.

The ratios of calculated and experimental activation rates per atom, normalised to ^{239}Pu fission, are listed in Table 1. The agreement is that expected from the uncertainties assigned to the FD5 data, and is probably adequate for practical purposes. It is interesting to note, however, that the consistency of the relative predictions of the important $^{54}\text{Fe}(n,p)^{54}\text{Mn}$ and $^{59}\text{Ni}(n,p)^{58}\text{Co}$ reactions would be considerably improved if more recent data were used, the ratio of their C/E values rising from the 0.80 obtained with FD5 to 0.98 with ENDF/B4.

Table I

CORROSION PRODUCT ACTIVATION DATA

Reaction: (Half-life)	Data Source UKNDL	Element Samples		C/E for Alloy Samples (CFR)			
		E* (mb)	C/E	FV548	PE16	M316	Stellite
$^{50}\text{Cr}(n,\gamma)^{51}\text{Cr}$ 27.7 days	-	31	0.80	0.75	0.75	0.77	1.08
$^{54}\text{Fe}(n,p)^{54}\text{Mn}$ 312 days	DFN 63	10.5	0.77	0.85	0.92	0.83	0.76
$^{58}\text{Fe}(n,\gamma)^{59}\text{Fe}$ 45.1 days	DFN965	9.8	0.82	0.83	0.83	0.83	-
$^{59}\text{Co}(n,\gamma)^{60}\text{Co}$ 5.27 years	DFN235	54	0.78)))	0.75
$^{60}\text{Ni}(n,p)^{60}\text{Co}$ 5.27 years	-	0.25	0.88)1.0	1.0	1.0)
$^{58}\text{Ni}(n,p)^{58}\text{Co}$ 70.8 days	DFN236	14.4	0.96	1.05	1.03	1.03	0.87
$^{181}\text{Ta}(n,\gamma)^{182}\text{Ta}$ 115 days	DFN328	664	1.13	-	-	-	-

*Effective cross section in PFR mockup core spectrum. Experimental accuracy $\pm 7\%$ (1 σ).

As a check that no significant sources of γ -activity were being missed in the few-day irradiations, the spectra from the steel plates that had been in Zebra for ~ 3 years confirmed that the main activities were indeed those identified in the shorter irradiations.

2. Measurements of the β -Decay Power from Fission

Calculations of the heat sources due to the accumulation of fission products and higher actinides in irradiated fuel are made using the summation code FISPIN and associated libraries of decay data and fission yields. As a part of the validation of this procedure for fast reactor design and safety applications, measurements have been made of the release of β -particle energy following irradiation of ^{235}U and ^{239}Pu at the centre of the ZEBRA PFR mock-up. The decay was followed for as long as allowed by the diminishing signal/background ratio and satisfactory results were obtained over a cooling period from about 20 seconds to one year.

Aluminium and melinex foils were used to catch and retain fragments emitted from thin deposits of ^{235}U and ^{239}Pu . The catcher foil technique had the advantage that the β -energy from the fragments could be measured without interference from the activity of the deposit or the capsule material. The retention of the fragments by the catcher was checked in subsidiary experiments. Immediately following the 10^5 -second irradiation the catcher foils were placed directly against the end window of a NE102A β -scintillation counter, the digitised output current from the anode of the photomultiplier being shown proportional to the rate of energy deposition. The absolute efficiency of the detector was established using a similar foil carrying a deposit of a standard source solution of ^{90}Sr - ^{90}Y . A typical decay curve is shown in Fig. 1. The overall accuracy is 3-5%.

Values of energy release rate from β -particles (plus conversion electrons and X-rays) following a 10^5 -second irradiation were calculated using FISPIN with UKFPDD-1 decay data and Crouch's 1979 compilation of fission-product yields. The mean ratios of calculated and experimental decay power over various cooling periods, and the standard deviation of the individual measurements within each period, are given in Table II.

The agreement is very satisfactory, and represents a notable improvement over that found with earlier data libraries which significantly overpredicted (by $\sim 15\%$) the decay power for cooling times less than ~ 1000 seconds. This improvement is attributed to a combination of better data on some of the short-lived nuclides and better methods of

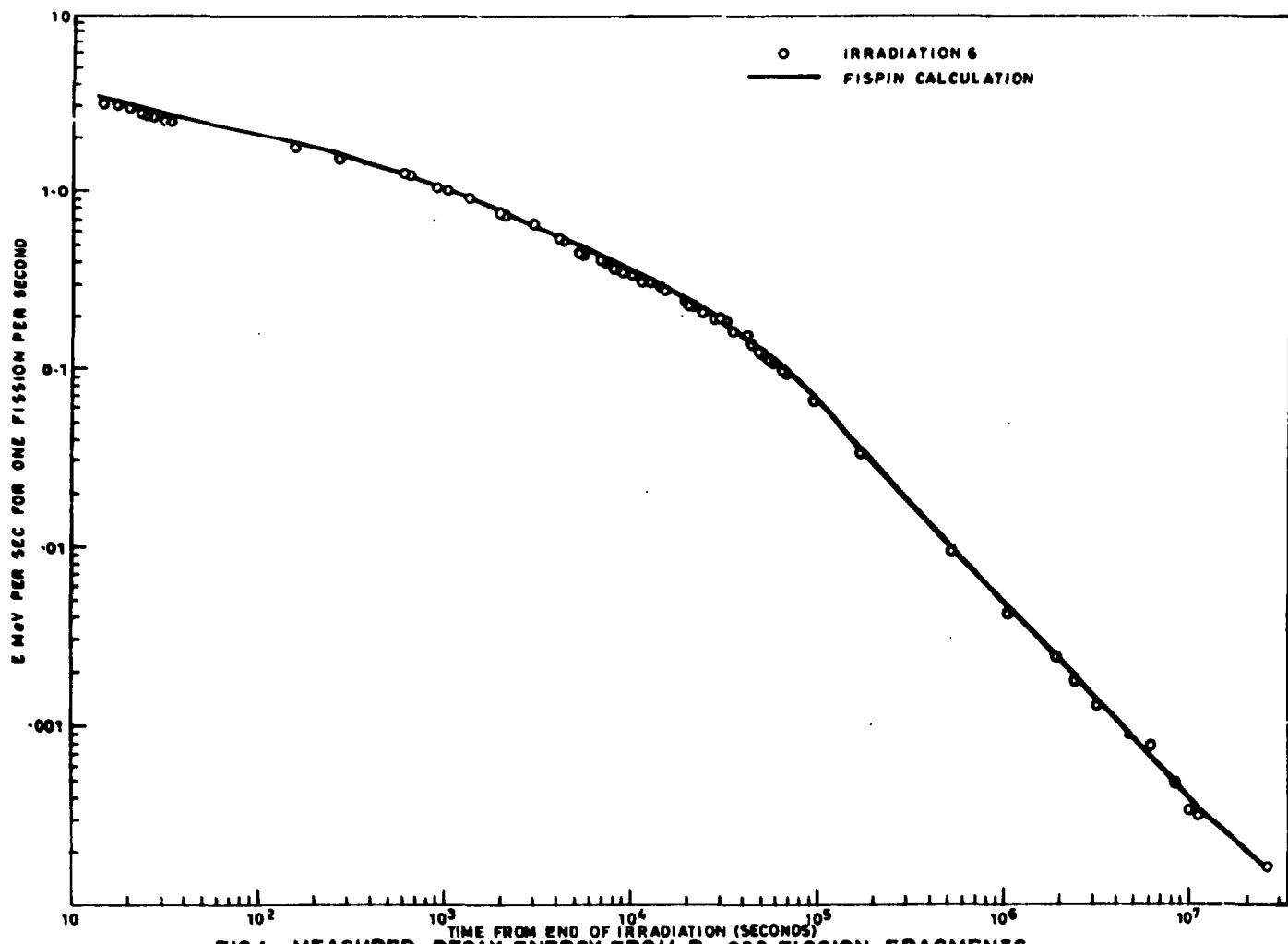


FIG.1 MEASURED DECAY ENERGY FROM PU-239 FISSION FRAGMENTS DURING PERIOD 15-2.7x10⁷ SECONDS FOLLOWING IRRADIATION

Fig.1. Measured decay energy from ²³⁹Pu fission fragments during period 15 - 2.7 x 10⁷ seconds following irradiation

estimating the mean β -energies in cases where no experimental evidence is available. There is no indication of a significant trend in C/E with cooling time over the period covered here, although further experiments to test the data beyond 1 year would be useful.

Table II
Analysis of β -Decay Experiments

Cooling Period (s)	C/E for β -Decay Power	
	^{235}U	^{239}Pu
<100	1.010 \pm 0.013	1.036 \pm 0.010
$10^2 - 10^3$	0.990 \pm 0.008	1.005 \pm 0.025
$10^3 - 10^4$	0.989 \pm 0.006	1.005 \pm 0.007
$10^4 - 10^5$	0.980 \pm 0.021	0.985 \pm 0.023
$10^5 - 2 \cdot 10^6$	1.016 \pm 0.051	1.025 \pm 0.067
$2 \cdot 10^6 - 3 \cdot 10^7$	0.981 \pm 0.059	1.037 \pm 0.055

Note: FISPIN calculations with UKFPDD-1 and Crouch-2 yields. The \pm are standard deviations of the C/E values for points within each time interval.

3. Survey of Alternative Absorbers

Because of possible endurance problems with boron-carbide, other potential materials for use in fast reactor control rods have from time-to-time been examined. To assist selection, a series of perturbation experiments on a range of samples were made in Zebra Core 12 (CFR-spectrum), a first screening being made on the basis of much earlier work in Zephyr. Samples of 10-50 g (where possible in metallic form) were inserted into a standard plate-cell for reactivity measurements against an unmodified cell using a critical-balance technique. A plutonium plate was used as normalisation.

The results are given in Table III in the form of "perturbation cross sections", which for highly absorbing samples are closely related to the spectrum-averaged capture cross sections; the contribution from scattering is expected to be < 50 mb. There are quite marked variations between different elements, which reflect the well known systematics, odd-nucleon nuclides having higher cross sections than their even-nucleon neighbours. Europium (151, 153) emerges the clear winner, with an absorbing power per atom similar to that of boron-10. On a worth/cm³ scale, europium-oxide (Eu₂O₃) is about 1.5 times higher than natural ¹²C. Rhenium metal (185, 187) also looks promising.

Table III

Absorber Survey in ZEBRA Core 12

Element	$\sigma^* \text{ mb}$	$\Delta\rho/\text{cm}^3$	Form
B	550 + 13	1	Carbide
Rh	500 ± 20	0.69	Metal
Pd	322 + 30	0.41	Metal
Ag	600 ± 30	0.66	Metal
In	463 ± 50	0.33	Metal
Sm	658 + 30	0.36	Oxide
Eu	2920 ± 150	<u>1.47</u>	Oxide
Gd	743 ± 55	0.37	Oxide
Tb	1270 + 55	0.68	Oxide
Dy	717 ± 30	0.35	Oxide
Ho	1043 + 50	0.55	Oxide
Er	535 + 40	0.28	Oxide
Tm	757 ± 50	0.40	Oxide
Yb	433 ± 50	0.24	Oxide
Lu	1076 + 50	0.57	Oxide
Ta	749 ± 40	0.79	Metal
Re	1190 ± 60	<u>1.49</u>	Metal
Pt	352 ± 35	0.44	Metal
Au	582 ± 35	0.65	Metal

Subsequent experiments with full-scale power reactor control rods have shown, however, that Eu_2O_3 (33 kg) has a worth only about 95% that of B_4C (10 kg). This is due to the influence of flux depression and neutron moderation effects, and emphasises the care needed in extrapolating from small sample results.

Boron-carbide remains the reference material for UK power reactor designs, with Eu_2O_3 a possible fall-back..

4. Production of Curium by Capture in ^{241}Am and ^{243}Am

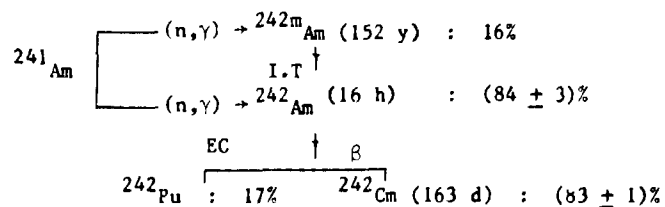
A knowledge of the cross sections of the higher actinides is required to predict the composition of irradiated fast reactor fuel. The production rates of the spontaneously fissioning nuclides ^{242}Cm and ^{244}Cm , by capture in ^{241}Am and ^{243}Am , are of particular interest, since the resulting neutron emission has important implications both for the monitoring of the reactivity of the core during maintenance and refuelling and for the design of the spent-fuel handling route. The relative importance of these two nuclides depends on the isotopic quality of the feed plutonium, on its storage time prior to loading (which determines the initial ^{241}Am content),

and on the cooling period following irradiation (the half-lives of ^{242}Am and ^{244}Am being 163 days and 18.1 years respectively).

Differential cross section measurements on the higher actinides present various difficulties, in particular the lack of adequate target materials, and considerable reliance is placed on theoretical models. Confirmation by means of well-defined integral experiments is therefore highly desirable. To meet this requirement, samples of ^{241}Am and ^{243}Am have been irradiated in ZEBRA to determine the partial capture cross sections leading to the respective curium isotopes. The irradiations were made in the central spectra of Assemblies 14 (similar to PFR), 12 and 16 (similar to CFR). The samples were irradiated as oxide, three 10 mg samples of ^{241}Am and three 20 mg samples of ^{243}Am being individually sealed in aluminium ampoules and inserted in aluminium plates of standard fuel ZEBRA dimensions. Following radiochemical separations, the curium yields were measured by alpha-counting and alpha-spectrometry techniques.

For the calculation, 37-group fluxes in the structure of the FD5 data set at the position of the americium samples were derived using the collision-probability code MURAL. These fluxes were then combined with the 37-group cross sections for ^{241}Am and ^{243}Am from the Harwell evaluations to obtain the required capture rates. The samples were sufficiently small that resonance-shielding effects could be neglected. The fission cross section of the ^{239}Pu flux monitor was taken from the FCL5 data.

The production of ^{242}Cm from ^{241}Am proceeds according to the following route:-



A factor of $0.84 \times 0.83 = 0.70$ must therefore be applied to the $^{241}\text{Am} (n,\gamma)$ cross section when predicting the ^{242}Cm yield. There are no such complications for ^{243}Am , where essentially all captures lead to ^{244}Cm .

The spectrum-averaged cross sections calculated with the above data are compared with the measured values in Table IV. The C/E values for ^{241}Am in the two spectra

Table IV
Curium Production Cross Sections

Sample	Core	Fluence n.cm ⁻²	Cross Section for Cm Production (barns)		C/E
			Experiment	Calculation	
241 _{Am}	PFR	2.60 x 10 ¹⁵	1.28 ± 0.10	1.12	0.88 ± 0.07
	CFR	2.97 x 10 ¹⁴	1.48 ± 0.11	1.25	0.84 ± 0.06
243 _{Am}	PFR	2.66 x 10 ¹⁵	1.32 ± 0.20	1.58	1.20 ± 0.18
	CFR	2.16 x 10 ¹⁵	1.99 ± 0.29	1.73	0.87 ± 0.09

Note: Errors on cross sections ($\pm 1\sigma$) include 5% on determination of fluence via ²³⁹Pu fission rate., largely systematic to all values.

are very similar, with a mean (14 ± 7)% lower than unity. This result is not inconsistent with the errors of 10-15% assigned to the evaluated (n, γ) cross section; additionally, there is the 4% systematic uncertainty associated with the relative yield of the isomeric and ground states of ²⁴²Am. In the case of ²⁴³Am the experimental errors are greater, due primarily to the lower specific activity of the ²⁴⁴Cm product. While the different C/E values in the two spectra may be indicative of an incorrect energy dependence of the cross section, more precise measurements are clearly desirable.

Conclusion

This short review has indicated the rather broad contributions to integral data studies possible in a zero-power reactor, particularly when supported by sophisticated radiochemical techniques. Further ZEBRA work in this area is being planned. At the same time irradiations now in progress in the PFR will provide information on a wider range of actinide reactions that cannot be observed under low flux conditions.

The documents listed below contain more detailed accounts of some of the work described here.

REFERENCES

1. R.A.P. Wiltshire, H.H. Willis, F.J.G. Rogers, K.M. Glover, J.G. Cuninghame and D.W. Sweet. The Cross Section for the Production of ^{242}Cm from ^{241}Am in a Fast Reactor, AERE-R 7363 (1973).
2. D.W. Sweet. Actinide Fission Rate Measurements in ZEBRA, AEEW-R 1090 (1977).
3. M.F. Murphy, W.H. Taylor, D.W. Sweet and M.R. Marsh. Experiments to Determine the Rate of Beta Energy Release Following Fission of ^{239}Pu and ^{235}U in a Fast Reactor, AEEW-R 1212 (1979).
4. M.F. Murphy, D.W. Sweet, and W.H. Taylor. Tests of Some FD5 Activation Cross Sections by ZEBRA Irradiations. Proceedings of Specialists Meeting on Nuclear Data for Structural Materials, Geel, 1977, EUR 6108.

CINDA LISTINGS

Element		Quantity	Type	Energy		Documentation				Lab	Comments
S	A			Min.	Max.	Ref.	Vol	Page	Date		
Li	7	n,n Alpha-T	Expt-Prog	4.7 6	1.4 7	UKNDC	P96	52	3/80	HAR	Swinhoe + Table given thermal Li-6 (n,alpha-T) used as check.
C	12	Alpha-n	"			"	"	38	"	"	West + neutron yield from thick targets using alpha energies from 4 to 7 MeV.
Mg	NAT	"	"			"	"	38	"	"	" " "
Al	27	"	"			"	"	38	"	"	" " "
Si	NAT	"	"			"	"	38	"	"	" " "
Ti	NAT	n,gamma spec	Eval-Prog			"	"	37	"	"	Sowerby AERE-R 9502, (1979).
Fe	NAT	Reson Params	Expt-Prog	3.0 2	4.0 4	"	"	23	"	"	Gayther + Table given.
Fe	NAT	Alpha-n	"			"	"	38	"	"	West + neutron yield from thick targets using alpha energies from 4 to 7 MeV
Fe	NAT	n,alpha	"	1.4 7		"	"	52	"	"	Cookson + α angular dist.
Fe	56	n,proton	Eval-Prog	1.4 7		"	"	87	"	NPL	Ryves + value = 109.2 ± 1.0 mb
Ni	NAT	n,alpha	Expt-Prog	1.4 7		"	"	52	"	HAR	Cookson + α angular dist.
Ni	60	n,proton	"	1.4 7		"	"	54	"	"	Lees + 128 ± 13 mb
Ni	62	n,alpha	"	1.4 7		"	"	54	"	"	Lees + 20.1 ± 2.1 mb
Zr	NAT	Alpha-n	"					38	"	HAR	West + neutron yield from thick targets using alpha energies from 4 to 7 MeV.

CINDA LISTINGS

Element		Quantity	Type	Energy		Documentation				Lab	Comments
S	A			Min.	Max.	Ref.	Vol	Page	Date		
Nb	93	n,inelastic	Expt-Prog	4.4	6	UKNDC	P96	79	3/80	WIN	Taylor + Isomer result = 155 ± 45 mb
Nb	93	n-2n	"	1.4	7	"	"	87	"	NPL	Ryves + Provisional result 475 ± 14 mb
Nb	93	n,alpha	"	1.4	7	"	"	87	"	"	Ryves + Provisional result 5.53 ± 0.16 mb
Ta	181	n,2n	"	1.4	7	"	"	87	"	"	Ryves + Provisional result 1310 ± 39 mb
Au	197	n,2n	"	1.4	7	"	"	87	"	"	Ryves + Provisional result 2025 ± 61 mb for 6.1 day isomer.
Au	197	n,2n	"	1.4	7	"	"	87	"	"	Ryves + Provisional result 139 ± 7 mb for 9.7 hour isomer.
UO ₂	NAT	Alpha-n	"			"	"	38	"	HAR	West + neutron yield from thick targets using alpha energies from 4 to 7 MeV.
UC	NAT	"	"			"	"	38	"	"	" " "
U	238	n,2n	"	1.4	7	"	"	87	"	NPL	Ryves + Provisional result 778 ± 23 mb
U	235	n,f spec	"	5.0	5 7.0 6	"	"	97	"	BIR	Walker + spectrum of delayed neutrons. Graph given.
Am	243	Evaluation	Eval-Prog			"	"	38	"	HAR	Lynn + T.B.C.
Am	241	n,gamma	Expt-Prog	Fast		"	"	70	"	HAR	Glover + yield of ²⁴² Cm
Am	243	n,gamma	"	"		"	"	70	"	"	Glover + yield of ²⁴⁴ Cm.
Cm	242	Half-life	"			"	"	72	"	"	Wiltshire T.B.C.

1. NUCLEAR PHYSICS DIVISION, AERE, HARWELL

(Division head: Dr. J.E. Lynn)

Introduction

Nuclear data measurements in Nuclear Physics Division are diverse and are performed on a variety of sources. Individual research items are labelled with a single letter indicating on which accelerator the experiments were performed. These labels are as follows:

Cockcroft-Walton Generator	A
3 MV pulsed Van de Graaff Generator IBIS	B
6 MV Van de Graaff Generator	C
14 MeV Tandem Generator	D
45 MeV Electron Linac	E
Variable Energy Cyclotron	G
Synchrocyclotron	H

In the contents pages there is a cross reference to the accelerator where a measurement was made (when this applies).

The material for this contribution is taken from the chapter on Nuclear Data and Technology for Nuclear Power in the 1979 Nuclear Physics Division Progress Report AERE PR/NP27.

1. NUCLEAR DATA AND TECHNOLOGY FOR NUCLEAR POWER

1.1E The new machine for the electron linac laboratory (J.E. Lynn, M.S. Coates, P.P. Thomas and B.P. Clear)

The 136 MeV electron linac was formally opened on 6th July 1979 by Dr. W. Marshall, the Deputy Chairman of the A.E.A., as part of the Authority's Jubilee celebrations. Although at that time an electron beam had been successfully accelerated using all 8 sections of the completely assembled machine, the full range of contractually specified acceptance tests on machine performance had not been carried through by the manufacturers. This commissioning programme has proceeded since then, but more slowly than anticipated. Experimental work is now expected to start by Spring 1980.

The production problems (see PR/NP 26, p.12) encountered with the tantalum targets to be used for the initial neutron production in the Fast Neutron and Condensed Matter Cells have been overcome and both targets are ready for use. The first uranium targets (see PR/NP 26, p.12) for both Cells are in an advanced state of manufacture. Metallurgy Division have produced Zircaloy clad uranium plates to the required specification for the Condensed Matter target for all but the thickest plates. It was decided to make these of tantalum so that the manufacture of the assembly could be completed on an acceptable time scale. The neutron output from this composite assembly of plates will be only 7% lower than that from a complete Zircaloy clad uranium arrangement. The Fast Neutron target assembly of uranium plates contained in helium filled tantalum cans is complete.

Some of the previously reported difficulties with the pulsed magnet development (PR/NP 26, p.12) have been resolved and it is hoped to try a pulse magnet under operating conditions after the first few weeks of experimental trials on the installation. For this work conventional steady field magnets will be used in the electron beam lines to the targets. The first pulse magnet will be used to switch pulses between the Booster Cell and either the Fast Neutron or the Condensed Matter Cell.

1.2E Capture cross sections of structural materials (Relevant to request numbers 474-483, 519, 521)

Analysis of the neutron resonances in iron observed with the 270 l liquid scintillator is now complete. Some of the results of this analysis, and further developments in the calculation of the efficiencies of capture detectors to be used in

future measurements are described below.

1.2.1 Detector efficiency (R.B. Thom (Imperial College of Science and Technology

In the previous progress report (PR/NP26, p.14) methods for determining the gamma-ray efficiency and neutron sensitivity of the 270 l liquid scintillator capture detector were described. These properties have also been studied for other types of capture detector. In particular the gamma-ray response of a Moxon-Rae detector has been investigated using the gamma-ray Monte Carlo code GAMOC⁽¹⁾, modified to trace the trajectories of recoiling Compton electrons. The ideal Moxon-Rae detector is designed to produce an efficiency which is proportional to the incoming gamma-ray energy. Experimentally a small departure from linearity is observed resulting in an enhanced efficiency for the detection of low energy gamma-rays. An important consequence of this effect would be in the normalisation of capture data via the capture cross-section of a "reference" material such as gold. The capture spectrum of a heavy nucleus tends, in general, to be composed of more low energy gamma-rays than that typical of the nucleus of a structural material. The present calculations indicate that this effect would lead to an error in normalisation of ~5%.

The gamma-ray detection properties of a cylindrical cell containing 0.4 l of C₆D₆ liquid scintillator are currently being investigated. A response proportional to incoming gamma-ray energy is achieved by the method proposed by Maier-Leibnitz⁽²⁾ of applying a suitable weighting function to the pulse amplitude spectrum. The weighting function is derived from pulse amplitude spectra observed with standard gamma-ray sources and from Monte Carlo calculation. Fig. 1.1 shows a typical weighting function in comparison with that calculated at the Geel laboratory⁽³⁾ for the same experimental conditions.

(1) R.B. Thom, Ph.D. thesis (University of London) to be published.

(2) H. Maier-Leibnitz, private communication to R.L. Macklin and J.H. Gibbons (Phys. Rev. 159 (1967) 1009).

(3) G. Rohr, private communication (1979).

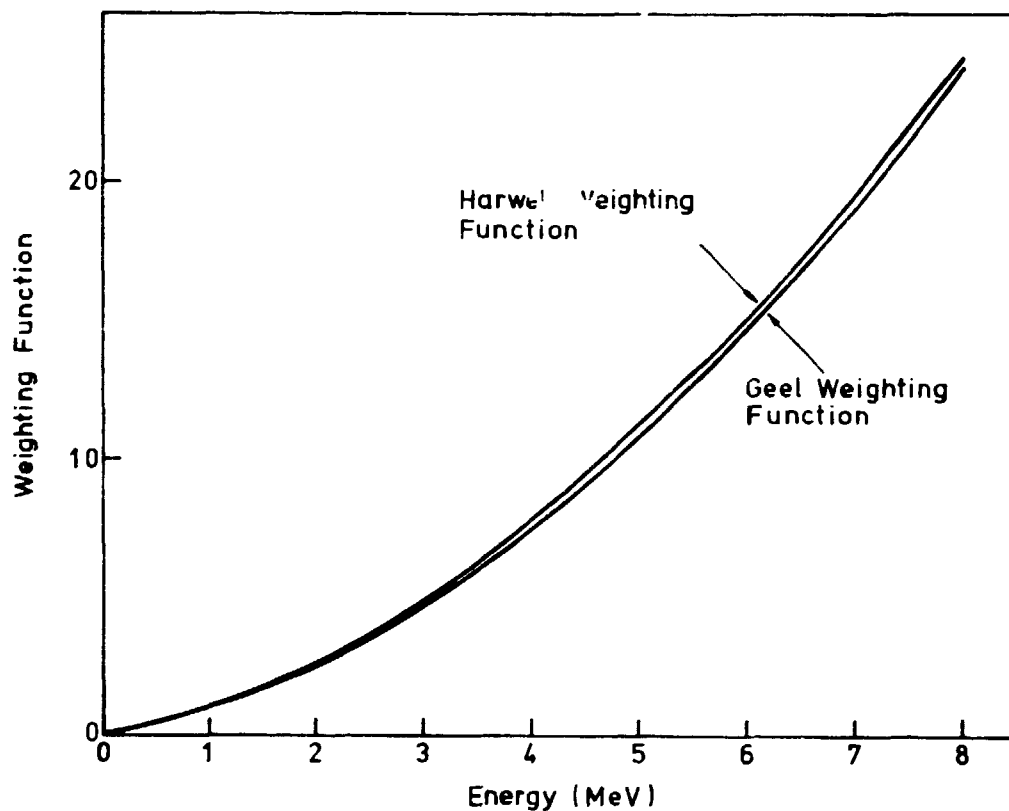


Fig. 1.1 Pulse amplitude weighting function for a typical total energy ("Maier-Leibnitz") detector

1.2.2 Resonance parameters of iron (D.B. Gayther, M.C. Moxon, R.B. Thom and J.E. Jolly)

The resonance in ^{56}Fe at 1.15 keV accounts for a large fraction of that component of the Doppler effect in a fast reactor which arises from its structural materials. Values for the parameters of this resonance were given in the last progress report (PR/NP26, p.21). However, when the analysis of the nickel data recommenced recently a slight anomaly in the raw capture yield data was revealed. The anomaly increased with the time-of-flight of the neutron incident on the sample, and has been traced to an error in the deadtime correction. The effect of this error on the measured capture cross sections is most marked at the lower neutron energies. The final values for the total width and the neutron width of the 1.15 keV resonance are respectively 2.5% and 29% smaller than previously reported.

Table 1.1 gives the results of the analysis of the capture measurements on natural metallic iron obtained from a least squares fit to the data using the program REFIT(1); only the statistical error obtained from the least squares fit to the data is quoted. Parameters for all but a few minor resonances are determined up to 40 keV and from 40 to 200 keV we are able to comment on the latest parameters for ^{56}Fe evaluated by Perey(2).

Table 1.1

Neutron Resonance Parameters of Natural Iron up to 40 MeV Incident Energy

A	J	ℓ	E_R (eV)	$\frac{ag\Gamma_n\Gamma_\gamma}{\Gamma}$ (eV)	Γ_n (eV)	Γ_γ (eV)
-	-	-	319.954+0.078	$(2.75+1.67) \times 10^{-6}$		
58	-	>0	359.339+0.106	$(3.51+0.25) \times 10^{-5}$	$(11.9+0.8) \times 10^{-3*}$	0.25+0.14
-	-	-	399.070+0.247	$(2.67+0.30) \times 10^{-5}$		
56	†	1	1152.597+0.010	$(4.44+0.01) \times 10^{-2}$	$(52.6+0.16) \times 10^{-3}$	0.6148+0.0058
57	-	>0	1630.74+0.16	$(1.08+0.04) \times 10^{-3}$		
56	-	>0	2352.9+0.8	$(3.61+0.29) \times 10^{-4}$		
-	-	-	2633.1+1.9	$(2.53+0.58) \times 10^{-4}$		
58	-	>0	2781.6+4.1	$(1.69+0.46) \times 10^{-4}$		
-	-	-	3714.5+3.3	$(3.21+0.40) \times 10^{-4}$		
57	0	0	3890.5+25.7	$(2.10+0.31) \times 10^{-3}$	[212]	0.385+0.057
-	-	-	4058.3+5.5	$(2.55+0.55) \times 10^{-4}$		
-	-	-	4244.1+3.9	$(3.72+0.56) \times 10^{-4}$		
-	-	-	4497.2+10.5	$(2.16+0.62) \times 10^{-4}$		
57	-	>0	4754.0+2.5	$(7.81+0.82) \times 10^{-4}$		
57	-	>0	5926.7+12.4	$(8.86+2.57) \times 10^{-4}$		
57	1	0	6209.9+22.6	$(1.51+0.08) \times 10^{-2}$	[368]	0.920+0.048
-	-	-	6693.5+8.4	$(1.26+0.34) \times 10^{-3}$		
57	-	>0	7221.7+2.9	$(9.10+0.54) \times 10^{-3}$	[5.35]	0.984+0.058*
54	†	0	7657.1+27.4	$(8.79+0.21) \times 10^{-2}$	[1097]	1.518+0.036
57	-	>0	7930.9+6.9	$(3.58+0.08) \times 10^{-3}$		
57	-	>0	9253.8+31.3	$(9.07+4.57) \times 10^{-3}$		

Table 1.1 (continued)

Neutron Resonance Parameters of Natural Iron up to 40 MeV Incident Energy

A	J	ℓ	E_R (eV)	$\frac{ag_n^{\Gamma} \Gamma_Y^{\dagger}}{\Gamma}$ (eV)	Γ_n (eV)	Γ_Y (eV)
54	-	>0	9479.0+1.2	$(3.40 \pm 0.11) \times 10^{-2}$	[1.20]	1.143+0.036*
58	0	0	10350.6+70.6	$(2.58 \pm 1.30) \times 10^{-3}$	[416]	0.8+0.42
54	-	>0	11167.8+1.8	$(4.07 \pm 0.10) \times 10^{-2}$	[7.7]	0.773+0.019*
57	-	>0	12140.8+38.9	$(8.8 \pm 6.0) \times 10^{-4}$		
56	-	>0	12475.0+39.1	$(2.58 \pm 0.64) \times 10^{-3}$		
57	-	>0	12838.1+11.8	$(8.51 \pm 0.84) \times 10^{-3}$	[6.15]	0.889+0.088*
57	-	>0	13361.5+43.9	$(2.18 \pm 1.12) \times 10^{-3}$		
54	-	>0	13598.3+54.3	$(1.82 \pm 0.67) \times 10^{-3}$		
57	-	>0	13973.8+8.7	$(7.08 \pm 0.29) \times 10^{-2}$	[2.6]	2.31+0.18*
54	-	>0	14444.2+4.0	$(3.42 \pm 0.10) \times 10^{-2}$	[1.4]	0.997+0.050*
56	-	>0	17747.8+18.5	$(1.33 \pm 0.12) \times 10^{-2}$		
57	-	>0	18192.3+27.1	$(1.23 \pm 0.17) \times 10^{-2}$	[2.34]	1.23+0.26*
54	-	>0	19262.5+41.8	$(7.26 \pm 1.47) \times 10^{-3}$		
56	-	>0	20186+128	$(4.67 \pm 2.59) \times 10^{-3}$		
57	-	>0	21257.4+62.7	$(5.29 \pm 1.38) \times 10^{-3}$	[5.07]	0.534+0.154*
56	-	>0	22754.7+4.9	0.134+0.007	0.199+0.0056*	[0.55]
54	-	>0	23125.9+27.8	$(1.34 \pm 0.18) \times 10^{-2}$		
56	†	0	27574.1+26.9	0.779+0.015	[1476]	0.850+0.013
54	-	>0	30522.5+50.7	$(3.32 \pm 0.44) \times 10^{-2}$	[7.69]	0.620+0.088*
56	-	>0	34126.0+7.8	0.400+0.011	[0.56]	0.358+0.016*
54	-	>0	35118.1+56.2	$(4.82 \pm 0.25) \times 10^{-2}$		
56	-	>0	36621.7+14.3	0.234+0.010		
56	-	>0	38243.3+5.5	0.285+0.007	[1.91]	0.377+0.010*

[] assumed parameter used to determine the other parameters.

* g_n^{Γ} or g_n^{Γ}

† a is the fractional isotopic abundance

All uncertainties are expressed as one standard deviation and are obtained only from fits to the data.

Fig. 1.2 shows the fit to the data in the region of the 1.15 keV resonance in ^{56}Fe for the 2 mm sample. The main peak is at an energy of 1.150 keV. The broad peak above the resonance is due to higher energy neutrons scattered by the potential cross section and then captured in the region of the resonance at subsequent collisions. Fig. 1.3 shows the observed data (again for the 2 mm sample) and the least squares fit together with the capture cross section derived from the resonance parameters in the neutron energy region 5 to 9 keV and 24 to 32 keV respectively.

In the neutron energy region below 10 keV we observed eight resonances not previously reported. These were observed in all three samples, the 2 mm being a sample of very pure iron (99.9999%). For the purpose of analysis these resonances were assigned to ^{57}Fe and we used the average detection efficiency for that isotope in calculating the yields.

All uncertainties are expressed as one standard deviation and those quoted in the table are obtained only from the fits. In addition there is an uncertainty in the normalisation of the data to the gold capture cross section of $\pm 10\%$. The uncertainty of ± 50 mm in the flight path gives an additional error in the resonance energy of $\pm 0.01\%$ which in most cases is much greater than that obtained from the least squares fit.

The total width of the important resonance at 1.15 keV is accurately determined from the fit to our data to be 0.6674 ± 0.0059 eV. Uncertainties in the effective temperature used in the Doppler function and uncertainties in the time-of-flight resolution function give an additional uncertainty of ± 0.014 eV. Changes in the normalisation of up to 20% have a negligible effect on the total width. The neutron width is 0.0526 ± 0.0002 eV with an additional uncertainty of 0.0053 to take into account uncertainties in the normalisation. The difference between the total and neutron width gives a value of 0.615 eV for the radiation width (with a total error of ± 0.016 eV).

Another important resonance (from a reactor point of view) is the s-wave resonance in ^{56}Fe at ~ 27 keV. Assuming a neutron width of 1476 eV for this resonance(3), we obtain a value of 0.850 ± 0.013 eV for the radiation width. It should be noted that all the resonances shown in Fig. 1.3b have been included in the calculation of the capture yield in the energy region 24 to 35 keV as well as using multi-level R-matrix formalism for the cross section.

In the energy region from 40 to 200 keV we have compared a capture yield calculated from resonance parameters given in an evaluation of ^{56}Fe by F. Perey(2) with our

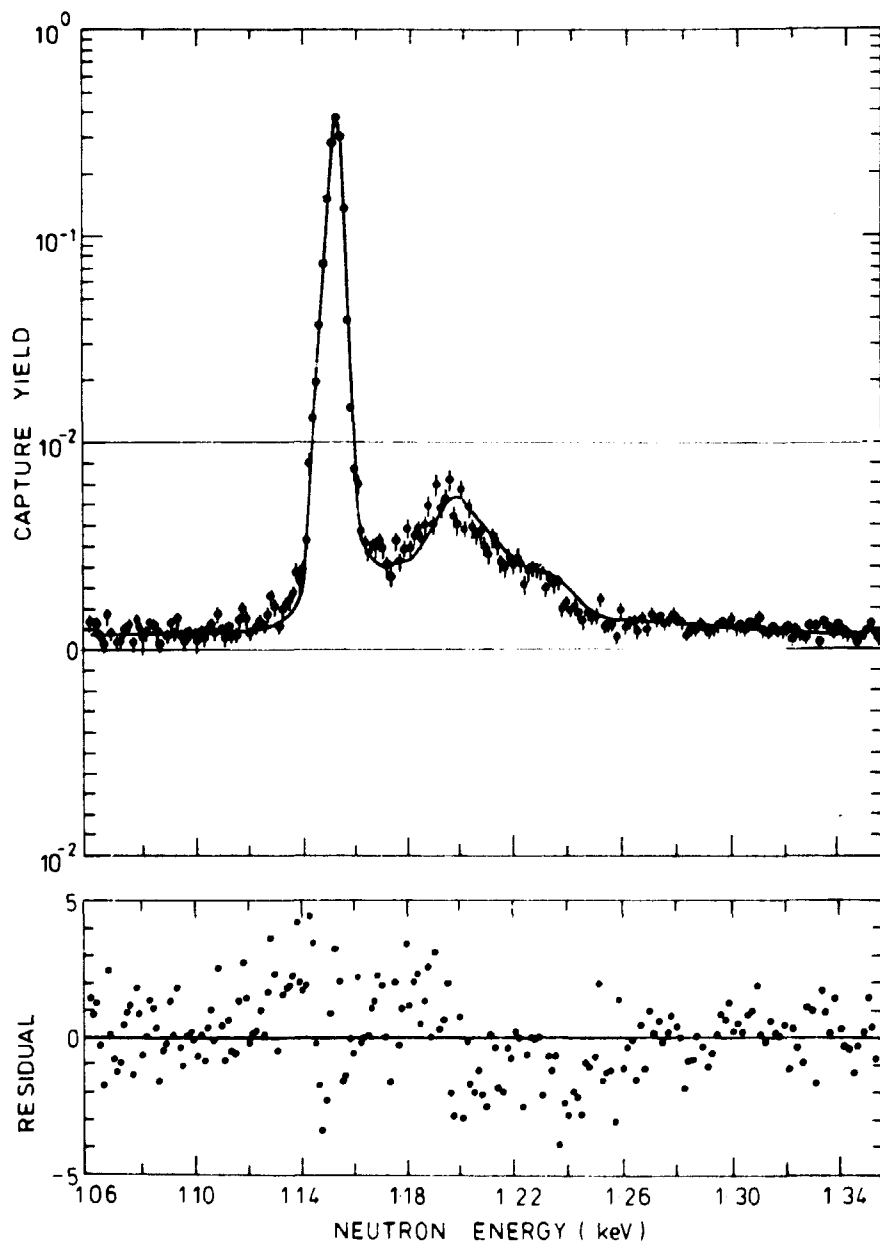


Fig. 1.2. (a) The continuous curve is a least squares fit to the measured capture yield (x) for a sample of natural iron (2 mm) in the region of the 1.15 keV resonance of ^{56}Fe . Note change of ordinate scale at 10^{-2} from logarithmic to linear.

(b) The scatter of the residuals, (observed minus the calculated yield divided by the uncertainty in the observed yield), indicate the quality of the fit.

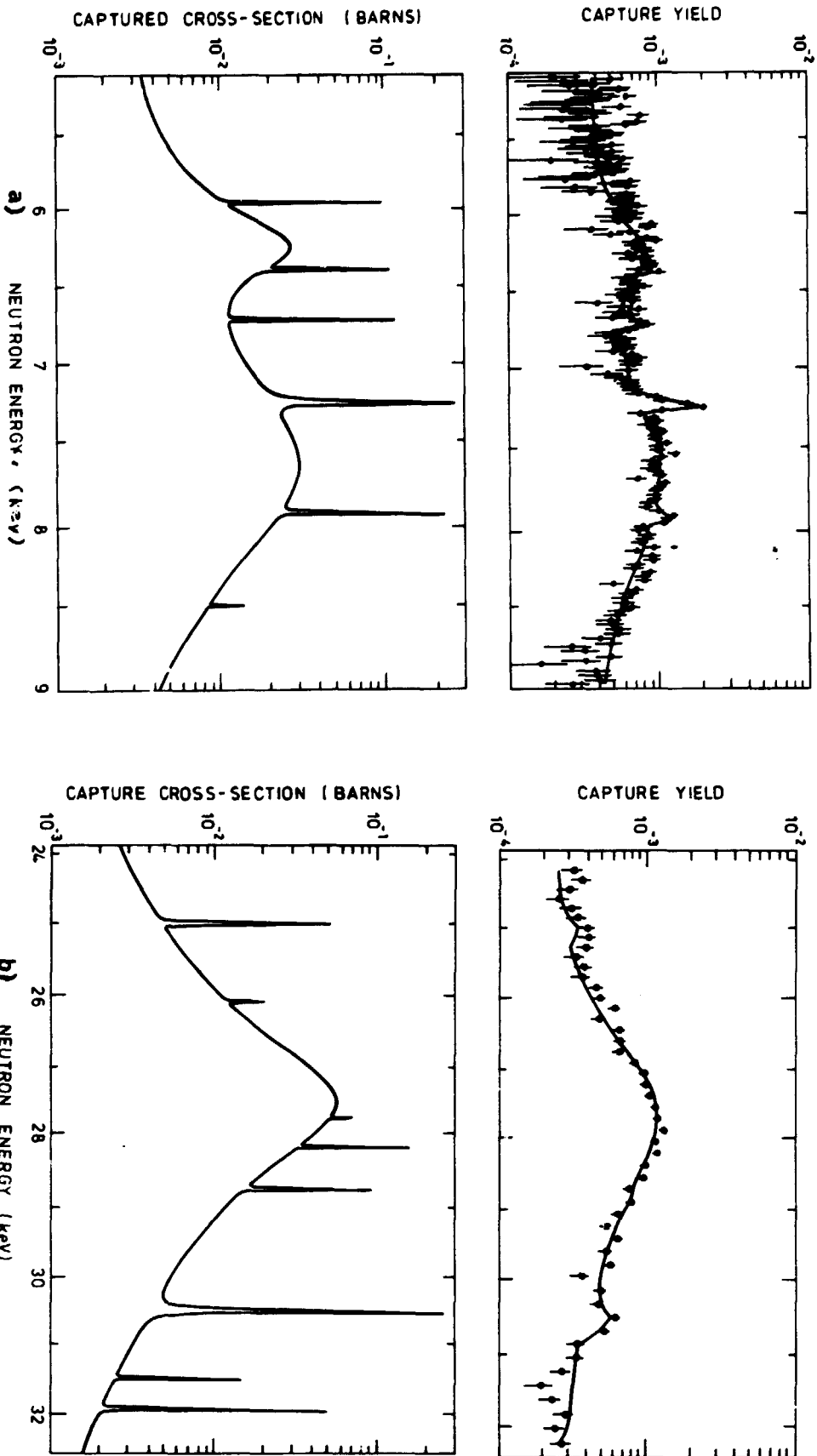


Fig. 1.3. In both cases the continuous curve is a least squares fit to the measured capture yield data; the Doppler broadened capture cross section derived from the fit is shown above. In (a), the parameters for the resonances at 6.36 and 9.53 keV were held fixed; in (b), only the parameters for the resonances at 27.6 keV and 30.5 keV were varied.

data. The agreement is poor, in some energy regions the calculated yield being as much as twice the experimental value.

-
- (1) M.C. Moxon, Proc. of Specialists Meeting on Neutron Data of Structural Materials for Fast Reactors, Geel (1977) 644.
 - (2) F.G. Perey, G.T. Chapman, W.E. Kinney and C.M. Perey, Proc. of Specialists Meeting on Neutron Data of Structural Materials for Fast Reactors, Geel, (1977) 530.
 - (3) M.C. Moxon and J.B. Brisland, Proc. of Specialists Meeting on Neutron Data of Structural Materials for Fast Reactors, Geel (1977) 689.

1.3H Neutron transmission measurements on structural materials (G.D. James, D.B. Syme and I.L. Watkins) (Relevant to request numbers: 326, 450, 451, 474, 519, 522, 551, 601, 605)

Neutron transmission measurements for structural materials continued on the synchrocyclotron until the machine ceased operation on 31st March. Thirty-six measurements were carried out bringing the total number of measurements made on continually improved versions of the time-of-flight spectrometer to ninety-one. The transmission samples used and the basic experimental parameters are given in Table 1.2. The samples include separated isotopes of ^{53}Cr , ^{54}Fe and ^{57}Fe , on loan from ORNL as well as samples of natural iron, nickel and titanium. Measurements on carbon and sulphur were included to check the energy scale. Twenty-two of the measurements were made with permanent filters (Al, AlMn, NaF) which provide in-situ indication of the background at several discrete energies corresponding to strong resonances in these materials. The accelerated pace of data taking has meant that data processing is not complete and only two of the runs taken this year have been completely processed.

To represent the background curve in the permanent filter runs, a cubic spline fitting routine has been brought into use by J.P. Argyle and P.A. Hay-Jahans. This routine works well for the AlMn filter but not as well for the NaF filter where there are four background points within a narrow energy range. Results taken with and without a permanent filter for $^{56}\text{Fe}_2\text{O}_3$ (see PR/NP26, p.28, sequence numbers 52 and 53) show close agreement. Nevertheless, there is a component of background which is not revealed by either method of background measurement. This is thought to arise from neutrons, close in energy to the spectrum neutrons, which emerge from the water moderator after scattering in a magnet pole face. This effect is being investigated by Monte Carlo calculation (see this report Section 1.5).

Table 1.2

Neutron Transmission Measurements on the Synchrocyclotron 1979

Sequence Number	Sample ⁽¹⁾ Material	Thickness (atom/barn)	Path ⁽²⁾ (m)
56	⁵³ Cr ₂ O ₃ (AlMn)	0.0049	50
57	30mm Fe(NaF)	0.2549	100
58	12mm Fe(NaF)	0.1023	100
59	⁵⁶ Fe ₂ O ₃	0.1331	100
60	36mm C	0.314	100
61	⁵³ Cr ₂ O ₃	0.08887	100
62	⁵³ Cr ₂ O ₃ (NaF)	0.08887	100
63	30mm Fe(NaF)	0.2549	100
64	12mm Fe(NaF)	0.1023	100
65	6mm Fe(NaF)	0.05164	100
66	2mm Fe(NaF)	0.01721	100
67	18mm Ni(NaF)	0.1642	100
68	6mm Ni(NaF)	0.5480	100
69	3mm Ni(NaF)	0.2740	100
70	60mm Fe(NaF)	0.5097	100
71	6mm Ti(NaF)	0.03416	100
72	9mm Ti(NaF)	0.05131	100
73	18mm Ti(NaF)	0.1022	100
74	⁵⁷ Fe ₂ O ₃	0.1431	100
75	⁵⁷ Fe ₂ O ₃ (NaF)	0.1431	100
76	⁵⁷ Fe ₂ O ₃	0.1431	100
77	⁵⁴ Fe ₂ O ₃	0.1104	100
78	36mm C	0.314	100
79	⁵⁴ Fe ₂ O ₃ (C)	0.1104	100
80	18mm C	0.1563	50
81	⁵⁴ Fe ₂ O ₃	0.01431	50
82	⁵⁴ Fe ₂ O ₃	0.1099	50
83	⁵⁴ Fe ₂ O ₃ (Al)	0.1099	50
84	⁵⁴ Fe ₂ O ₃ (NaF)	0.1099	50
85	⁵⁴ Fe ₂ O ₃ (NaF)	0.01431	50
86	⁵⁴ Fe ₂ O ₃	0.01431	50
87	⁵⁴ Fe ₂ O ₃ (Al)	0.1099	50

Table 1.2 (continued)

Neutron Transmission Measurements on the Synchrocyclotron 1979

Sequence Number	Sample ⁽¹⁾ Material	Thickness (atom/barn)	Path ⁽²⁾ (m)
88	⁵⁴ Fe ₂ O ₃ (NaF)	0.1099	50
89	⁵⁴ Fe ₂ O ₃	0.1099	50
90	18mm C	0.1562	50
91	S	0.467	50

Notes

1. Parentheses denote permanent filter material present during both sample in and sample out runs.
2. All 50 m measurements are taken with a ⁶Li-glass detector and a minimum channel width of 5ns. All 100m measurements are taken with an NE110 detector and a channel width of 2.5ns.

At present, various improvements are being made to data handling and storage.

1.4H Background evaluation in synchrocyclotron transmission data (D.B. Syme)

Conventional 'notch filter' measurements were taken as part of the synchrocyclotron neutron transmission data (PR/NP26, p.27) and were used to deduce the neutron background. An investigation of some inconsistencies in these results has revealed limitations of this method for higher energy neutrons and for compact cyclotron sources. Techniques are being developed to better characterise the backgrounds in such conditions.

Neutron time-of-flight measurements above a few keV face an additional background due to the 2.2 MeV gamma-rays produced by thermal neutron capture in hydrogen in the moderated source. These events have a characteristic broad time distribution with a 20-30 μ s decay and so contribute significantly only at the shorter times. For the usual range of flight paths (20-200m) this effect is negligible below a few keV. At higher energies it must be measured and removed from the data before the neutron background can be determined. The required measurements have been made for the synchrocyclotron data.

The sensitivity of the notch filter technique itself decreases towards higher energies because the resonance peak cross section available to the notch filter falls as 1/E. More fundamentally, the finite width of the resonances used in the notch filter

($\Delta E/E = 2-20\%$) prevents observation of the background neutrons close in energy to that of the 'in-time' neutrons. One of the main components of the background is due to source room return and is different in energy from the in-time neutrons by an amount related to the ratio of the source enclosure size to the flight path length. For a compact source enclosure like the synchrocyclotron this energy difference is of the order of a few percent and so may not be properly observed by the notch filter measurements. For a typical linac the source enclosure is larger and this background is reduced but its energy difference is increased. In this case, a larger fraction of the smaller background will be observed in the notch filter, although this fraction will vary with the width of the observing resonance.

In order to determine unperturbed backgrounds from the previous notch filter measurements, the effect of the filters on the expected source and background spectra are being calculated in detail. A Monte Carlo simulation of the source and background spectra is described in the next section.

1.5H Monte Carlo simulation of the synchrocyclotron moderated source (R.B. Thom,

T.M. Horscroft and D.B. Syme)

The Monte Carlo neutronics code MORSE(1) was used to model the required geometry and to track neutrons originating in the tungsten target of the synchrocyclotron to their exit at the face of the adjacent water moderator. For a given input neutron energy the results are in the form of a bidimensional array of exit neutron intensity versus energy and time. Separate spectra were recorded for neutrons which had visited the synchrocyclotron magnet poles in their histories. The geometry of target and moderator has been described previously(2). The tungsten target lies 7 mm below the midway plane between the iron magnet poles which have a 30 cm gap and 127 cm radius.

Some preliminary results are given in Fig. 1.4 for source neutrons of 1 MeV and two different energy bands of moderated neutrons. Final results will be summed over the source energy spectrum. The solid histograms are for the 'in-time' neutrons which have travelled directly from source to moderator before moderation. These show the characteristic time dependence of moderator spectra,

$$\phi(x) \sim 1/2 x^2 e^{-x}; \quad x = t/\Sigma v.$$

Here t is the moderator time delay, Σ is the macroscopic scattering cross section and v is the neutron velocity. The lower energy neutrons peak later and are broader in

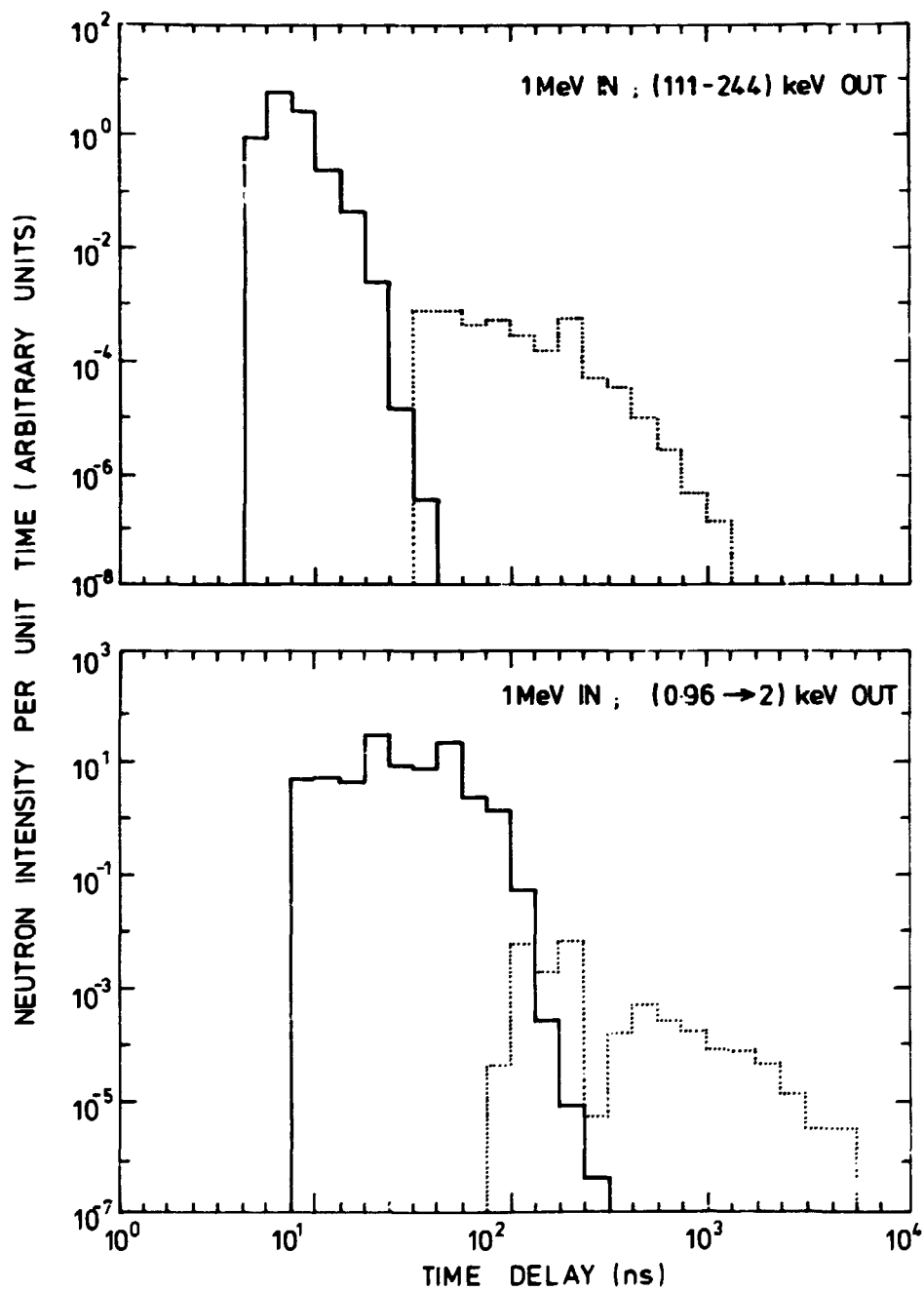


Fig. 1.4. Monte Carlo calculations for the neutron source and moderator of the Harwell synchrocyclotron. Time spectra are shown for moderated neutrons in a (112-244) keV energy bin (top) and a (0.96-2) keV energy bin (bottom). Both were generated by a delta function pulse in the source target at time zero, and with energy 1 MeV. The solid histograms are for neutrons which have entered the moderator directly from the source target and the dashed histograms are for neutrons which have been reflected from the magnet poles, some 15 cm from the source-moderator assembly.

time as expected. The dashed histograms are for 'background' neutrons which have in their histories returned to the moderator from the magnet pole. These have similar shapes but are delayed and broadened with respect to the 'in-time' spectra. The delays and broadening are consistent with the ideas of the previous contribution.

We intend to fit the 'in-time' and the 'background' spectra by functional forms of type $\phi(x)$, to determine the variation with energy of these and to use this parameterisation to predict the effective resolution function and the background for any required neutron energy and flight path. The effect of notch filters will be calculated and compared with the experimental results.

-
- (1) MORSE-GC, 'General Purpose Monte Carlo Multigroup Neutron and Gamma-Ray Transport Code with Combinational Geometry', RISC Computer Code Collection-203.
 - (2) G.D. James, D.B. Syme, P.H. Bowen, A.D. Gadd and I.L. Watkins, in Neutron Data for Structural Materials for Fast Reactors. K.H. Bockhoff (Editor) (Pergamon Press, Oxford, 1979), 571.

1.6 An assessment of the accuracy requirements on higher actinide nuclear data for fast reactors (B.H. Patrick and M.G. Sowerby)

A sensitivity study has been carried out to assess the adequacy of the nuclear data needed for fast reactor calculations of the arisings of minor actinides, the alpha-contribution to decay heat and the neutron output from irradiated fuel. The study is based on a fast reactor outer core sub-assembly of mixed oxide fuel containing AGR plutonium as a fraction, 0.296, of the heavy element content. A calculation was performed in which the sub-assembly was "irradiated" for ~1 year leading to a burn-up of 8.26%. The fuel was assumed to have been stored for 4 years prior to the irradiation and afterwards the composition was followed during a cooling period of up to 10 years.

The inventory code FISPIN⁽¹⁾ and a one group fast reactor library were used for the simulated irradiation. Sensitivity coefficients were obtained by first running a standard case, followed by a number of other cases in each of which one cross section or half-life value was altered. The code calculates the changes in the atom density of each isotope resulting from neutron capture, fission, (n,2n) reactions and radioactive decay, the sensitivity coefficients of the reactor parameters of interest being derived from the computed atom densities. The sensitivity coefficients were then compounded with the corresponding nuclear data uncertainties to arrive at a total uncertainty which is the net result of inaccuracies in the actinide nuclear data. Covariance terms

between the different items of nuclear data were neglected as they are expected to be small compared with the variances.

Table 1.3

Estimated Uncertainties on Selected Reactor Quantities Following Irradiation of Fast Reactor Fuel

Quantity	Required Standard Deviation (%)	Estimated Uncertainty*		Nuclear Data Contributing Most to Uncertainty
		Short Cooling Times (≤ 1 y) (%)	Long Cooling Times (~ 4 y) (%)	
Production of ^{236}Pu	50	100	100	$^{237}\text{Np}(n,2n)$
Production of ^{238}Pu	20	8.3	8.7	$^{241}\text{Am}(n,\gamma)^{242}\text{gAm}$, $^{238}\text{Pu}(n,f)$
Production of ^{241}Am	50	6.2	5.0	$^{241}\text{Am}(n,\gamma)^{242}\text{gAm}$, $^{241}\text{Pu } T_{\frac{1}{2}}$
Production of ^{243}Am	50	10	10	$^{242}\text{Pu}(n,\gamma)$, $^{243}\text{Am}(n,\gamma)$
Production of ^{242}Cm	50	17	15	$^{241}\text{Am}(n,\gamma)^{242}\text{gAm}$, $^{241}\text{Am}(n,\gamma)^{242m}\text{Am}$
Production of ^{244}Cm	50	22	22	$^{243}\text{Am}(n,\gamma)$, $^{242}\text{Pu}(n,\gamma)$
Alpha-decay heat	$\ll 5$	15	5	$^{241}\text{Am}(n,\gamma)^{242}\text{gAm}$, $^{242}\text{Cm}(n,f)$
Total decay heat	5**	5.5	3.0	$^{241}\text{Am}(n,\gamma)^{242}\text{gAm}$, $^{242}\text{Cm}(n,f)$
Spontaneous fission neutron output		15	20	$^{241}\text{Am}(n,\gamma)^{242}\text{gAm}$, $^{243}\text{Am}(n,\gamma)$
(α,n) neutron output		18	13	$^{241}\text{Am}(n,\gamma)^{242}\text{gAm}$, (α,n) yields
Total neutron production	10 (reactivity) 20 (shielding)	14	18	$^{243}\text{Am}(n,\gamma)$, $^{241}\text{Am}(n,\gamma)^{242}\text{gAm}$ ^{242}Cm spontaneous fission branching ratio

*Uncertainties are given as one standard deviation. No account is taken of uncertainties arising from sources other than nuclear data.

**Including uncertainties arising from fission product decay.

The results of folding together the data uncertainties and the calculated sensitivity coefficients are given in Table 1.3. Also shown are the standard deviations applicable at the present time as suggested by Baker(2) (these may need to be

reduced when a fast reactor programme is established). The results show that, with the exception of ^{236}Pu , the uncertainties in the production of the minor actinides are considerably smaller than current requirements. But the uncertainties on the nuclear data which affect the decay heat are still too large to allow the alpha-contribution to be estimated with sufficient precision and the same is true of the total decay heat when allowance is made for the contribution from uncertainties in the fission product decay. The uncertainty on the total neutron production rate seems to meet the shielding needs but requires more accurate data if the reactivity criterion is to be satisfied.

The last column in Table 1.3 indicates the nuclear data which contribute most to the uncertainties in the various reactor quantities. By comparing the current uncertainties on these data with the reactor needs, it is possible to deduce the accuracies required for the nuclear data if the needs are to be satisfied. The requirements of highest priority are listed in Table 1.4.

Table 1.4
Nuclear Data Requirements of Highest Priority

Quantity	Present Standard Deviation (%)	Required Standard Deviation (%)	Purpose
$^{237}\text{Np}(n,2n)$	100	25	Production of ^{236}Pu
$^{241}\text{Am}(n,\gamma)^{242g}\text{Am}$	20	8	Total heat generation
		10	Total neutron production
$^{243}\text{Am}(n,\gamma)$	25	10	Total neutron production
^{242}Cm spontaneous fission branching ratio	10	5	Total neutron production
(α,n) yields	30	10	Total neutron production

(1) R.F. Burstall, Risley report ND-R-328(R) (1979).

(2) A.R. Baker, NPDE, Risley, private communication (1979).

1.7 An Evaluation of the Prompt Capture Gamma-Ray Spectrum of Natural Ti Produced by Thermal Neutrons (M.G. Sowerby)

In response to a request, an evaluation has been performed of the prompt capture gamma-ray spectrum of natural Ti produced by thermal neutrons. This spectrum is difficult to measure accurately and completely because

- (a) de-excitation of the compound nucleus is mainly a statistical process and hence there can be so many gamma-rays of different energy emitted that they cannot all be identified independently;
- (b) the response of some gamma-ray detectors is not always ideal. For example a simple Ge(Li) detector looking at gamma rays of 3 MeV will produce 3 peaks in its pulse height distribution corresponding to the full energy, single escape and double escape peaks and a distribution of pulse heights corresponding to the Compton effect. This means that it is difficult to determine the energy spectrum of low intensity gamma-rays with such a device, and
- (c) the number of capture events and hence the absolute intensities of the gamma-rays are not usually well-known.

For natural Ti these problems are further aggravated because there are five stable isotopes though ^{48}Ti is responsible for ~95% of the thermal captures.

Examination of the available measurements of gamma-ray spectra showed that though most experiments give gamma-ray energies which agree well, there is a great variation in the values of the gamma-ray intensities. For the Ti isotopes it is expected that, due to single particle effects, there will be strong primary transitions to the low lying states in the compound nucleus. In assessing the Ti data it is therefore necessary to find out if there are a significant number of primary transitions to the states above ~4 MeV excitation energy, which are individually too weak to observe but may contribute significantly to the total gamma-ray energy. Rasmussen et al⁽¹⁾ consider that for their measurements of natural Ti there are no appreciable unresolved transitions and this conclusion is supported by the results of Adyasevich et al⁽²⁾. The recommended capture gamma-ray spectrum is therefore based on the measurements of Rasmussen et al corrected so that they are self consistent and renormalised to give the correct gamma-ray energy per capture event. The results of the work have been published⁽³⁾.

(1) N.C. Rasmussen, Y. Hukai and T. Inouye, AD688955 (1969), also known as ACCRL-69-0071.

(2) B.P. Adyasevich, L.V. Groshev and A.M. Demidov, J. of Nucl. En., 3, (1956) 258.

(3) M.G. Sowerby, AERE-R 9502 (1979).

1.8 Evaluation of differential nuclear data for ^{243}Am (J.E. Lynn, B.H. Patrick, M.G. Sowerby and E.M. Bowey)

Work has resumed on the evaluation of the differential nuclear data for ^{243}Am , with the aim of producing a file for inclusion in the U.K. Nuclear Data Library. Theoretical calculations are used to provide the required data for the parts where no measurements exist and these calculations are essentially complete. A set of resonance parameters has been chosen for neutron energies up to 250 eV and appropriate parameters determined for bound levels in order to give good agreement with the shape of the total cross section in the thermal region. The evaluation of the measured fission cross section data in the fast region has begun.

1.9 Nuclear data files (E.M. Bowey)

Copies of the ENDF/B-V data files, recently released by the U.S. Department of Energy, are now held on magnetic tape at Harwell. Those programs required to access these data files (CRECT, LISTFC and others) have been converted for use on the Harwell IBM 370/3033 computer.

Some progress has been made in the construction of the ^{243}Am file for the U.K. Nuclear Data Library (see preceding section).

1.10D (α, n) yields from light elements (D. West and A.C. Sherwood)

(Relevant to request numbers 16, 17, 113, 118, 119, 160, 195-199, 258, 259, 275, 286)

Measurements have continued at a similar level of activity as in the previous year. Thick target yield measurements of the following substances have now been concluded: Mg, Al, Si, C, UO_2 , Fe, Zr and type M316 stainless steel.

UC has been measured at 17 energies and some additional measurements, using a production sample taken from a fuel element, are planned.

Work has started on the yields of Be, B and certain compounds containing these materials. Preparations are in hand to enable Li and Na to be measured. The latter elements of course require special handling arrangements to prevent surface oxidation and chemical attack by moisture in the air.

The correction factors which must be applied to the raw data have only recently become available and have not yet been used to deduce the final results for any of the sets of otherwise completed data. The correction factors include

- (1) Neutron absorption in the ^{241}Am and other materials of the calibration source (~0.2%). Absolute neutron flux measurements for our system using Au foils measured by NPL are now available which will enable this (and other) corrections to be evaluated.

- (2) Neutron leakage from the detector system using the ^{241}Am -Be calibration source (~1%). Computations using MONK are now available and are reported in section 1.18.
- (3) Neutron absorption in the target holder, Faraday cup and beam tube when inserted in the moderator block has been measured directly using 4 radioactive (α, n) sources, Am-Be, Am-B, Am-F and Am-Li, with and without the beam tube assembly in the moderator block.

The effect of a strongly absorbing target, B, has also been measured. The neutron absorption in the beam-tube target assembly varied from $2.03 \pm 0.05\%$ for Am-Be neutrons to $3.95 \pm 0.15\%$ for Am-Li neutrons. In the presence of a boron target the corresponding values were 2.45% and 4.44%. The integration program outputs a value of the rms radial coordinate (in cylindrical geometry) of the neutron counts observed which provides some measure of the energy of neutrons in a particular yield measurement. This quantity can be used to assign the relevant absorption correction (in the range 2-4%) for an actual yield measurement.

Thick target yields of compounds and mixtures

Thick target data are often required for compounds or mixtures whose constituents have only been measured separately. A method of doing this without knowing the differential cross sections as a function of energy or making major approximations has been published(1).

The method assumes that the Bragg law of additivity of the stopping powers of its constituents applies in the compound. It also makes use of the fact that the stopping powers of all elements vary with energy in the same way. That is for two elements i, j

$$\frac{dE}{d(\rho x)}_j = C_{ji} \frac{dE}{d(\rho x)}_i \quad (1)$$

where C_{ji} is approximately a constant independent of α -particle energy.

It was shown that the neutron yield from a compound is then given by

$$Y_{\text{compound}} = \sum_j a_j A_j C_{ji} \frac{Y_j / \sum_j a_j A_j C_{ji}}{a_j A_j C_{ji}} \quad (2)$$

independently of any assumptions other than those stated above. The summation extends

over the j constituents of which $j = 1$ is used as a reference material. a_j is the number of atoms of atomic weight A_j in the compound and Y_j is the thick target (α, n) yield of the pure element j at the energy in question.

To test this relation we can use some of our directly measured values of yield in compounds of two elements and in the pure elements. Data for two cases are available in which, to minimise the experimental data required, the yield of one of the constituents is negligible, namely UC and BeO.

Using relation (2) it follows that for UC

$$C_{U,C} = \left(\frac{dE}{d(\rho x)} \right)_U / \left(\frac{dE}{d(\rho x)} \right)_C = \left(\frac{Y_C}{Y_{UC}} - 1 \right) \frac{A_C}{A_U} \quad (3)$$

Hence from the measured yields Y_C and Y_{UC} at a particular α -particle incident energy one can, from relation (3), work out the required ratio of stopping power of U and C for relation (2) to be obeyed. The hypotheses used in deriving (2) are then tested by comparing these values of relative stopping with the direct values obtained from tables of stopping power. Fig. 1.5(a) shows the derived values of $C_{U,C}$ plotted, as points, against incident α -particle energy in the range 4 to 7 MeV which includes the energies of the vast majority of actinide α -particle emitters of technological interest.

The solid lines are the values of $C_{U,C}$ obtained from tables of stopping power by Williamson et al⁽²⁾ (curve B) and by Ziegler⁽³⁾ (curve A). Since $C_{U,C}$ is not exactly constant with energy it is necessary to take account of the fact that the effective value of $C_{U,C}$ will depend slightly on the way the (α, n) yield of C varies with energy. This has been done for only the Williamson et al values in Fig. 1.5(a) and is shown as the dotted curve C. The difference between the derived $C_{U,C}$ values and those from the tables is in the region of 10%.

Because of the wide difference of Z between U and C this is a very severe test of relation (2).

The case of BeO where the atomic numbers of the constituents are closer is shown in Fig. 1.5(b). Here the Ziegler values have been weighted to include the variation of the Be yield with energy to give the dotted curve D.

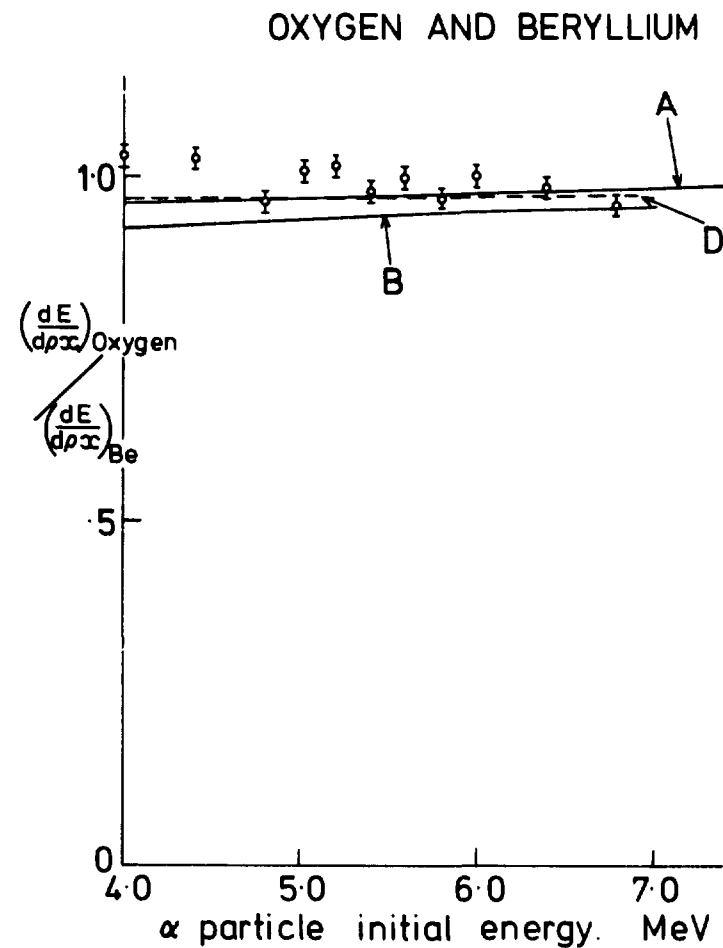
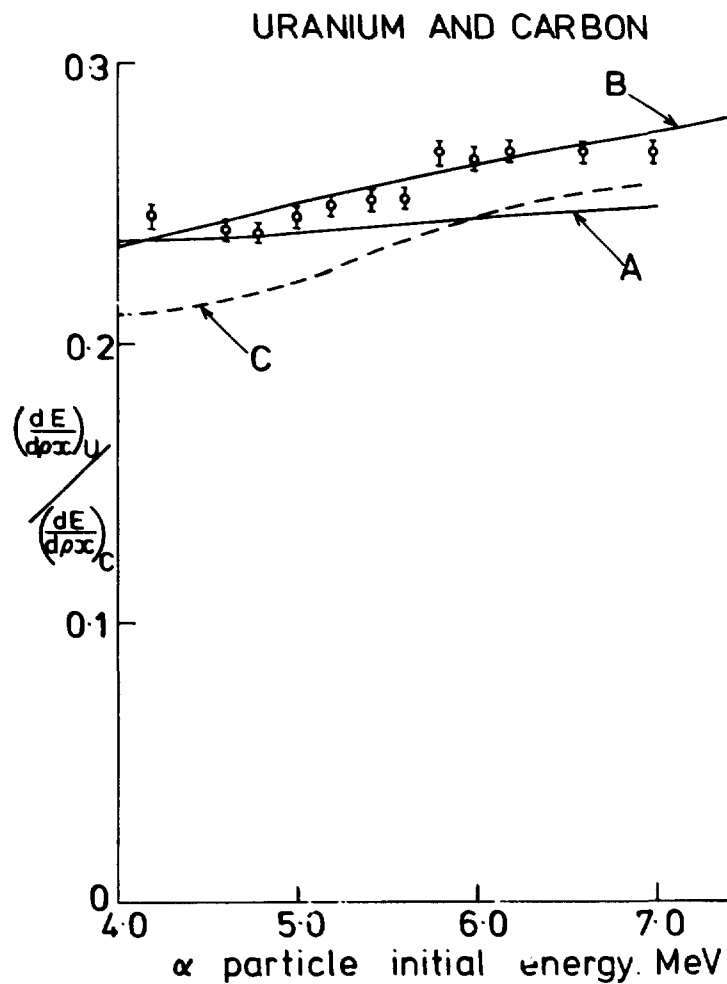


Fig. 1.5. Comparisons of the derived values, plotted as experimental points, from the thick target yields of neutrons in C and UC and in Be and BeO respectively. A = values from Ziegler tables at the initial α -particle energies, B = values from the tables of Williamson et al at the initial α -particles energies, C = values from the tables of Williamson et al weighted according to the differential C(α ,n) yield as the α -particle slows down, D = values from Ziegler tables weighted according to the differential Be(α ,n) yield as the α -particle slows down.

The difference between the derived and tabular values of $C_{O,Be}$ is at most 5% if the Ziegler values are used and 9% if the Williamson et al values are used.

One concludes that relation (2) is good to 10% in these two cases and that at present there may be little point in examining the matter further unless more precise direct measurements of $dE/d(\rho x)$ are also made.

-
- (1) D. West, The calculation of neutron yields in mixtures and compounds from the thick target (α, n) yields in the separate constituents, AERE-R 9372 (1979).
 - (2) C.F. Williamson, J.P. Boujot and J. Picard, CEA R 3042 (1966).
 - (3) J.F. Ziegler, Helium: Stopping power and ranges in all elemental matter (The stopping and ranges of ions in matter. Volume 4) Pergamon Press (1977).

1.11 Safeguards Research

1.11.1 Theoretical analysis of the Variable Dead Time Counter (VDC) (E.W. Lees and B.W. Hooton)

Strictly speaking, the VDC refers to a data analysis procedure (PR/NP26, pp.54-58) used with neutron coincidence counters (NCC). NCC are used in Safeguards work for the passive, non-destructive assay of Pu mass by measurement of the ^{240}Pu content. The VDC analysis method utilises the fact that neutrons from spontaneous fission are correlated in time and that after the usual dead time corrections are performed, one is left with a residual proportional to the number of correlated neutrons, i.e. proportional to the number of spontaneous fission events and hence to the mass of ^{240}Pu .

$$M_{240} \propto X = b - \frac{c}{1 - cd} \quad (1)$$

where b is the true count rate, c is the count rate measured in a scaler with non-extending dead time d .

Stanners⁽¹⁾ proposed an improvement to the VDC analysis by defining the quantity

$$Y = \sum_{i=1}^m (n_i - 1) \quad (2)$$

where n_i (≥ 2) is the number of pulses in the i th pulse group from a fission event which have a random appearance rate of m per second. He claimed that

$$Y = X \left[1 - E_1 - \frac{cd}{1 - cd} E_2 \right]^{-1} \quad (3)$$

where E_1 and E_2 are complicated functions of c , d and a parameter q . The parameter q is meant to describe the mean time interval between the leading neutron and the next neutron in a pulse group from the same fission event.

Clearly, equation (3) implies that Y can go to infinity and then become negative and indeed does so for large ^{240}Pu samples, e.g. for $M_{240} = 574$ g, $b = 64757$ s $^{-1}$, $c = 12614$ s $^{-1}$, $d = 63.54$ μ s resulting in $X = 1210$ and $Y = -52$. However, the definition of Y in equation (2) prohibits negative values of Y ; thus either the derivation of (3) is incorrect or the definitions of E_1 and E_2 are wrong.

We have studied the derivation of equation (3) carefully, and believe the following aspects are not fully accounted for in that equation:

- (i) The parameter q describing the time interval between detected neutrons from the same fission event depends on the number of neutrons in the pulse train. In fact, we have shown⁽²⁾ that if the probability of detecting a neutron following a fission event can be described by an exponential function with characteristic die-away time τ , then for n detected neutrons from the same fission event,

$$q(n) = \tau / (n - 1)$$

Consequently, E_1^n and E_2^n are functions of n . Using $q(n)$ in equation (3) retards the divergence of the denominator, but for the example given above, Y is still negative (≈ -2).

- (ii) The derivation of equation (3) assumes that the probability of capture for a neutron in the detector falls off exponentially with time. This is not strictly true (e.g. PR/NP26, p.56) and we have investigated the effect of using the measured capture probability distribution to calculate E_1^n and E_2^n by numerical integration. Fig. 1.6 shows the results for the calculation of $q(n)$ where clearly the interval probabilities follow an exponential behaviour more closely than does the die-away time. Using these $q(n)$ only changes the values of Y by a few per cent.

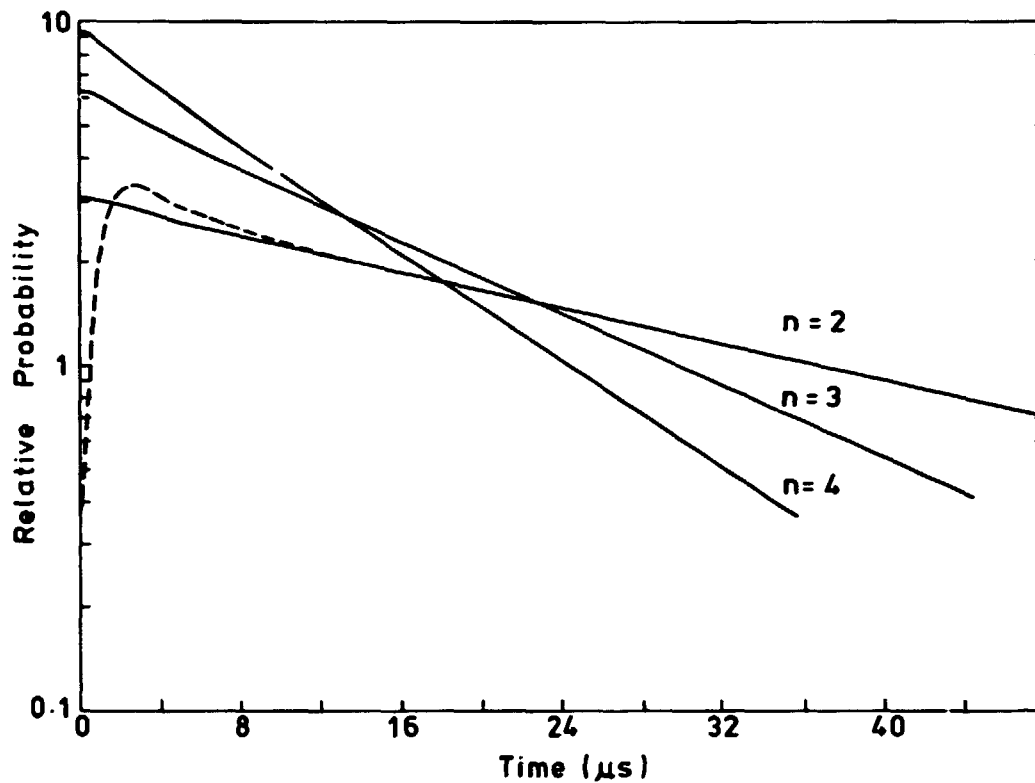


Fig. 1.6. The probability functions for intervals between the leader and a second neutron in a group of n neutrons in a detector with a capture probability distribution as given by the dashed curve. For times greater than $16 \mu s$, the $n = 2$ and die-away curves are identical.

(iii) In deriving (3), the interaction of dead times from detected neutrons in the same group is only taken into account for events of multiplicity 2. Higher multiplicity events ($n > 2$) are not considered.

(iv) In deriving (3), the dead times are assumed to be randomly distributed with a mean rate of appearance c . For large samples with extensive neutron multiplication, the neutrons will appear in correlated bunches and this assumption is invalid.

As a result of investigating (iii) and (iv), we have reached the conclusion that the most useful technique for a theoretical understanding of the VDC analysis is to

resort to Monte Carlo calculations⁽³⁾.

-
- (1) W. Stanners, private communication 1977 in ref. 2.
 - (2) E.W. Lees and B.W. Hooton, AERE-R 9168 (1978).
 - (3) B.W. Hooton and E.W. Lees, Int. Meeting on Monitoring of Pu-contaminated Waste, JRC-Ispra, September 1979.

1.11.2 A model for studying coincidence systems used in plutonium assay (B.W. Hooton and E.W. Lees

The model for studying coincidence systems (PR/NP26, p.51) has been further developed and applied to several analysis algorithms. A modification which is more economical in the use of random numbers and computing time has been successfully implemented and applied to four algorithms for plutonium measurement.

The first two algorithms, the Variable Dead Time Counter and the Stanners modification, which are described in PR/NP25, p.51 have been shown to be in error by about 7% for 50g of ²⁴⁰Pu. Both of these algorithms are approximations which do not have a sound theoretical basis.

A new algorithm, the Extended Dead Time (EDT) Algorithm has been tested and found to be theoretically sound. However, it suffers from low statistical accuracy at high counting rates. It is based on the distribution function S(D) for the time interval between consecutive pulses D. This function, shown in Fig. 1.7, can be sampled using a counter with an extending dead time D₁. Such a counter will count all events in S(D) with a value of D > D₁. If D₁ is given a value D₁ >> τ, the die-away time in the well counter, then since S(D) is exponential in this region the counter registers

$$A = \int_{D_1}^{\infty} \lambda^2 e^{-\lambda t} dt = \lambda e^{-\lambda D_1}$$

This measurement can be used to calculate λ, the exponential component in S(D).

The total area of the S(D) distribution T, is greater than λ by an amount which is proportional to the number of coincidences and the two measurements can be used to derive the amount of plutonium in the sample.

The 'singles' rate at large values of D arises from (α,n) events and fissions in which one or more neutrons are detected; this rate is given by

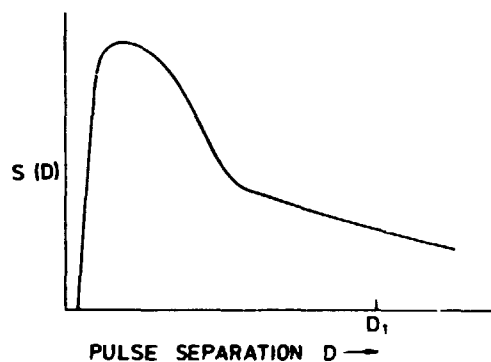


Fig. 1.7. The distribution function for the separation in time D of consecutive pulses

$$\lambda = (\alpha, n) + F(1 - P_0)$$

where P_0 is the probability of detecting zero neutrons from a fission source of strength F and (α, n) is the measured (α, n) rate. The total rate is given by

$$T = (\alpha, n) + \bar{\nu} F \epsilon$$

where ϵ is the detection efficiency. The quantity

$$T - \lambda = F(\bar{\nu} \epsilon - (1 - P_0))$$

is proportional to F .

The weakness of this algorithm is that at high counting rates very few pulse spacings have $D > D_1$ and it is difficult to obtain a high statistical accuracy for λ .

The shift register algorithm analyses the distribution function for events occurring at a separation time t irrespective of whether another event has intervened or not. The distribution function for this situation is shown in Fig. 1.8 and it is a constant for $t \gg \tau$, the die-away time of the well counter. The constancy of $S(t)$ enables it to be measured accurately even at high rates. The effect of a dead time in the discriminator will be to distort the distribution near $t = 0$ but this will have

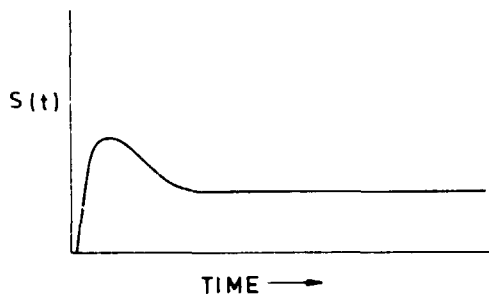


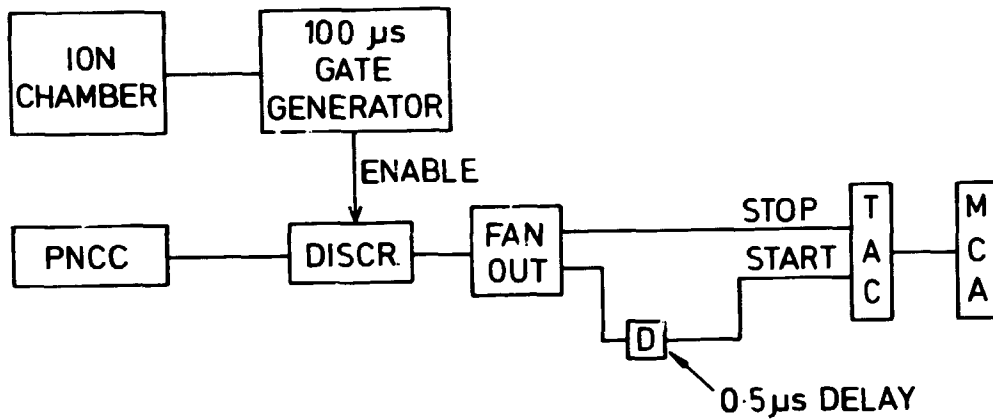
Fig. 1.8. The distribution function for the separation in time t between any two pulses, irrespective of any intervening pulse

little effect on a practical measurement. The shift register algorithm has been tested using the model and found to be valid up to at least 1 Kg of ^{240}Pu . The model will be applied to larger masses of plutonium and to the effects of neutron multiplication when the shift register part of the model has been modified to study register overflow effects.

1.11.3 N.M.A.C.T. portable neutron coincidence counter (PNCC) (E.W. Lees and F.J.G. Rogers (NMACT))

Last year, we reported (PR/NP26, pp.54-58) on the measurement of the physical properties of the PNCC used by NMACT in the passive, non-destructive assay of Pu mass by measurement of the ^{240}Pu content. To complete this work we have analysed our measurements on the time distribution between neutrons as detected by the PNCC from the same fission event.

The measurements were made with a spontaneously fissioning ^{252}Cf source mounted in an ion chamber placed at the centre of the PNCC. The detection of a fission fragment was used to generate a 100 μs 'enable' gate as shown schematically in Fig. 1.9. Any neutron events detected by the PNCC within this 100 μs interval, were fed directly to the STOP input and through a small delay to the START input of a time-to amplitude converter (TAC); clearly the TAC records the time interval, less the small delay, between the first neutron pulse and the next one following a fission event.



TAC \equiv Time - to - amplitude convertor

MCA \equiv Multi - channel analyser

Fig. 1.9. Schematic diagram of the electronic equipment used to measure the time distribution in the PNCC between neutrons from the same fission event.

The results are displayed in Fig. 1.10. The data are well described in the time range 10 to 70 μ s by a single exponential with a time constant $\tau = 38.45 \pm 0.43 \mu$ s where the quoted error is purely statistical. The best fit straight line shown in Fig. 1.10 has a χ^2 per degree of freedom of 1.05. Beyond 70 μ s the data deviate from the exponential behaviour for reasons arising from the method of measurement.

The mean time interval of neutrons from the same fission event can be theoretically calculated if the lifetime (die-away time) of a neutron in the detector is described by a pure exponential function of time(1). It was shown in PR/NP26, p.56 that the die-away time did not follow a single exponential behaviour ($\tau = 39 \mu$ s) until 25 μ s after the fission event. However, it would appear that the interval probabilities between neutrons from the same fission event exhibit better exponential dependence than the die-away curve from which it is derived. This can be demonstrated theoretically (this report, section 1.11.1).

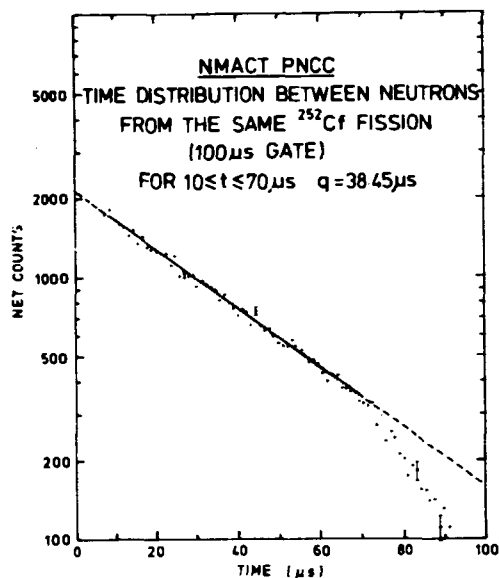


Fig. 1.10. The time distribution between neutrons from the same fission event as measured by the NMACT PNCC.

In conclusion, the experimentally measured value of $q = 38.45 \pm 0.43 \mu\text{s}$ is slightly less than the exponent of the die-away time, which is in good agreement with the predictions of Appendix B in ref. 1. This result, however, disagrees with the value of $\sim 23 \mu\text{s}$ which was empirically deduced by Stanners(2). The discrepancy has been discussed elsewhere in more detail(1) and is due to Stanner's choice of q to produce a straight line calibration of ^{240}Pu mass and NCC response; such a response is physically unrealistic because of the effects of neutron multiplication.

(1) E.W. Lees and B.W. Hooton, AERE-R 9168 (1978).

(2) M. Stanners, private communication (1977) in reference 1.

1.11.4 Calculations of neutron multiplication and its effect on the response of neutron coincidence counters (E.W. Lees, B.W. Hooton and F.J.G. Rogers (NMACT))

Our previous calculations(1) of the effects of neutron multiplication on the

response of neutron coincidence counters (NCC) used in Safeguards were hampered by a lack of detailed knowledge of the geometry and density of the doubly sealed Pu samples. Special samples have since been prepared and Table 1.5 shows the results for a NCC with the analysis procedure of both the variable dead time counter (VDC) method⁽²⁾ and also the Bönnel shift register (SR) method⁽³⁾. The VDC experimental results and the theoretical calculations including the effects of neutron multiplication are in very good agreement up to 500 g PuO₂. Above 500 g PuO₂, experiment and theory diverge rapidly; this is doubtless due to the breakdown of the derivation of Y in VDC analysis (see this report, section 1.11.1).

Table 1.5

Theoretical and experimental results for PuO₂ samples of well defined geometry and density (²⁴⁰Pu ~20% by mass)

PuO ₂ Mass (g)	VDC Analysis		Shift Register Analysis	
	Theory	Experiment	Theory	Experiment
113.0	79	79	46	60
224.9	161	159	93	125
450.0	337	332	195	269
900.0	681	810	394	641

The SR results do not agree with theory at any of the mass values studied which is at first sight surprising since the same detector was used in both measurements. The likely cause of the discrepancy appears when we consider in some detail how the Bönnel version of the SR is applied. Basically, the time correlation of neutrons is measured in two gates or registers whose time separation is greater than the mean lifetime of a neutron in the detector. Thus, one gate measures the real + accidental 'coincidences' and the other measures the accidental 'coincidences'. In the Bönnel form, there are two physically separate gates and, for electronic reasons, the widths of these gates are not identical. Thus, a factor f is introduced to multiply the real + accidental count rate (R + A) so that the effective widths of the two gates are identical. The factor f is determined by solving the equation

$$f \times (R + A) - A = 0$$

which must be true for a random (α, n) neutron source.

However, in practice $R + A$ and A are large numbers with a small difference and so f must be known very accurately. As an example, Table 1.6 shows the effect of various values of f on the experimental results. Furthermore, experimental evidence tends to imply that f is slightly dependent on the count rate, increasing in value with increasing count rate.

Table 1.6

Sensitivity of Experimental Results Obtained with the Shift Register Analysis to the Factor f

PuO ₂ Mass (g)	Counts/300 s		Shift Register Response (s ⁻¹)		
	R + A	A	f = 1.00	f = 1.03	f = 1.055
113.0	76094	62517	45	53	59
224.9	266991	243101	80	106	129
450.0	988344	964182	81	179	262
900.0	4199401	4236787	-125	295	645

Clearly, this is unsatisfactory and a new version of the SR similar to that employed by LASL⁽⁴⁾ is about to be tried by NMACT. In this version, only one gate is present and this is interrogated twice on a prompt and delayed cycle to estimate the accidental coincidences. Further comparisons with theory will await the satisfactory performance of this new SR.

-
- (1) J.W. Lees and B.W. Hooton, AERE-R 9168 (1978).
 - (2) R. Berg et al., EUR 5158e (1974).
 - (3) K. Böhnel, KFK 2203 Karlsruhe (1975).
 - (4) N. Ensslin et al., Nucl. Mat. Management 7 (1978) 43.

1.12A (n, α) cross sections (J.A. Cookson, M.A. Langton* and C. Wise*)
(Relevant to request numbers: 502-9, 576-84, 424-30)

Measurements have been made of the angular distributions of the (n, α) cross sections for natural Fe and Ni at a mean neutron energy of 14.7 MeV, over an angular range of 0° to 134° in the laboratory. The technique used a telescope (see PR/NP25, p.45) consisting of 4 proportional counters filled with hydrogen and a small amount of methane, and a CsI scintillation counter. Difficulty was encountered in obtaining a target of Cr, the third element for which (n, α) measurements are required, but one has now been made on a thick tantalum backing and measurements will be carried out as soon as possible.

The extension of the (n, α) measurements to energies below 14 MeV will require the use of the Tandem accelerator. A number of modifications to the counter telescope are being tried out prior to this, including the possible use of a silicon surface-barrier detector in place of the CsI scintillator. In order to permit the use of the maximum available beam currents a new gas cell with double helium-cooled beam entry windows has been made.

1.13 Verification of tritium activation measurements by ${}^6\text{Li}(n,\alpha\text{t})$ cross section determination (M.T. Swinhoe* and C.A. Uttley)
(Relevant to request numbers: 78-85)

The previous progress report (PR/NP26, p.39) reported ${}^7\text{Li}(n,n'\alpha\text{t})$ cross section measurements which were carried out to fulfill fusion reactor blanket data requirements. These results were 26% lower than the ENDF/B-IV evaluation, and a measurement of the thermal cross section of ${}^6\text{Li}(n,\alpha\text{t})$ was mentioned as a check on the tritium counting system. This measurement, carried out using the cadmium ratio method, has caused considerable difficulty due to a variation in ${}^6\text{Li}/{}^7\text{Li}$ isotopic ratio from pellet to pellet. This has been overcome by dissolving the original LiOH material and drying at 120°C to give homogeneous material. During the course of this measurement a method was developed to measure the ${}^6\text{Li}/{}^7\text{Li}$ ratio of the various samples used, and this will be described elsewhere in this report (section 3.15). Values for the ${}^6\text{Li}(n,\alpha\text{t})$ thermal cross section have been obtained for three different ${}^6\text{Li}/{}^7\text{Li}$ ratios, and these are shown in Table 1.7 together with the standard value. The two highest concentrations of ${}^6\text{Li}$ required corrections for self-shielding effects of 17 and 23%. The effect of

*Physics Department, University of Birmingham

self-shielding on the lowest concentration was negligible. The significant contributions to the error on the measurement are: from tritium counting ($\pm 2.2\%$); the reactor flux ($\pm 2\%$); the ${}^6\text{Li}/{}^7\text{Li}$ ratio for the lowest concentration pellet ($\pm 5\%$); and for the two higher concentrations the correction for self-shielding ($\pm 3\%$). The agreement between the measurements and the standard value of the ${}^6\text{Li}$ cross section gives confidence in the results of the ${}^7\text{Li}(n,n'\alpha)$ cross section which are shown in Table 1.8.

Table 1.7

Results of ${}^6\text{Li}(n,\alpha)$ cross section measurement

${}^6\text{Li}/{}^7\text{Li}$ ratio from Mass Spectrometry	Measured ${}^6\text{Li}$ Cross Section (barns)	Standard ${}^6\text{Li}$ Cross Section (barns)
$(7.5 \pm 0.4) \times 10^{-5}$	924 ± 54	936 ± 4
$(6.02 \pm 0.05) \times 10^{-3}$	936 ± 40	
$(9.40 \pm 0.08) \times 10^{-3}$	946 ± 41	
$(9.40 \pm 0.08) \times 10^{-3}$	994 ± 43	

Table 1.8

Measured Values of the ${}^7\text{Li}(n,n'\alpha)$ Cross Section

Neutron Energy MeV	${}^7\text{Li}(n,n'\alpha)$ Cross Section Millibarns
4.7	68.6 ± 15
5.64	269 ± 27
7.47	318 ± 26
9.72	314 ± 21
9.77	310 ± 19
11.76	289 ± 15
14.1	228 ± 8
14.1	235 ± 8

1.14E Measurements of the $^{60}\text{Ni}(n,p)^{60}\text{Co}$ and $^{62}\text{Ni}(n,\alpha)^{59}\text{Fe}$ cross sections at 14.7 MeV neutron energy (E.W. Lees and B.H. Patrick)

The opportunity to make these measurements occurred during our investigation (PR/NP26, p.69) into the $^{238}\text{U}(\gamma,\alpha)$ and $^{238}\text{U}(n,\alpha n')$ reactions(1) where we used thin Ni foils as monitors in irradiations on the intense ($\sim 5 \times 10^{11}$ n/s) d-T neutron generator at AWRE Aldermaston.

Our measurement of the $^{238}\text{U}(n,\alpha n')$ cross section at 14.7 MeV was determined relative to the standard $^{58}\text{Ni}(n,p)$ and $^{58}\text{Ni}(n,2n)$ cross sections, using the induced gamma-ray activity in the samples as measured with a Ge(Li) detector. It was immediately evident from a study of the gamma-ray spectra, illustrated in Fig. 1.11, that decay lines resulting from neutron interaction with the minor isotopes of Ni in the thin foil were occurring and that these were sufficiently intense to allow determinations of the $^{60}\text{Ni}(n,p)^{60}\text{Co}$ and $^{62}\text{Ni}(n,\alpha)^{59}\text{Fe}$ cross sections relative to the $^{58}\text{Ni}(n,p)$ and $^{58}\text{Ni}(n,2n)$ cross sections. The measured activity was followed over a period of 8 weeks as illustrated in Fig. 1.12. The observed half-lives for the decays were all in agreement with the accepted values.

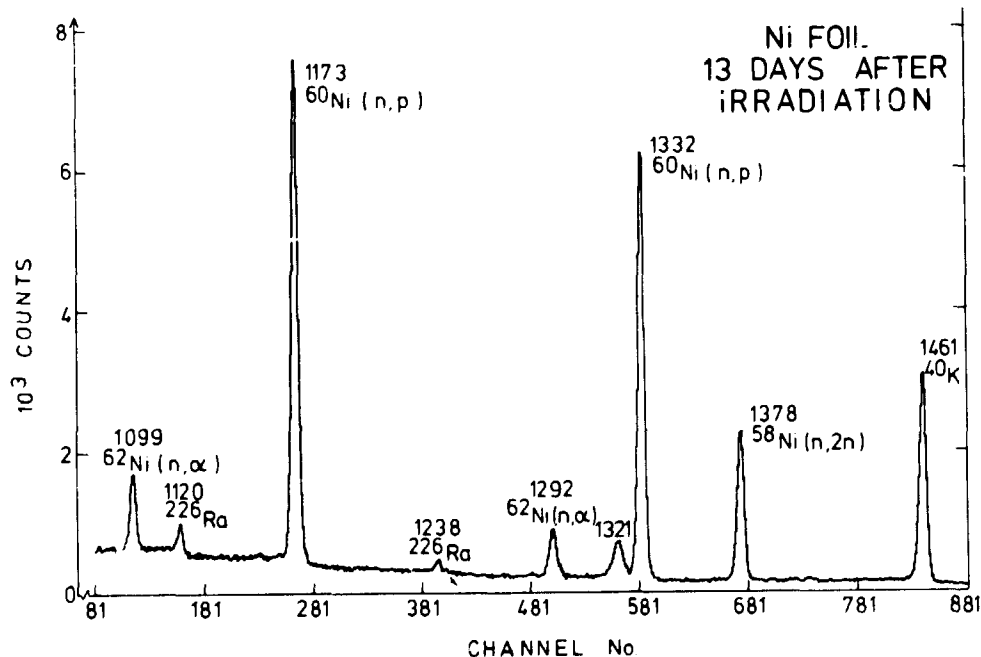


Fig. 1.11. The gamma-ray spectrum between 1.08 and 1.48 MeV from a thin Ni foil 13 days after irradiation in a neutron flux of energy 14.7 ± 0.2 MeV. The energies of the peaks are given in keV. Note that since the half-life of the ^{57}Ni resulting from $^{58}\text{Ni}(n,2n)$ reactions is only 36.16 h, this line has decayed by a factor of ~ 400 since the end of the irradiation.

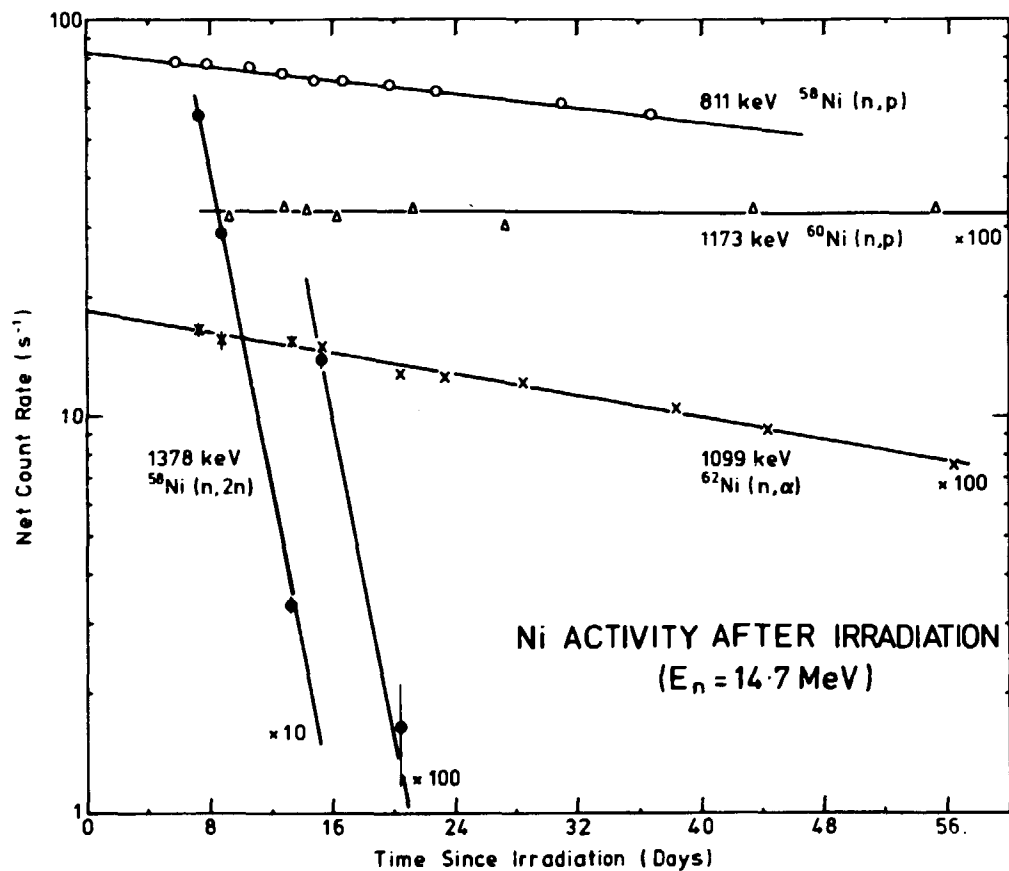


Fig. 1.12. Observed decay activities as a function of time for the thin Ni foils after irradiation in a neutron flux of energy 14.7 ± 0.2 MeV. The scale factors for the 1173, 1099 and 1378 keV lines are to enable them to be plotted on the chosen scale

The ratio of the $^{58}\text{Ni}(n,2n)$ to the $^{58}\text{Ni}(n,p)$ cross section was measured to be 0.1040 ± 0.0034 in excellent agreement with the ENDF/B IV dosimetry file evaluation of $33.9 \text{ mb}/335 \text{ mb} = 0.1012$. Assuming $335 \text{ mb} \pm 10\%$ for the $^{58}\text{Ni}(n,p)$ cross section at 14.7 MeV neutron energy, then the present work implies cross sections of $128 \pm 13 \text{ mb}$ for the $^{60}\text{Ni}(n,p)$ reaction and $20.1 \pm 2.1 \text{ mb}$ for the $^{62}\text{Ni}(n,\alpha)$ reaction.

Tables 1.9 and 1.10 list recent measurements of these cross sections; more experimental information and details of the various references can be found in our report⁽²⁾. The ENDF/B IV evaluation of 116 mb for the $^{60}\text{Ni}(n,p)$ reaction

closely follows the Geel data and is seen to be low with respect to the other measurements. For the $^{62}\text{Ni}(n,\alpha)$ cross section, the present measurement is in agreement with previous measurements and is more precise.

Table 1.9
Recent Measurements of the $^{60}\text{Ni}(n,p)^{60}\text{Co}$ Cross Section in the
Vicinity of 14.7 MeV Neutron Energy

Neutron Energy (MeV)	σ (mb)	Reference
14.7**	114 ± 8	Geel 1965
14.8	130 ± 40	Kazakh 1969
14.7 ± 0.2	$137 \pm 17^*$	Durham 1973
14.6	134 ± 11	Kyushu 1978
14.7 ± 0.2	128 ± 13	Present work

**Interpolated between 14.42 MeV (118 mb) and 14.99 MeV (109 mb)

* Renormalised relative to ENDF/B IV evaluation of 104 mb for the cross section for the $^{56}\text{Fe}(n,p)^{56}\text{Mn}$ reaction

Table 1.10
Measurements of the $^{62}\text{Ni}(n,\alpha)^{59}\text{Fe}$ Cross Section in the
Vicinity of 14.7 MeV neutron Energy

Neutron Energy (MeV)	σ (mb)	Reference
14.8	17 ± 4	Kazakh 1969
14.7	22.8 ± 3.9	Kharkovski 1975
14.6	25.8 ± 3.3	Kyushu 1978
14.7 ± 0.2	20.1 ± 2.1	Present work

(1) E.W. Lees, B.H. Patrick and S. Lindley, J. Phys. G: Nucl. Phys. 5 (1979) 1307.

(2) E.W. Lees, B.H. Patrick and S. Lindley, AERE-R 9390 (1979).

1.15 The response of solid state track recorders to fast neutrons (B.W. Hooton, A.V. Haque* and C.B. Beasant*)

The previously reported response of cellulose nitrate to neutrons (PR/NP26, p.37) has been interpreted in terms of a theoretical response to secondary charged particles. An expression for the theoretical response of solid state track recorders (SSTR) has been derived by considering the number of tracks intersected by the etching plane, Fig. 1.13. These tracks are considerably different from those produced by charged particles incident on the surface and these differences can be summarised as follows.

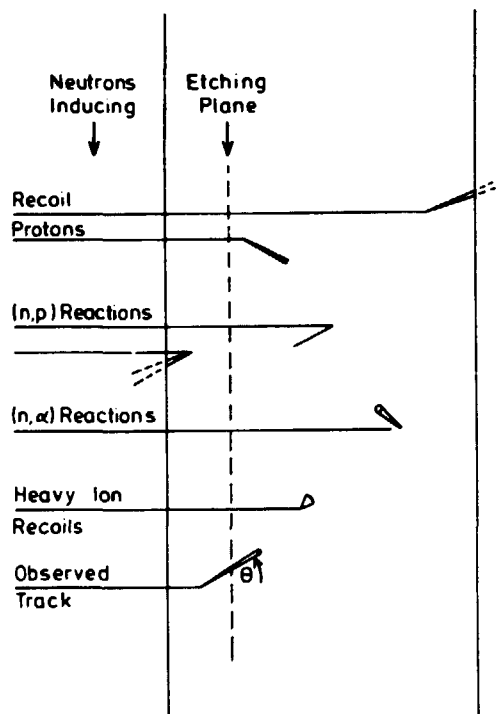


Fig. 1.13. An illustration of the production of secondary charged particles within a material bombarded with neutrons

1. The tracks originate from all points within the volume of the SSTR in a uniformly distributed manner.
2. The tracks appear in all directions but do not have an isotropic distribution.

*Imperial College of Science and Technology

3. Some tracks will be caused by particles leaving the surface of the SSSTR. In this situation the direction of etching is opposite to the direction of increasing ionisation damage.
4. The tracks are caused by different nuclear particles, protons, alpha particles and recoil ions.
5. At any stage of etching the observation plane will intersect tracks at all stages of production, ranging from the beginning of a track to the end of its range.

The theoretical response can be obtained by projecting the observable path length $L_1(\theta, E_0)$ of a particle of type 1 at an angle θ to the direction of an incident neutron beam of energy E_0 . This projection $L_1(\theta, E_0) \cos\theta$ must be integrated over all angles and summed over all particle types to obtain the total response. The basic equation for the number of tracks per unit area per incident neutron

$$T_1 = \int N_1 (d\sigma/d\omega) L_1(\theta, E_0) \cos\theta d\omega$$

can be evaluated if the reaction cross section and observable track lengths are known. The response to thermal neutrons is particularly simple since 0.58 MeV protons from the $^{14}\text{N}(n,p)^{14}\text{C}$ reaction $Q = +0.626$ MeV produce all the tracks. This isotropic distribution of proton tracks of length L leads to a total number of tracks per neutron given by

$$T = \frac{N_1 \sigma_1 L}{2}$$

where N_1 is the number of ^{14}N nuclei per unit volume. At higher neutron energies, where (n,α) reactions and heavy ion recoils produce tracks, the basic equation needs detailed evaluation using the kinematics and angular distributions of the reactions. The results are in good agreement with experiment when corrections are applied to take effects of etching and observational efficiency into account. These corrections consider

- (a) The enlargement of tracks by the etching process.
- (b) The minimum size of track that can reasonably be measured under a microscope and registered as a track.

(c) Effects due to the observers subjective approach to track recognition.

(d) Depth of focus effects.

An explicit expression has been derived for the depth of focus effect but the other effects require empirical corrections to the basic theory. These corrections should have little effect on the shape of the response as a function of neutron energy.

1.16 Studies of parallel plate avalanche detectors (D.B. Syme and A.M. Rolls*)

Measurements of neutron-induced fission cross sections in the more highly alpha active actinides make stringent demands on detector technology. Recently parallel plate avalanche chambers have been used^(1,2). These have favourable pulse height discrimination between fission fragments and alpha particles and intrinsically narrow pulses which enable high rates to be withstood. We have developed such chambers with narrow pulse widths and improved time resolution and a version with an enhanced sensitivity to gamma-rays. It should be possible to develop a detector with a pulse 'width' of the order of 10^{-9} s for applications to the above measurements and to the detailed observation of the microstructure in the 5×10^{-9} s wide pulse from the Harwell linac.

At present a pulse of 1.5×10^{-9} s F.W.H.M. has been obtained from a 2.5 cm diameter detector operating at 700 V over a 0.5 mm gap containing flowing acetone vapour at a pressure of 18 torr. The timing resolution was 0.39×10^{-9} s, measured by passing ^{252}Cf alpha particles through two chambers in series. Such thin walled detectors can be used around external targets for angular distribution measurements.

Using the strong exponential variation of the gain with applied field, the detector can be tuned to observe selectively different particles according to their mode of energy loss. Good separation of ^{252}Cf alpha pulses from noise was obtained and the fission fragments were well separated at much higher pulse height. Data taken at the same gain, showed that the recoil electrons from ^{60}Co gamma rays could be detected. When the field was lowered, first the electron pulses and then the alpha pulses were reduced in height and became assimilated into the noise peak, leaving the more highly ionising fission pulses clearly visible. The fission peak has two components corresponding to the different rates of energy loss from the light and heavy fragments. These data were taken with a ^{252}Cf source mounted outside the chamber which had a 3 mm gap, a 5 μm Al entrance window and was operated at 690 V with 14 torr of acetone

*University of Surrey

vapour.

While the efficiency for detection of charged particles is nearly unity, the best efficiency for detection of gamma rays is understandably low in these thin walled detectors ($\sim 10^{-5}$). It can be made essentially zero by reducing the gain and this is an advantage for fission studies. By making thick-walled chambers the number of gamma interactions in the wall and the number of recoil electrons produced are increased and the optimised gamma sensitivity has been improved to 5×10^{-4} . Thick-walled detectors with sub-millimetre gaps are being constructed in order to obtain narrower pulse widths and optimum gamma sensitivity for the linac application.

-
- (1) J. Christiansen, "Investigation of delayed fission in ^{236}U ", Internal report, Physikalisches Institut der Universitat, Erlangen, Nuremberg (1975).
 - (2) F. Kaeppler, "Counter techniques for highly radioactive samples", Internal report, Institut fur Angewandte Kernphysik, Karlsruhe (1978)

1.17 A fission chamber for the intercomparison of fast neutron flux density measurements (D.B. Gayther)

The design of this chamber, which is to be used in the forthcoming international intercomparison of flux density measurements organised by the Bureau International des Poids et Mesures, was discussed in PR/NP26, p.35. The main components of the multiplate chamber are now ready and have been manufactured under the supervision of Dr. J.W. Leake of the Instrumentation and Applied Physics Division, AERE. Final assembly awaits completion of the set of fission foils which are being prepared in the Chemistry Division, AERE. Four out of the ten ^{235}U foils have been made and satisfactory uniformity of the fissile layer thickness has been verified by several methods including the nuclear microprobe on the IBIS accelerator. A low geometry alpha-counter has been constructed in the Chemistry Division for accurate mass assay of the fissile deposits.

1.18 Neutron Monte Carlo studies (B.W. Hooton and A.R. Talbot)

Many of the systems used for passive or active neutron measurements on plutonium and uranium require detailed design to optimise the neutron spectra. The program MONK⁽¹⁾ has been used for many of these studies and has also been applied to calculate the neutron leakage from the equipment used to determine thick target (α, n) yields. This equipment (PR/NP25, p.47) was simulated by the geometry given in Fig. 1.19 and neutrons from an Am/B source spectrum were tracked through the system and compared to experimental results obtained using a calibrated source. The total leakage from the

polyethylene part of the equipment was computed to be 0.5% in good agreement with other calculations.

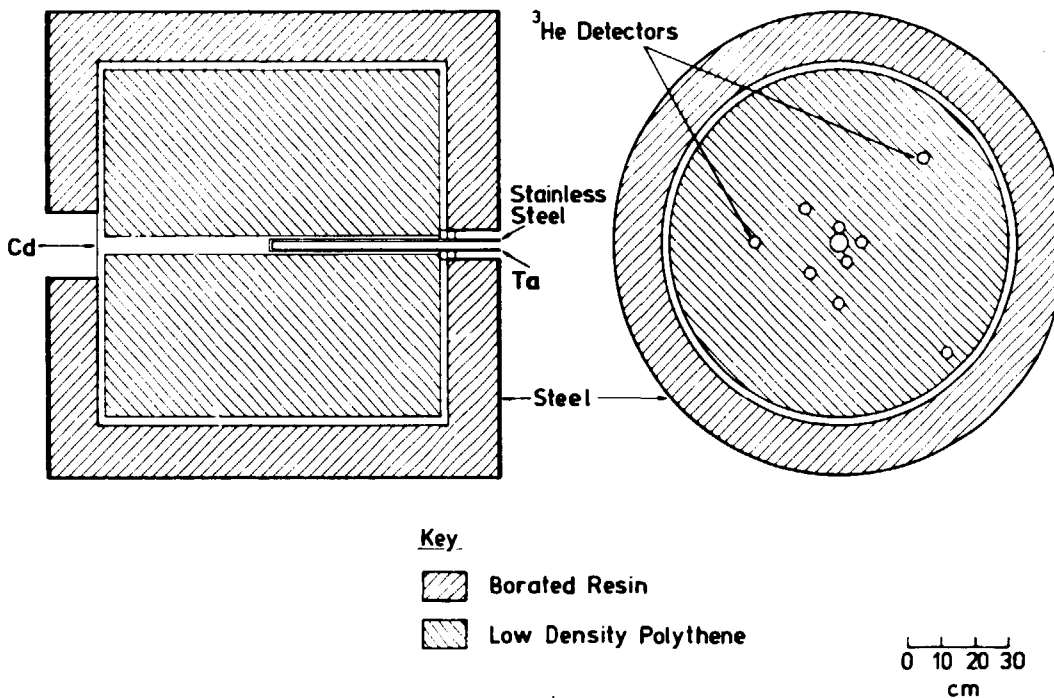


Fig. 1.14. MONK geometry used for the neutron counter

A much more stringent test of the program was obtained by comparing the computed and experimental counts in each of the ^3He detectors at different radii. This comparison is shown in Table 1.11 and confirms the validity of the method.

Table 1.11
A Comparison of Experimental and Monte Carlo Results for
Counts at Various Radial Coordinates

Radius (cm)	4	5.75	7.5	12	14.5	17.5	25	35	45
Experiment	1217	1129	917	441	267	154	36	6.3	1.3
Monte Carlo	1217	1086	921	441	283	180	51	6	2

The radial variation of neutron flux is sensitive to neutron energy and a quantitative calculation of this well known fact was carried out to evaluate the technique as a coarse neutron spectrometer. The results for six ^3He counters contained in a slab of polythene at distances D from the front face are given in Table 1.12 for limited statistics. The results for 2.0 and 2.5 MeV neutrons incident normally on the front face are similar but 14.0 MeV neutrons could readily be distinguished. This technique could be used to recognise (d,d) and (d,t) neutrons generated in a plasma.

Table 1.12

Monte Carlo Results for Neutron Counts in ^3He Detectors at a Distance D from the Front Face of a Polyethylene Block

E_n (MeV)	D(cm)					
	1	5	8	13	18	25
2.0	341	461	384	347	175	81
2.5	269	406	385	320	214	64
14.0	66	92	114	140	116	67

(1) V.S.W. Sherriffs, MONK - A general purpose Monte Carlo neutronics program, SRD R86 (1978).

1.19 The status of the Harwell version of FISPIN (D.A.J. Endacott)

The Harwell version of the FISPIN code, which calculates fission product and actinide arisings and structural material activation following a reactor irradiation has been modified and improved during the year so that it will have the same features as the Risley version, FISPIN 5⁽¹⁾. Further work is required before the versions can perform and output identical calculations.

The updated data libraries for use with the code are provided by UKAEA Risley and trouble was experienced during the year in reading the data tapes prepared on the ICL 2980 computer with the IBM 3033 computer at Harwell.

Test cases run at Risley are now being run at Harwell to enable the updated libraries and computer code to be tested and debugged.

(1) R.F. Burstall, ND-R-328(R) (1979).

1.20B Neutron sensitivity of two neutron capture detectors (G.L. Cleland*, S.J. Hall*
D.B. Gayther, J.E. Jolly)

A series of experiments has been carried out on two 'hydrogen-free' scintillators to determine their sensitivity to neutrons. The scintillators were NE226 (fluorocarbon based) and NE230 (deuterium based) each used in a detector 5 cm thick. The results were used to evaluate the materials' suitability for neutron capture detectors which must have a low sensitivity to scattered neutrons.

The work was done with mono-energetic neutrons from the ${}^7\text{Li}(p,n){}^7\text{Be}$ reaction (using the IBIS 3 MeV Van de Graaff at Harwell) over the energy range 25-220 keV. The tests were done on both free standing and shielded detectors.

The average efficiency of the unshielded NE230 detector was about 10^{-4} . The NE226 was in general a factor of 2 more sensitive although at low energies this increased to a factor of 10, due to a resonance in the neutron capture cross section of fluorine at 30 keV. The use of shielding increased the sensitivity by an order of magnitude.

*Kelvin Laboratory, University of Glasgow.

2. CHEMICAL NUCLEAR DATA

2.1 Report from the Chemical Nuclear Data Committee (J.G. Cuninghame, (AERE), Chairman)

The main committee has met twice during the year, as has the data Files Sub-committee under the chairmanship of Mr. B.S.J. Davies (CEGB, Berkeley). Dr. R. Bett (AERE) has taken over as secretary from Mr. I.C. McKean.

The following pages give detailed reports on individual items of work carried out in the area of chemical nuclear data but three important items may be singled out from amongst the numerous activities of the committee.

(a) The Data Library now contains up to date evaluated data on fission product, activation product, heavy element and actinide decay, and fission yields. It is readily available, and is in use as input data for inventory codes and for general purposes.

(b) The 7th edition of the Chemical Nuclear Data Request List has been prepared in consultation with users of the data and is issued as CNDC(79)P.15.

(c) The further development of the large computer code CASCADE and its associated codes has now been completed by Mr. G. Evangelides (Imperial College) and is in use. It seems probable that these codes will have extensive use as a practical means for obtaining data from evaluated data files such as ENSDF in a digestible form, as well as for the original CASCADE purpose of converting level scheme data into radiation data sets.

2.2 Fission Measurements

2.2.1 ZEBRA-BIZET experiments to study the effects of change of reactor neutron spectrum on fission yields (J.G. Cuninghame and H.H. Willis (AERE))

ZEBRA was closed down for core rearrangement after the last progress report, but is now available again and we are carrying out a series of 4 irradiations in core BZD/1, each irradiation to comprise one capsule containing ^{235}U , ^{238}U and ^{239}Pu samples in the core, and one in the breeder island. During the pause we irradiated ^{239}Pu and ^{235}U samples in well-known neutron spectra in GLEEP and have been able to use the results to correct anomalies in the early ZEBRA results caused by calibration problems.

2.2.2 Mass and kinetic energy distributions of fragments formed in the heavy ion induced fission of ^{208}Po (J.G. Cuninghame and J.A.B. Goodall (AERE); J.E. Freeman, G.W.A. Newton, V.J. Robinson, J.L. Durell, G.S. Foote, I.S. Grant (Manchester University), J.D. Hemingway (Universities Reactor, Risley)

In this work the ^{208}Po compound nucleus has been made by the nuclear reactions ($\alpha + ^{204}\text{Pb}$), ($^{12}\text{C} + ^{196}\text{Pt}$) and ($^{160} + ^{192}\text{Os}$), each reaction being investigated at two

or three different excitation energies. We have studied fission fragments by both on-line coincidence counting and by radiochemical methods for all the reactions. We determined isotopic yield distributions for seven different fission product elements and from them obtained the average number of neutrons associated with each fission event. We determined mass and kinetic energy distributions from the on-line measurements, taking account of the effects of pre- and post-fission neutron emission. The mass distributions are well fitted by the statistical theory, at a temperature corresponding to an excitation about 10 MeV above that at the saddle point. No evidence is found for an increase of kinetic energy with increasing angular momentum of the compound nucleus. In Fig. 2.1 we show the isotopic mass distributions measured for the system

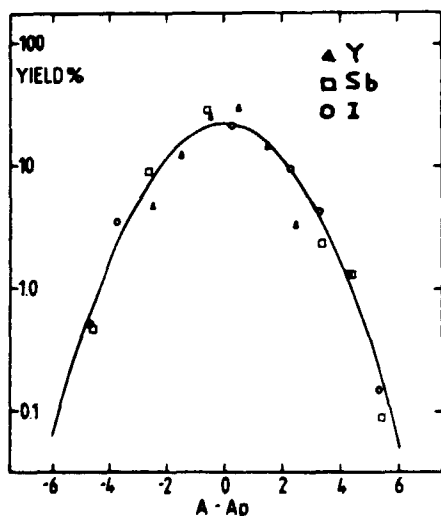


Fig. 2.1 Isotopic mass distributions for the system $^{12}\text{C} + ^{196}\text{Pt}$ at 93 MeV. Experimental points are normalised to 100% for each element.

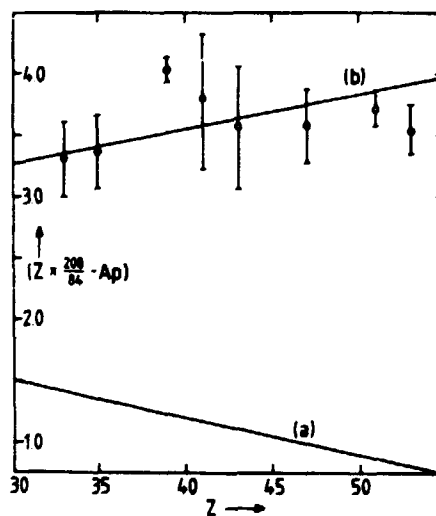


Fig. 2.2 Most probable mass as a function of Z for the system $^{12}\text{C} + ^{196}\text{Pt}$ at 93 MeV. The calculated distribution (a) is for the primary fragments; (b) is for the final fragments assuming $\bar{\nu} \propto A_p$

($^{12}\text{C} + ^{196}\text{Pt}$) at 93 MeV excitation. Experimental points are normalised to 100% for each element. Fig. 2.2 shows the most probable mass as a function of Z for the same system. The calculated distribution (a) is for the primary fragments; (b) is for the final fragments assuming $\bar{\nu}$ (the average number of post-fission neutrons emitted by the fragments) $\propto A_p$ (the most probable fragment mass for an element). Figure 2.3 shows the

measured mass and kinetic energy distributions. This work has been reported in reference (1).

(1) Mass and kinetic energy distributions of fragments formed in the heavy ion induced fission of ^{208}Po : authors as above: Int. Symp. Phys. & Chem. of Fission, Julich 14-18 May 1979: IAEA-SM-241/D2.

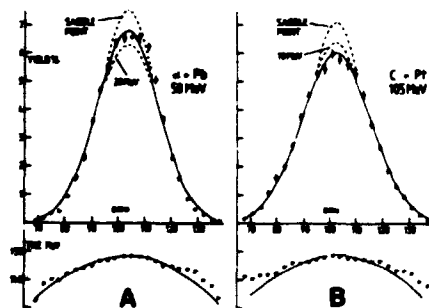


Fig. 2.3 Overall mass and kinetic energy distributions in ^{208}Po fission. The full line assumes an excitation above the saddle point of 10 MeV for the $d + \text{Pb}$ data. 20 MeV for the $\text{C} + \text{Pt}$ data

2.2.3 The competition between fission and neutron emission in Po compound nuclei
(J.G. Cuninghame and J.A.B. Goodall (AERE), J.E. Freeman, G.W.A. Newton,
V.J. Robinson, J.L. Durrell, G.S. Foote, I.S. Grant (Manchester University),
J.D. Hemingway (University Reactor, Risley))

When a compound nucleus such as ^{208}Po is made by high energy reactions, fission and neutron emission compete, with the result that there are always several lighter Po compound nuclei contributing to the fission. Fission from all these nuclei must be taken into account in order to obtain mass and kinetic energy distributions such as those in Section 2.2.2.

We have measured cross-sections for the $2 \rightarrow 0$ ground state band transitions in even-even Po nuclei in the $(\alpha + ^{204}\text{Pb})$ and $(^{12}\text{C} + ^{196}\text{Pt})$ reactions and compared the results with calculations made using the ALICE evaporation code. Fig. 2.4 shows these results for the second reaction.

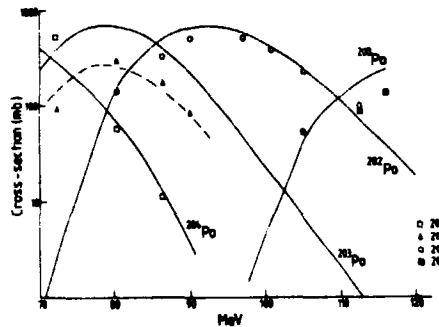


Fig. 2.4 Comparison of measured $^{196}\text{Pt}(^{12}\text{C}, xn)$ cross sections with the predictions of the ALICE code

2.2.4 A study of some of the neutron deficient isotopes of Po (R. Bett, J.G. Cuninghame, H.E. Sims (AERE), I.S. Grant and P. Misaelides (Manchester University))

We are making measurements of the excitation functions for formation of neutron deficient Po isotopes in order to back up the work described in Sections 2.2.2 and 2.2.3. To look at the heavier ones we are using the reaction ($^{12}\text{C} + ^{195}\text{Pt}$) which leads to the compound nucleus ^{207}Po , while for the lighter ones we are using ($^{20}\text{Ne} + ^{182}\text{W}$) leading to ^{202}Po . Measurements, using on-line γ - γ coincidence spectrometry with Ge(Li) detectors are currently underway.

2.2.5 The effect of angular momentum and excitation energy on mass, kinetic energy and prompt neutron distributions of highly fissile nuclei (R. Bett, J.G. Cuninghame and H.E. Sims (AERE), I.S. Grant and P. Misaelides (Manchester University))

We have previously investigated the reactions ($^{209}\text{Bi} + ^{15}\text{N}$) giving the ^{224}Th compound nucleus and ($^{232}\text{Th} + ^1\text{H}$) giving ^{233}Pa ; (the two compound nuclei have almost identical fissility parameters). To complete the experimental work we have now made measurements on the ($^{206}\text{Pb} + ^{18}\text{O}$) reaction, leading to ^{224}Th . The raw data from all these measurements are now being processed.

2.2.6 The competition between fission, spallation and deep inelastic transfer in heavy ion induced reactions (H.E. Sims (AERE), R.J. Smith, G.W.A. Newton and V.J. Robinson (Manchester University))

Yields of various fission and spallation products and also of deep inelastic transfer products are being measured for the reactions $^{165}\text{Ho} + ^{16}\text{O}$ (fission + spallation) and $^{93}\text{Nb} + ^{16}\text{O}$ (deep inelastic transfer + spallation) at a variety

of excitation energies. First indications are that deep inelastic transfer reaction yields are higher than expected from the results of other workers.

2.2.7 The role of angular momentum in nuclear reactions (R. Bett (AERE), E.M. Shaw, G.W.A. Newton and V.J. Robinson (Manchester University))

Experimental excitation functions and isomer ratios have been compared with Blann's Hybrid Model theoretical calculations for the reactions $^{103}\text{Rh}(\alpha, xn)^{107-x}\text{Ag}$, for $x = 1-5$. As shown in Fig. 2.5, excitation functions are in good agreement with the predictions, at least for $x = 1-4$. Values found for the isomer ratios are low and suggest that there is a large fraction of "spin tunnelling" from the high spin state to the low spin state.

2.2.8 Fission-spallation competition in the A = 200 mass region (H.E. Sims (AERE), S.M.A. Hoffman, G.W.A. Newton and V.J. Robinson (Manchester University))

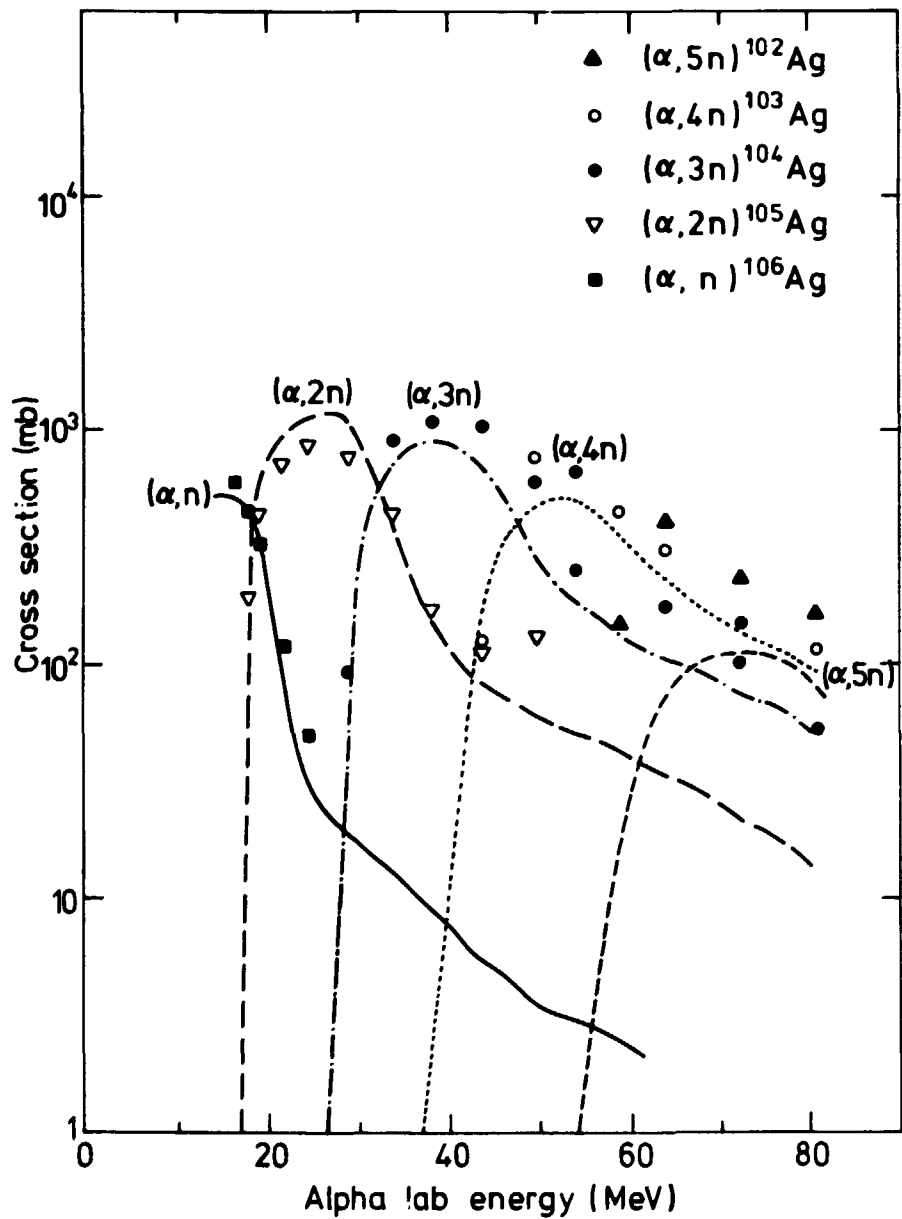
Absolute cross sections for fission and spallation in the compound nucleus ^{197}Tl formed from the reaction $^{181}\text{Ta} + ^{16}\text{O}$ are being measured. The work is complicated by lack of decay scheme data in this mass region and experiments are also in progress to rectify this.

2.2.9 Angular momentum studies in heavy ion induced fission (H.E. Sims (AERE), A. Szymanski, G.W.A. Newton and V.J. Robinson (Manchester University))

Isomer ratios have been measured for the various yttrium and technetium isotopes produced from high energy fission of ^{169}Tm bombarded with ^{20}Ne and ^{16}O . Mass yield curves have also been obtained; Figure 2.6 gives an example of these. The isomer ratio data are being compared with those resulting from spallation in the systems $^{93}\text{Nb}(\alpha, xn)^{97-x}\text{Tc}$ and $^{85}\text{Rb}(\alpha, xn)^{89-x}\text{Y}$.

2.2.10 Tritium yields in thermal and fast fission (I.C. McKeen and E.A.C. Crouch (AERE))

Very little progress has been made because the 'Zebra' reactor at Winfrith has been engaged on an international programme, the irradiation conditions for which were unsuitable for our yield determinations.



EXCITATION FUNCTIONS FOR Rh(α,xn) Ag REACTIONS

Fig. 2.5. Excitation Functions for Rh(α,xn)Ag Reactions

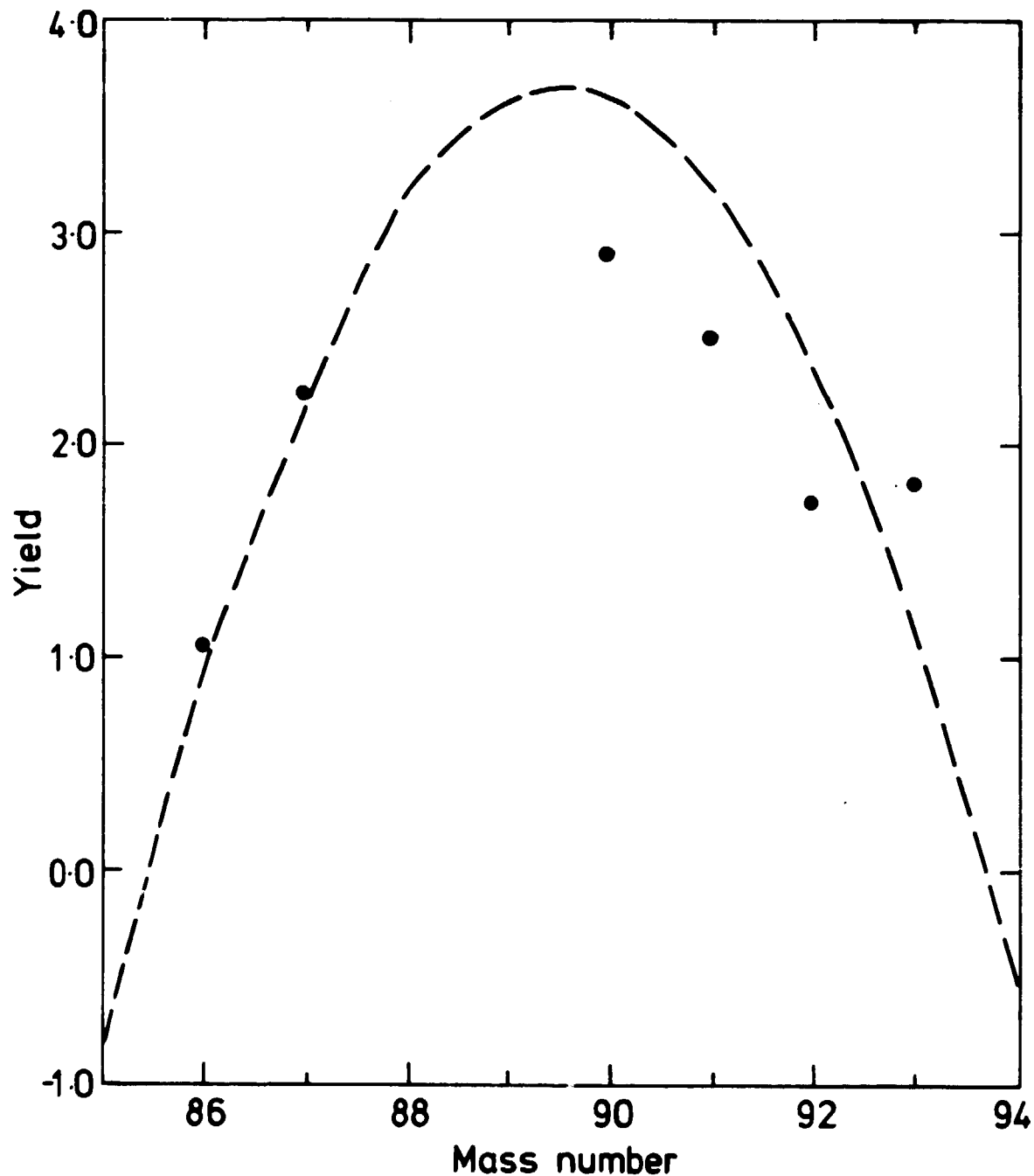


Fig. 2.6. Gaussian fit to mass yield curve for Y isotopes in the reaction $^{169}\text{Tm} + ^{16}\text{O}$ at 181 MeV

2.3 Cross Section Measurements

2.3.1 Integral Experiments to measure the partial capture cross section for the production of ^{242}Cm and ^{244}Cm (Mrs. K.M. Glover and R.A.P. Wiltshire (AERE)) (relevant to request numbers 1604, 1607 and 1672)

The programme of work continues to measure the production rates of the

spontaneously fissioning nuclides ^{242}Cm and ^{244}Cm by capture in ^{241}Am and ^{243}Am in fast reactor spectra using the ZEBRA reactor at Winfrith(1). Table 2.1 shows the results of measurements made in Core 12, 14 and 16.

Table 2.1
Curium - Production Cross Sections

Sample	Core	Fluence ($n\text{ cm}^{-2}$)	Cross Section for Cm Production (barns)		C/E
			Experiment, E	Calculation, C	
^{241}Am	14	2.60×10^{15}	1.28 ± 0.10	1.12	0.88 ± 0.07
	12	2.97×10^{14}	1.48 ± 0.11	1.25	0.84 ± 0.06
^{243}Am	14	2.66×10^{15}	1.32 ± 0.20	1.58	1.20 ± 0.18
	16	2.16×10^{15}	1.99 ± 0.20	1.73	0.87 ± 0.09

The C/E values for ^{241}Am in the two spectra are very similar and are consistent with the errors of 10-15% assigned to the calculated cross sections. Additionally there is a systematic uncertainty associated with the relative yields of the isomeric and ground states of ^{242}Am .

In the case of ^{243}Am the experimental errors are larger, primarily due to the lower product yield, and this is reflected in the C/E values. To resolve the discrepancy of approximately two standard deviations between the two C/E values, further measurements taken to greater fluence are needed.

A further series(2) of irradiations in ZEBRA is planned beginning January/February 1980. Measurements will be made in more than one spectral position, and include measurements of the ^{242m}Am partial capture cross section, if sufficient Am isotopes are available. Isotopically pure ^{241}Am is currently being separated from all the remaining stocks of electromagnetically pure ^{241}Pu . 2 mg ^{241}Am have been irradiated in DIDO for the preparation of fresh ^{242}Cm spike with minimum ^{243}Cm content.

(1) Nuclear data of higher Pu and Am isotopes. NNDC Brookhaven National Laboratory, 20-22nd November, 1978. Mrs. K.M. Glover and R.A.P. Wiltshire (Harwell), D.W. Sweet (Winfrith).

(2) J.E. Sanders, J. Marshall, D.W. Sweet and W.H. Taylor (Winfrith), Mrs. K.M. Glover and R.A.P. Wiltshire (Harwell). Some aspects of fast reactor operation studied in ZEBRA. Int. Symp. on Fast Reactor Physics, Aix-en-Provence, September, 1979.

2.3.2 Measurement of neutron cross sections in PFR (E.A.C. Crouch, I.C. McKean, J.G. Cuninghame and H.H. Willis (AERE), W. Davies, D.J. Lord and V.M. Sinclair (DNPDE), N.R. Daly (AWRE))

Details of this programme, which will check cross section data in neutron spectra similar to CFR, were given in UKNDC(75)P71, page 53. Irradiation of most of the capsules, which contain ^{108}B , ^{235}U , ^{238}U , ^{239}Pu , ^{240}Pu , ^{241}Pu , ^{242}Pu , ^{241}Am and ^{243}Am , is now complete, and they are now held in the Post Irradiation Examination caves. Analyses will be done at DNPDE, AWRE and AERE.

2.4 Half Life Measurements

2.4.1 ^{242}Cm half life (R.A.P. Wiltshire and A.J. Eccles (AERE))

The half life of ^{242}Cm is being redetermined by direct alpha decay. Data are being accumulated from four sources counted at intervals in a low geometry counter, together with alpha spectrometry measurements using a surface barrier detector. The curium stock has been analysed mass spectrometrically. From all the experimental data it is hoped that an accuracy of ± 0.2 per cent will be achieved for the half life of ^{242}Cm .

2.4.2 ^{237}Np Decay Data (Mrs. K.M. Glover, M. King, B. Whittaker and D. Brown (AERE))

Further samples of ^{237}Np have been radiochemically separated from the ^{233}Pa daughter for measurements of the ^{237}Np γ -ray intensities. There was negligible interference from ^{233}Pa in the γ -ray spectra obtained.

To evaluate the ^{237}Np decay scheme, relative alpha intensity data are needed and information on this topic is rather sparse. Accurate measurements of these relative intensities are planned using vacuum evaporated sources and a high resolution surface barrier detector.

Investigations of potential problem areas in the redetermination of the half life of ^{237}Np by specific activity measurements are proceeding. The corrections to be applied to large area sources in low geometry counters are being checked experimentally. The stoichiometric compound $\text{Cs}_2\text{NpO}_2\text{Cl}_4$ will be used in the half life redetermination. The effect of caesium on source thickness, source uniformity and self-absorption is being studied.

A medium geometry counter has been designed and is in course of construction. This will enable sources from relatively low specific activity material e.g. $\text{Cs}_2\text{NpO}_2\text{Cl}_4$, to be counted with high precision, whilst at the same time minimising effects due to self absorption.

2.5 Data File Sub-committee (B.S.J. Davies, A. Tobias (BNL), B. Aldred, V. Barnes (BNFL), Mrs. K.M. Glover, H.E. Sims (AERE), M.F. James, A.L. Nichols (AEEW), D.G. Valiis (AWRE))

The sub-committee is responsible for the development and maintenance of the data files which together constitute the UK Chemical Nuclear Data Library, the current status of which is shown in Table 2.2.

An assessment of the data was recently published by Nichols⁽¹⁾, placing particular emphasis on the Actinide decay data identified as important at the first IAEA Advisory Group Meeting in Karlsruhe, 1975. It includes a list of data compilations and evaluations published since then which are relevant to heavy element decay.

A paper describing proposed improvements to the decay data files, with particular reference to decay heat calculations, was presented⁽²⁾ at the UK Nuclear Data Forum.

Two of the individual files are now discussed in more detail.

(1) A.L. Nichols, Current status of evaluated heavy element decay data for reactor calculations: problems and anomalies. AEEW-R1251 (1979). Presented at IAEA Second Advisory Group Meeting on Transactinium Isotope Nuclear Data, Cadarache, May 1979.

(2) A.L. Nichols, and A. Tobias, UK Nuclear Data Forum, Winfrith, December, 1979.

2.5.1 Fission product decay data

Revised data for about 100 fission product nuclides have been prepared, and merged into the existing recommended data set in the file UKFPDD/1. Testing of the amended file is under way. In addition, measured values of half lives of short-lived nuclides have been substituted for theoretical values for about 75 fission products in the provisional version of the file UKFPDD/2.

Efforts are being made at the Berkeley Nuclear Laboratories of the CEEGB, to reduce the quantity of theoretical data within the Fission Product Data File. Measured decay scheme data for approximately 60 nuclides have recently become available and, when evaluated will replace the corresponding theoretical values currently filed. About 25 of these decay schemes have now been evaluated.

2.5.2 Heavy element and actinide decay data

Data for 95 nuclides, from a target of 119(1) have now been included in the ENDF/B5 format, in the Heavy Element and Actinide Data File, and a further 7 decay schemes have been evaluated. The file will eventually contain data on spontaneous fission decay.

Table 2.2

UK Chemical Nuclear Data Library
Status October, 1979

Data File	Present Status	File Development
1. Fission Product decay data	Exists as UKFPDD/1. Derived from merging Tobias 1973 data with US ENDF/B4.	Data for about 100 nuclides have been replaced by new data to form part of the provisional version of UKFPDD/2. Being reviewed by James (AEEW). Half-lives for 50 nuclides and decay schemes for 50 nuclides being evaluated by Tobias (BNL).
2. Activation Products of Structural Materials, Decay Data	Available in ENDF/B4 format for 91 nuclides.	Maintenance and improvements are planned beginning mid-1980 by Nichols (AEEW).
3. Heavy Element and Actinide Decay Data	Data for 95 nuclides in file in ENDF/B5 format, excluding detailed spontaneous fission data (to follow).	Data evaluated for a further 6 nuclides. 18 nuclides await evaluation.
4. Fission Yields	Available in ENDF/B4 format, based on Crouch's second round of adjustment. Data refers to fission product ground states only.	Further round of adjustment based on extended criteria is complete. The ENDF/B4 format is being fully utilised to accommodate both isomeric and ground state yields.
5. Delayed Neutrons	Tomlinson data are still recommended.	New evaluation by Crouch (AERE) under way.
6. (n,n) cross sections	None in file.	Data being compiled by James (AEEW).

(1) Nichols, A.L., James, M.F., Summary report of the second meeting of the IAEA Co-ordinated Research Programme for Transactinium Isotope Decay Data, Aix-en-Provence, 1979.

2.6 Fission Product yields: assessments and consistent sets
(E.A.C. Crouch (AERE))

A steady flow of fission product yields is being published and they are incorporated into the library prior to assessment and further use.

The consistent sets are now based on adjustments to estimated chain and independent yields using minimisation of χ^2 for the following constraints:

- (a) The sum of the adjusted chain yields is 2.0.
- (b) The sum of the adjusted chain yields multiplied by the mass number is equal to the mass number of the fissile nuclide plus one, minus the mean total neutron emission.
- (c) The sum over all mass-numbers of the product of the adjusted chain yield with the sum of the products of atomic number with the fractional independent yields (adjusted) is equal to the atomic number of the fissile nuclide.
- (d) For each mass number the sum of the adjusted fractional independent yield is equal to 1.0.
- (e) Fission products of given atomic number Z occur in several mass chains A(Z) of the low mass peak of the yield/mass curve. Fission products of the complementary atomic number ($Z_F - Z$) occur in several mass chains of the high mass peak of the yield/mass curve $A'(Z_F - Z)$. Then

$$\sum_{A(Z)} \text{FIY}(A,Z) \cdot Y(A) - \sum_{A'(Z_F - Z)} \text{FIY}(A', (Z_F - Z)) \cdot Y(A') = 0$$

where $\text{FIY}(A,Z)$ is the adjusted fractional independent yield for nuclide A,Z and $Y(A)$ is the adjusted chain yield for mass number A.

At Winfrith the consistent sets are used to calculate the after heat in a shut-down reactor. So far the agreement with experimental results has improved as the constraints are applied. The division of fission products between isomeric states has been applied using the results of calculations of the ratios to be expected, and the set is to be tested at Winfrith.

Delayed neutron emission probabilities have been assessed and should be tested soon.

2.7 Computer Code Development

2.7.1 Development of CASCADE; a computer code to convert evaluated decay scheme data into radiation data sets (J.C. Cuninghame (AERE), G. Evangelides (Imperial College), A.L. Nichols (AEEW) and D.G. Vallis (AWRE))

'CASCADE' is a Fortran IV program which by examining decay routes through intermediate states converts nuclear decay scheme data to radiation emission sequences and intensities. It uses data stored in a format produced by an associated program 'FELIX' from ENSDF format input data, which it can supplement by performing theoretical calculations.

The output is in ENDF/B4 or 5 format as required. It may be catalogued by a further program, 'CASCAT', which can edit, list or sort according to nine pre-programmed, or one user-definable ordering modes. CASCAT can also assemble together the output of several CASCADE runs.

The recent development of CASCADE was carried out by G. Evangelides under an extra-mural research contract with Imperial College. ENSDF data were used to extend and improve the original data base, the techniques were developed, operations improved and use of the program documented and demonstrated. A major constraint has been the inconsistencies in the ENSDF data file, and these are being listed. Over 1300 nuclides have been processed by FELIX to CASCADE input format, and about 350 nuclides have been processed by CASCADE. The Chemical Nuclear Data Committee's Data File Sub-committee is to identify nuclides which should be studied using CASCADE.

Dr. H.E. Sims at AERE Harwell is the custodian of CASCADE.

The following documents relating to CASCADE will be issued shortly:-

- (a) CASCADE - Reference Manual. CNDC(79)P10, AERE-R9611

A Computer Program for the Interpretation Analysis and Evaluation of Nuclear Decay Schemes.

- (b) CASCADE - Computer User's Manual. CNDC(79)P11, AERE-R9612

A Computer Program for the Interpretation Analysis and Evaluation of Nuclear Decay Schemes.

- (c) FELIX - Reference and Computer. CNDC(79)P12, AERE-R9613

User's Manual.

A Computer Program for the Conversion of NSDF/ENSDF Compilations to CASCADE Input Format.

(d) CASCAT - User's Manual.

CNDC(79)P13, AERE-R9614

A Computer Program using SORT/MERGE for ordering, listing and editing CASCADE produced Radiation Catalogues.

2.7.2 Improvements to the GAMANAL γ -ray analysis code (J.A.B. Goodall and H.A. Sims (AERE))

The following additional facilities have now been added to GAMANAL:-

- (a) Spectral data can now be read from floppy disks as well as from Dectape.
- (b) Shape and other counter data can be fed in for all detectors which have been used to obtain the spectra which are stored on tape or disk for processing. These data are then automatically selected for corresponding counters as required, without the need for user intervention.

2.7.3 Improvements to PDP 11 Pulse Height Analyser software J.G. Cuningham, J.A.B. Goodall (AERE); A.G. Hayton, E. Adlington (F. International)

The existing software is being improved so that control and display will be via a graphics terminal which may be remote from the computer. On return to the RT11 monitor, all pulse height analyser data will be preserved for later restoration to the program if required.

A code is being developed for acquiring and storing four parameter data from a variety of sources, and processing under up to sixteen constraints prior to GAMANAL analysis.

A further code enables the PDP 11 to be linked to the central computer for two way data transfer, and control of GAMANAL analysis.

3. REACTOR PHYSICS DIVISION, AEE, WINFRITH

(Division Head: Dr. C.G. Campbell)

3.1 The UK Nuclear Data Library (R.W. Smith and J. Story)

New editions of the general purpose tape ND1 and dosimetry tape ND1-3 have been prepared and will be distributed shortly to AERE, AWRE Risley and the NEA Nuclear Data Bank. ND1 contains files for 80 materials, of which 16 were not included in the last release of this tape in 1973, and improvements have been made to several of the other files. Lately the Pa-233 evaluation has been revised in the resolved resonance range (up to 37 eV); the new file has DFN-59A. Work has been resumed on the re-evaluation of the resonance parameters of the iron isotopes.

The resonance cross section programme SIGAR has been extensively revised and rewritten, to improve its accuracy and capabilities; the new version, labelled SIGAR-7, also gives a clearer and more detailed print-out. A user's guide is in draft form, but needs some revision.

The programme MINIGAL, which calculates thermal average and resonance integral cross-sections from UK data files, has also been revised and has been implemented on the ICL-2980 computer. This called for some re-structuring of the binary mode formats of the UKNDL, which had used file-marks as sub-file markers. These modifications are being extended to other UKNDL editing codes, and should greatly facilitate their implementation on IBM computers as well as the ICL-2900 series.

3.2 Libraries of Fission Product Decay Data and Yields (M.F. James)

The fission product libraries that are currently recommended in the UK for summation and inventory programmes are UKFPDD-1⁽¹⁾ for decay data, and Crouch 2⁽²⁾ for yields, as described in the UK Chemical Nuclear Data File Status Table in last year's Progress Report⁽³⁾; both of these libraries are in ENDF/B4 format. Series of calculations have been made using these libraries with the FISPIN⁽⁴⁾ and FISP⁽⁵⁾ codes, for comparison with measured values of decay heat. Agreement between calculation and experiment is good for ^{235}U ; for ^{239}Pu the experimental situation is less clear as there are significant discrepancies between different measurements of decay heat for this nuclide.

Work is continuing to improve both libraries; and a revised set of yields (Crouch 3) has already been produced by E.A.C. Crouch (Harwell). These have had additional constraints applied, which force the yields of complementary elements to be equal.

Fig. 3.1 compares the total decay heat calculated using these yields with that calculated using Crouch 2 yields, which do not have these particular constraints. For ^{235}U fission, relatively small changes in the yields are necessary to satisfy the constraints, so that the consequent change in decay heat is negligible except at short cooling times. For ^{239}Pu fission, on the other hand, the changes in yields are larger, presumably because there are fewer measured values, and there is a small but significant increase in decay heat.

Revisions to the decay data library are being made mainly at CEGB, Berkeley Nuclear Laboratories; these will lead to inclusion of detailed spectral data for more fission products, although it is worth noting that the existing library UKFPDD-1 already has more spectral information than other comparable libraries of the same vintage. Some decay heat calculations have already been performed with the data from the first stage of this revision; the effects of the new data are again more marked for ^{239}Pu than for ^{235}U fission.

It is anticipated that subject to satisfactory testing the new decay data and yield libraries will be made generally available towards the end of 1980.

-
- (1) A. Tobias. CEGB Report RD/B/N4179 (1977).
 - (2) E.A.C. Crouch. Atomic Data and Nuclear Data Tables 19, 417 (1977).
 - (3) UKNDC(79)P94, p.83.
 - (4) R.F. Burstall, ND-R-328(R) (1979).
 - (5) A. Tobias. CEGB Report RD/B/N4303 (1978).

3.3 Measurement of the $^{93}\text{Nb}(n,n')^{93\text{m}}\text{Nb}$ Excitation Function (W.H. Taylor, K. Randle, M.F. Murphy)

A measurement has been made to test the feasibility of measuring the above function using the DYNAMITRON machine at the Birmingham Radiation Centre. A pack of thin Nb, Ni and Fe foils were irradiated in a beam of 4.4 ± 0.4 MeV neutrons for twenty hours and the absolute levels of induced activities determined using X and γ -ray spectroscopy. The beam intensity was measured (using the $^{58}\text{Ni}(n,p)$ and $^{54}\text{Fe}(n,p)$ reactions) to be $4.75 \times 10^7 \pm 4\%$ n.cm⁻²s⁻¹ and the value obtained for the $^{93}\text{Nb}(n,n')^{93\text{m}}\text{Nb}$ cross section at 4.4 ± 0.4 MeV was $(0.155 \pm 0.045)\text{b}$. For useful measurements this $\pm 29\%$ uncertainty must be reduced to less than $\pm 5\%$. This could be achieved by increasing the beam intensity by a factor of five and the efficiency of the X-ray spectrometer by a factor of ten.

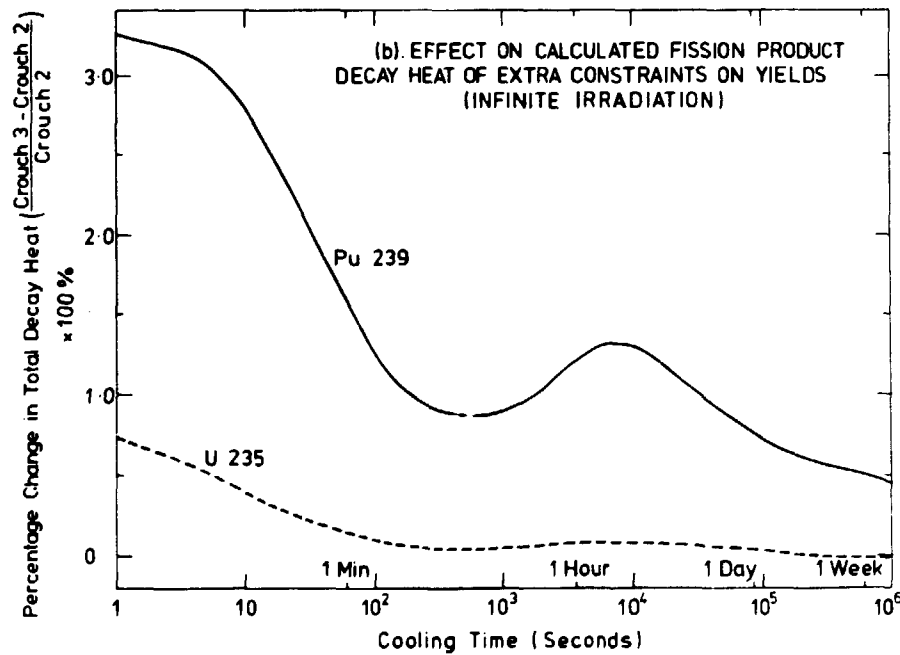
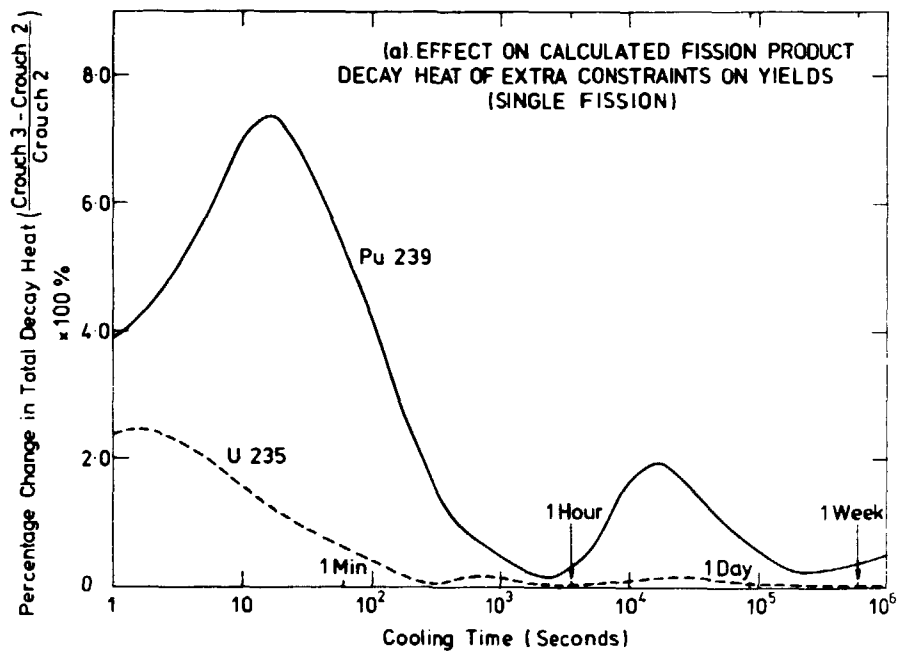


Fig. 3.1. Effects on the calculated fission product decay heat as a function of time resulting from using fission yields with additional constraints. The case for a single fission is shown in (a) and that for an infinite irradiation in (b).

4. CEGB RESEARCH DIVISION, BERKELEY NUCLEAR LABORATORIES

(Section Head: Dr. L.K. Burton)

4.1 ^{235}U Fission Product Gamma Spectra: A Comparison Between Experiment and Calculation (A. Tobias)

A report⁽¹⁾ with the following abstract has been issued:

Recent measurements of ^{235}U fission product gamma spectra (ORNL), after reduction to a broad group structure, were compared with results of corresponding summation calculations which were made with the UKFPDD-1 fission product data base. In order to facilitate convenient integration of the summation results, weighted sum of decaying exponentials were accurately fitted to them using an iterative least-squares method.

The comparisons between experiment and calculation reveal significant deficiencies in data for short-lived nuclides which prevent the accurate calculation of short-term ($\leq 100\text{s}$) gamma spectra by means of summation calculations. Simple rescaling of these summation results is found to be unsatisfactory. Discrepancies between experiment and calculation for gamma energies $> 5\text{ MeV}$ are also examined briefly and possible causes for them are discussed.

(1) A. Tobias. CEGB Report RD/B/N4667 (1979).

4.2 Decay Heat (A. Tobias)

A report⁽¹⁾ with the following abstract has been issued:

Many aspects of the nuclear fuel cycle require accurate and detailed knowledge of the energy release rate from the decay of radioactive nuclides produced in an operating reactor. In addition to the safety assessment of nuclear power plant, decay heat estimates are needed for the evaluation of shielding requirements on fuel discharge and transport routes and for the safe management of radioactive waste products extracted from spent fuel during reprocessing. The decay heat estimates may be derived by either summation calculations or Standard equations.

This paper reviews the development of these evaluation methods and traces their evolution since the first studies of the 1940's. In contrast to many of the previous reviews of this subject, both actinide and fission product evaluation methods are reviewed in parallel. Data requirements for summation calculations are examined and a

summary given of available codes and their data libraries. The capabilities of present day summation methods are illustrated through comparisons with available experimental results. Uncertainties in summation results are examined in terms of those in the basic nuclear data, irradiation details and method of calculation. The evolution of decay heat Standards is described and a brief examination made of their reliability and ability to provide suitably conservative decay heat estimates. Finally, to illustrate the use of present summation methods, comparisons are given of both the actinide and fission product decay heat levels from typical fuel samples in a variety of reactor systems.

(1) A. Tobias. CEBG Report RD/B/N4611 (1979) and Progress of Nuclear Energy (in press).

5. PHYSICS DEPARTMENT, NATIONAL RADIOLOGICAL PROTECTION BOARD

(Head of Department: J.A. Reissland)

5.1 Neutron Facility (C.L. Harvey, E.A. Pook)

The Board's accelerator is a SAMES TB8 and has been described previously in UKNDC(78)P88, p.109. Deuteron beam currents of 5 mA and 2 mA have been obtained in the 0° and 30° beam lines respectively. A tritium target in the 0° arm has yielded 7×10^{11} neutron per second. A yield of 10^{12} neutron per second is expected from a new target.

5.2 Neutron Detection (A.G. Sherwin, J.C.H. Miles and J.B. O'Hagan)

Various detector systems have been developed for the measurement and characterisation of the mixed neutron and gamma-ray fields produced by the SAMES accelerator and other neutron sources.

A fast neutron spectrometer system for measurements in the range 10 keV to 20 MeV consists of an organic liquid scintillator (NE213) and a set of four hydrogen filled spherical proportional counters, each detector covering a particular part of the energy range. A computer program(1) allows the neutron spectrum to be unfolded from the measured data by the same mini-computer that is used for the data acquisition. The dependence of the scintillator light output on particle energy has been studied and an accurate analytical function derived(2).

Ionisation chambers have been designed and constructed for the accurate determination of absorbed dose. Mixed field dosimetry, i.e. the separation of neutron and gamma-ray dose components can be achieved either by conventional subtraction methods or by a method based on the statistical analysis of the fluctuating ionisation current induced by the mixed field in a single ionisation chamber(3,4,5). This technique is particularly useful when the neutron dose component is a small fraction of the total dose.

Fission foils have been utilised as secondary standards in the measurement of fast neutron fluence(6,7). The foil of fissile material is placed in contact with polycarbonate film and the fission fragment tracks in the plastic are revealed by chemical etching.

(1) A.G. Sherwin, and J.B. O'Hagan, in NRPB/R & D 2, (1978) 202.

(2) A.G. Sherwin, and J.B. O'Hagan, in NRPB/R & D 3, (1979) 234.

- (3) A.G. Sherwin, in Proc. 2nd Symp. on Neutron Dosimetry in Biology and Medicine, Munich (EUR 5273), (1974).
- (4) A.G. Sherwin, in Monograph on Basic Physical Data for use in Neutron Dosimetry, (EUR 5629), (1976).
- (5) A.G. Sherwin, in Proc. 3rd Symp. on Neutron Dosimetry in Biology and Medicine, Munich, (1977).
- (6) J.C.H. Miles and A.G. Sherwin, in Monograph on Basic Physical Data for use in Neutron Dosimetry (EUR 5629), (1976).
- (7) J.C.H. Miles and A.G. Sherwin, Nuclear Instruments and Methods, 146, (1977), 503.

5.3 Iron Shielding Benchmark Experiment (Experimental: A.G. Sherwin, J.B. O'Hagan, J.C.H. Miles, C.L. Harvey. Theoretical: D.G. Jones)

The iron shielding benchmark experiment (UKNDC(78)P88, p.110) has now been completed. The beam of 14.6 MeV neutrons from the SAMES accelerator was attenuated by a two metre cube of iron and the responses of various activation and fission foils(1) were determined at various depths within the iron. These were compared with those predicted by neutron transport calculations (UKNDC(78)P88, p.110).

An investigation of possible sources of error in calculated flux values has shown that the fluxes in the first (source) energy group estimated using the Monte Carlo code, MORSE, were found to be in good agreement with the DOT values for thicknesses of iron up to 60 cm. Calculations with the 1-D discrete ordinates code, ANISN, showed that the most important factor influencing the results was the choice of cross section data set. There were appreciable differences between the spectra obtained using the EURLIB1 (1975) data set and those obtained using the EURLIB4 (1978) data set(2). A report of some of this work has appeared(1) and a more complete report will be available in the near future as will the full report on the shielding experiment.

-
- (1) J.C.H. Miles, 1: NRPB R & D 3, (1979) 232.
 - (2) E. Caglioti, EURLIB4: 120-group coupled neutron and gamma data library, ESIS, (1978).

5.4 Neutron Cross Section and Kerma Calculations (P.J. Dimbylow)

High energy neutron radiotherapy requires the extension of neutron cross section data from 20 MeV up to and possibly above 50 MeV for the main constituents of tissue. The calculation of total, elastic and reaction cross sections for C, N and O(1) using the computer programs NOPTIC (Nuclear OPTICAl Model) and SMOLDERS(2) (Statistical

Model Of Level Densities for the Evaluation of Reaction cross Sections) has been completed.

A new version of the program SMOLDERS has been developed to convert centre-of-mass exit channel energies produced by the evaporation model into particle and recoil nucleus spectra in the laboratory system from which kerma values can be obtained. Multiple particle cascade chains are treated as sequential two-body break-up reactions. In all processes the angular distribution of the emitted particles is assumed to be isotropic in the centre-of-mass system. The most important contributions to kerma in C, N and O are from the 3α reactions in C, (n,α) and (n,np) reactions in N and the (n,np) and 4α break-up reactions in O.

Work is in progress to investigate the effects of including discrete energy levels and precompound emission in the statistical model description of reaction mechanisms. The computer program, GNASH which was written for a CDC computer by Young and Arthur(3) has been converted to run on the IBM 3033 machine at Harwell. This program is a multistep Hauser-Feshbach code that includes precompound emission.

The evaluation of neutron cross section data is being extended to Al, Mg, P, S, Ar and Ca. Work is in progress on the optical model fitting of available total and elastic cross section data for these elements.

This project is part-funded by CEC contract 164-76 BIO UK.

-
- (1) P.J. Dimbylow, "A calculation of neutron cross sections for the elements H, C, N and O in the energy range 20-50 MeV", NRPB R-78, (1978).
 - (2) P.J. Dimbylow, "The high energy neutron cross section programs, NOPTIC and SMOLDERS", NRPB M-44, (1978).
 - (3) P.G. Young and E.D. Arthur, "GNASH: A pre-equilibrium statistical nuclear model model code for calculation of cross sections and emission spectra", LA-6947, (1977).

6. DIVISION OF RADIATION SCIENCE AND ACOUSTICS. NATIONAL PHYSICAL LABORATORY

(Superintendent: Dr. W.A. Jennings)

Various methods of measuring neutron fluence rate are being developed, intercompared and employed with a view to improving the accuracy of existing standards. The search for improved accuracy in the standardisation of radioactivity requires the development of new techniques and the determination of selected decay scheme data.

6.1 Neutron Source Calibrations (E.J. Axton, A.G. Bardell, S.J. Felgate)

Following the discovery last year of small traces of neutron absorbing impurities in the manganese bath the solution has been replaced by higher grade material and new measurements have commenced of the standard Ra-Be (γ, n) neutron source and of the hydrogen to manganese cross section ratio. Recently some doubt⁽¹⁾ has been cast on the validity of the value of 0.52 barns for the thermal neutron capture cross section of sulphur, which is relevant to this work. Methods of resolving this problem are under consideration.

(1) J.R. Smith. "The ^{252}Cf discrepancy and the Sulphur discrepancy". Proceedings of the International Conference on Nuclear Cross sections for Technology, University of Tennessee, Knoxville, Tennessee. 22-26 October 1979.

6.2 International Comparison of Neutron Source Emission Rate

This comparison, organised by the International Bureau of Weights and Measures (BIPM), is in progress. So far three laboratories have completed their measurements, but at the time of writing no further laboratories are yet ready to participate. The intercomparison is expected to terminate early in 1981.

6.3 Neutrons in the 1-1000 eV Energy Range (E.J. Axton and A.G. Bardell)

As reported last year (UKNDC(79)P94, p.90) no further progress has been made in the provision of a low energy neutron source based on the Van de Graaff accelerator, as the machine has not been available for this work. It is unlikely that this project will progress in the foreseeable future. Nevertheless, the measurements at a typical power station site reported last year⁽¹⁾ demonstrated a clear need for such a source. It was demonstrated that the multi-sphere technique which was used is capable of determining neutron dose-equivalent rates from neutrons in this low energy range.

(1) E.J. Axton and A.G. Bardell. "Neutron standards available at the National Physical Laboratory and the need for low energy standards". Proceedings of the advisory group meeting on Data for Reactor Dosimetry". IAEA, Vienna. 13-17 November 1978.

6.4 Intermediate Energy Neutrons (J.B. Hunt)

Due to the installation of the pulsed terminal with the Van de Graaff, no measurements have been made during the year in this energy region.

6.5 The Cross Section for the $^{56}\text{Fe}(n,p)$ Reaction for 14.73 MeV Neutrons (T.B. Ryves and E.J. Axton)

A value of (109.2 ± 1.0) mb for the cross section for the $^{56}\text{Fe}(n,p)^{56}\text{Mn}$ reaction for 14.73 MeV neutrons has been derived from a critical evaluation of measurements performed as part of an international comparison of fast neutron flux density organised by the BIPM between 1974 and 1978. This work is to be published in the proceedings of the International Conference on Nuclear Cross Sections for Technology, University of Tennessee, Knoxville, 22-26 October, 1979.

6.6 Neutron Cross Sections at 14.68 MeV (T.B. Ryves and P. Kolkowski)

Some activation cross sections for 14.68 MeV neutrons have been measured with a calibrated Ge(Li) detector. Provisional results are given in Table 6.1, relative to the $^{56}\text{Fe}(n,p)^{56}\text{Mn}$ cross-section of (109.9 ± 1.0) mb.

Table 6.1
Neutron Cross Sections at 14.68 MeV

Reaction	$T_{1/2}$	Cross Section mb	% Uncertainty 1σ	Notes
$^{93}\text{Nb}(n,2n)^{92\text{m}}\text{Nb}$	10.1 d	475	3	
$^{93}\text{Nb}(n,\alpha)^{90\text{m}}\text{Y}$	3.1 h	5.53	3	
$^{181}\text{Ta}(n,2n)^{180\text{m}}\text{Ta}$	8.1 h	1310	3	a
$^{197}\text{Au}(n,2n)^{196\text{g}}\text{Au}$	6.1 d	2025	3	b
$^{197}\text{Au}(n,2n)^{196\text{m}}\text{Au}$	9.7 h	139	5	b
$^{238}\text{U}(n,2n)^{237}\text{U}$	6.7 d	778	3	c

- a. The 93 keV γ -ray was counted, assuming a branching ratio of 0.243 ± 0.006 .
- b. The ratio of the cross sections was 14.6 ± 0.6 at 14.3 MeV, deduced from the shape of the $^{196\text{g}}\text{Au}$ decay following irradiation and hence independent of the detector efficiency.
- c. The 208 keV γ -ray was counted. Corrections were needed for interfering γ -rays from fission products and natural radioactivity.

In addition the $^{197}\text{Au}(n,\gamma)^{198}\text{Au}$ activation cross section at 14.3 MeV is being measured employing a Ti-T target on a thin aluminium backing, using a similar method to that of Peto et al(1). A provisional result of 1.5 mb (which includes 20% due to neutron scatter) has been obtained, in fair agreement with the value of 1 mb found by Drake et al(2) from measurements of capture γ -rays.

(1) G. Peto, J. Csikai, V. Long, S. Mukherjee, J. Banhalmi and Z. Miligy, Acta Phys. Slav. 25, (1975) 185.

(2) D. Drake, I. Bergqvist and D.K. McDaniels. Phys. Lett. 36B, (1971) 557.

6.7 The Decay Scheme of ^{180}Ta (T.B. Ryves)

The β^- and electron capture branching ratios in the decay of ^{180}Ta and the K internal conversion coefficient of the 93 keV γ -ray were deduced from coincidence measurements between β^- , γ and K X-rays and a measurement of the relative γ -ray intensities. The 1σ uncertainties in the branching ratios were estimated by a Monte Carlo technique. The half life was also measured, as $(8.152 \pm 0.006)\text{h}$. With reference to Fig. 6.1, the branching ratios were $a = (3.5 \pm 0.1)\%$, $b = (14.7 \pm 0.9)\%$, $c = (24.3 \pm 0.6)\%$ and $d = (57.6 \pm 1.0)\%$. The K internal conversion coefficient of the 93 keV γ -ray was (1.07 ± 0.03) , in good agreement with theory.

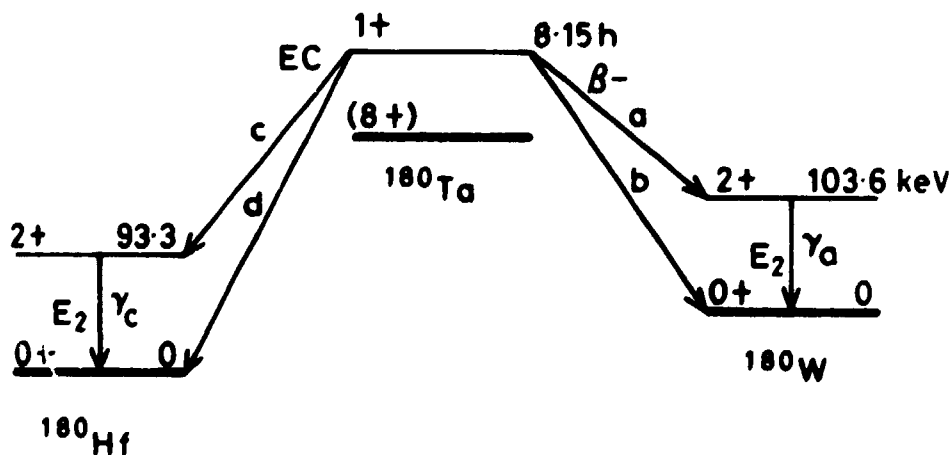


Fig. 6.1. The ^{180}Ta decay scheme

6.8 International Comparison of Neutron Fluence Rate (E.J. Axton)

At a meeting held in April 1979 at BIPM the following neutron energies and transfer methods were agreed for the forthcoming neutron fluence intercomparison.

Neutron Energy (MeV)	Transfer Methods		
	Fission Chamber	$^{115}\text{In}(n,\gamma)^{116}\text{In}$ Reaction	$^{115}\text{In}(n,n')^{115\text{m}}\text{In}$
0.144	X	X	
0.565	X	X	
2.5	X		X
5.0	X		X
14.8	X		X
Coordinator	AERE/NPL	NPL	BCMN

The coordinators have the responsibility to provide the hardware and a code of practice for using it, and also to plan the itinerary. It was felt that the coordinators would require about 1 year for preparation, so the intercomparison is scheduled to commence in April 1980 and last about two years.

6.9. Photoneutron Production in High Energy Electron and X-ray Beams Used for Radiotherapy (E.J. Axton, A.G. Bardell)

Measurements of the photoneutron contamination of the SL75/20 linear accelerator (made by the MEL Equipment Co. Ltd.) at Addenbrookes Hospital, Cambridge, by means of the multi-sphere technique described earlier have been completed and presented at an international conference on this subject held at the National Bureau of Standards in Washington in March 1979⁽¹⁾. The data were well fitted by a neutron spectrum comprising a primary Maxwellian emission spectrum, a slowing down spectrum and a thermal Maxwellian. Good agreement was obtained with earlier measurements⁽²⁾ on a prototype linear accelerator at 16 MV.

(1) E.J. Axton and A.G. Bardell. "Neutron production from Electron Accelerators used for Medical Purposes". Proceedings on Conference on Neutrons from Electron Medical Accelerators. National Bureau of Standards, Washington 8-10 April 1979. To be published.

(2) E.J. Axton and A.G. Bardell. "Phys. Med. Biol." 17 (1972) 293.

6.10 Fast Neutron Energies (V.E. Lewis and K.J. Zieba)

The variation of the activation cross sections for the (n,2n) reactions on ^{93}Nb and ^{90}Zr has been investigated for neutron energies between 13.5 and 14.7 MeV. The ^{93}Nb cross section is constant to within about $\pm 1\%$, whilst that for ^{90}Zr varies by a factor of about 1.8, i.e. approximately by 1% per 25 keV. Thus, the determination of the ratio of the induced activities of simultaneously irradiated samples of niobium and zirconium yields a sensitive measurement of neutron energy. This ratio was measured over the above range with a statistical standard deviation better than 1%. The neutron energies were determined using a silicon detector and observing the energies of alpha particles produced by the $^{28}\text{Si}(n,\alpha)^{25}\text{Mg}$ reaction. The estimated uncertainty was ± 20 keV at approximately 99% confidence level.

6.11 Reference Standard for Fast Neutron Absorbed Dose (V.E. Lewis, D.J. Young, D.J. Thomas, I.W. Goodier and J.L. Makepeace)

Progress on improvements to the Dosimetry accelerator has been slow due to staff shortages, but it is hoped to install the duoplasmatron ion source by mid-1980. Investigation of the sensitivities of various dosimeters, and the calibration of neutron fields has continued. A proton recoil telescope has been used for the measurement of the hydrogen KERMA in a d + T neutron field produced in a low scatter environment. The KERMA in tissue subsequently derived agrees with that measured using a tissue-equivalent ionisation chamber and utilising the appropriate, currently accepted ancillary physical data. The fluence derived from the telescope measurement agrees well with that determined by measuring the associated alpha-particle fluence.

Thermally stimulated exo-electron emission (TSEE) continues to show promise as a method for measuring the neutron and gamma-ray components of a mixed radiation field.

6.12 Nuclear Decay Scheme Measurements (P. Christmas, D. Smith, M.J. Woods, R.A. Mercer, L.E.H. Stuart, P. Cross and D.H. Makepeace)

The relative intensities of γ -rays from pure E2 transitions in the decay of $^{180\text{m}}\text{Hf}$ have been determined from conversion electron intensities measured with the iron-free, double-focussing beta-ray spectrometer together with calculated K- and L-shell conversion coefficients; see Table 6.2.

Table 6.2

Transition Energy (keV)	Gamma-ray Relative Intensity and Random Uncertainty (1σ)
93.3	21.94 ± 0.11
215.3	100
332.3	117.5 ± 0.8
443.2	100.7 ± 0.7

6.13 W-Value Measurements (D.J. Thomas and M. Burke)

Work on this long-term project will continue during 1980 both at Birmingham, where a new research fellow has been appointed, and at NPL.

7. UNIVERSITY OF EDINBURGH, DEPARTMENT OF PHYSICS

7.1 ^6He Emission Accompanying the Spontaneous Fission of ^{252}Cf (D.E. Cumpstey and D.G. Vass)

Last year we reported (UKNDC(79)P94, p.109) that we had carried out a multi-parameter study of the light particle emission in the fission of ^{252}Cf . The experimental details and a discussion of the measurements for the ^3H and ^4He emissions have now been published⁽¹⁾. Rare events corresponding to ^6He emission have also been identified in the data which were collected over ~30 days of continuous measurement. The ^6He events are well resolved from the others; ^5He , although emitted in fission, disintegrates before it can be detected.

In our experiment the energy threshold for the detection of He particles increased with mass number, and was rather high at 14.4 MeV for the ^6He particles. Nevertheless assuming that the ^6He energy distribution is Gaussian in form (as is the case to very good approximations for the ^3H and ^4He distributions), the total yield of ^6He was found by fitting a Gaussian curve to the measured high energy portion and taking the whole area under the curve as a measure of total yield. This gives the total yield of ^6He as $(2.0 \pm 0.7)\%$ relative to that of ^4He taken as 100%, which is in good agreement with previous measurements⁽²⁾.

The angular distribution of the ^6He particles with energies above 14.4 MeV relative to the light fragment direction is shown in Fig. 7.1. Corrections have been made for the effects of the recoil momenta imparted to the fragments by the ^6He particles. There is no sign of any polar emission.

(1) D.E. Cumpstey and D.G. Vass. A multiparameter investigation of the ^3H and ^4He emission in the fission of ^{252}Cf . Physics and Chemistry of Fission (Jülich, 1979), IAEA Vienna, and to be published in Nuclear Instruments and Methods.

(2) G.M. Raisbeck and T.D. Thomas, Phys. Rev. 172 (1968) 1272.
S.L. Whetstone and T.D. Thomas, Phys. Rev. 154 (1967) 1174.
S.W. Cooper, J. Cerni and R.C. Gatti, Phys. Rev. 154 (1967) 1193.

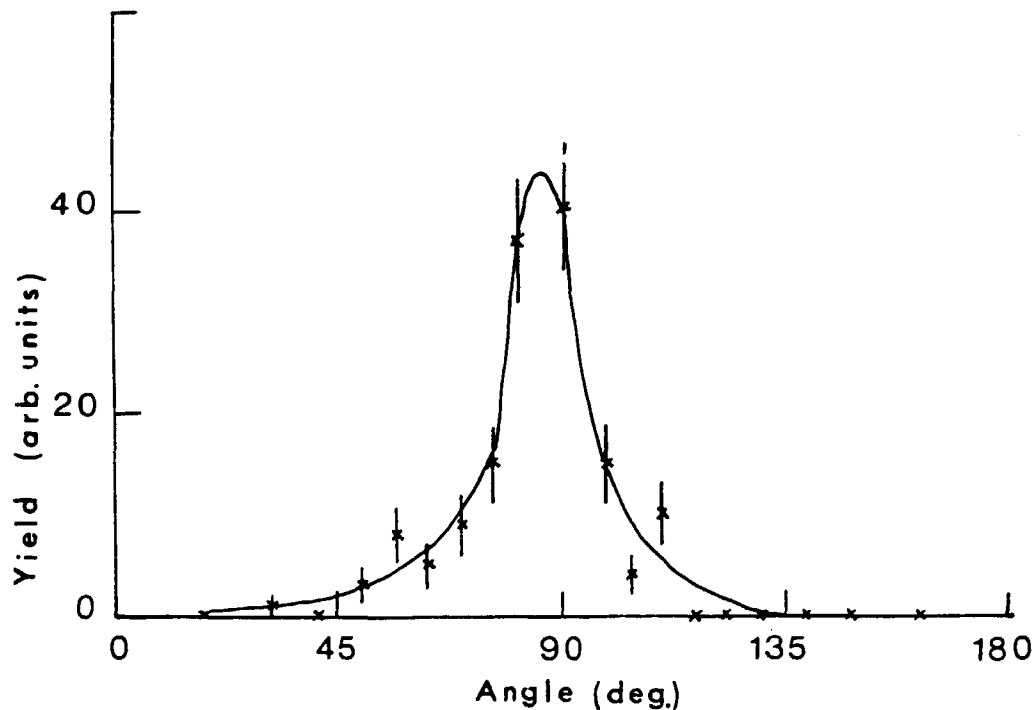


Fig. 7.1. Angular distribution of ${}^6\text{He}$ particles emitted in fission of ${}^{252}\text{Cf}$

7.2 Light Emission Accompanying Fission (G. Giacos and D.G. Vass)

A photomultiplier viewing a ${}^{252}\text{Cf}$ source mounted in vacuum is observed to respond to radiations emitted from the source. We have recorded for identical periods the pulse height spectra of the pulses from the photomultiplier with either (a) a 0.5 mm thick sheet of aluminium, (b) a 12.5 μm thick film of transparent mylar or (c) a similar but opaque film of mylar, placed in turn between the source and photomultiplier. The mylar film was made opaque simply by colouring it black using a "felt" pen.

The spectrum obtained in (a) was subtracted from that in (c) to give curve (1) in Fig. 7.2. We attribute this difference spectrum to the detection of scintillations produced in the perspex window of the vacuum system and/or the glass envelope of the photomultiplier by soft X-rays emitted from the source or nearby materials.

The difference spectrum obtained by subtracting the measurements in (c) from those in (b) is plotted as curve (2) in Fig. 7.2. We interpret this spectrum as due to the detection of light emitted directly from the source or its immediate vicinity. Many

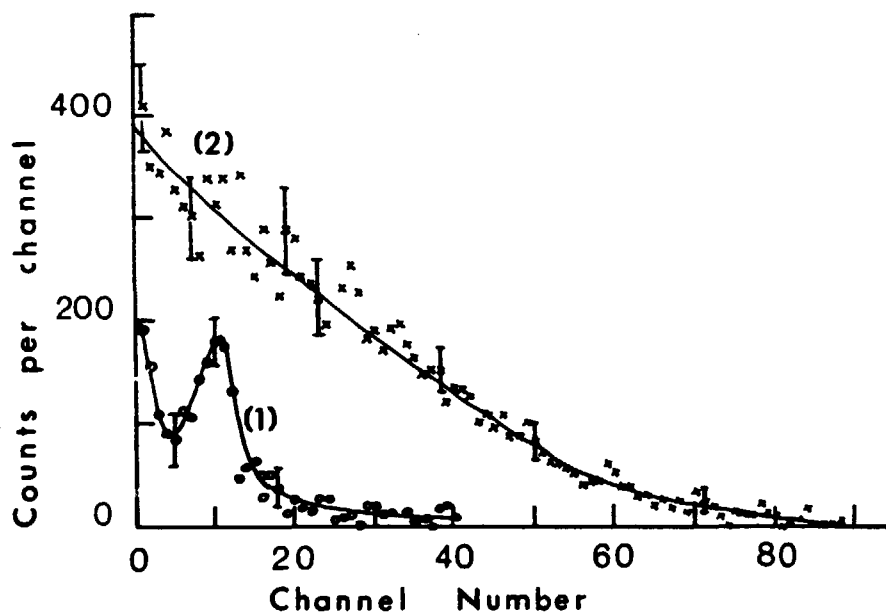


Fig. 7.2. Pulse height spectra due to (1) X-rays and (2) optical photons accompanying fission

different mechanisms can give rise to the emission of the light accompanying fission and we are investigating the phenomenon further.

Preliminary measurements indicate that timing signals may be derived from the light flashes to mark the instant of fission for use in time of flight spectrometry.

7.3 The Polarisation and Differential Cross Section for the Elastic Scattering of 16 MeV Neutrons (Amena Begum and R.B. Galloway)
(Relevant to request numbers 458, 616, 986)

Our first measurements of the polarisation of 16.1 MeV neutrons due to elastic scattering by Cu and Pb differed markedly for scattering angles around 20° from the values calculated with the optical model using global fit parameters(1).

Polarisation and differential cross section measurements were then made on Fe, Cu, I, W, Hg and Pb as reported last year (UKNDC(79)P94, p.110) and the global optical model calculations of polarisation showed a similar discrepancy around 20° . These measurements of polarisation and differential cross section have since formed the basis

of a search for optimum optical model parameters which have in turn been compared with the expectations from microscopic model calculations on elastic scattering. A full account of this work has just been published⁽²⁾

(1) R.B. Galloway and A. Waheed, Phys. Rev. C19 (1979) 268.

(2) Amena Begum, R.B. Galloway and F.K. McNeil-Watson, Nucl. Phys. A332 (1979) 349.

7.4 The Polarisation of 14 MeV Neutrons Due to Elastic Scattering (Amena Begum and R.B. Galloway)

Following the observation of a significant difference between the polarisation of 16 MeV neutrons elastically scattered through 20° by Cu and Pb and the values calculated from global optical models⁽¹⁾, a 20° double scattering measurement with 14 MeV neutrons was undertaken. The 14 MeV 20° polarisation magnitudes for elastic scattering by Cu and Pb were found to be similar to the 16 MeV values. Optical model calculations with selective variation of each parameter indicated that an improved fit to the 20° polarisation values could be obtained by altering the geometry of the spin-orbit potential. The fit was improved in the case of Cu by increasing the diffuseness and in the case of Pb by increasing the radius. A paper on the experiment and the analysis has just been published⁽²⁾.

(1) R.B. Galloway and A. Waheed, Phys. Rev. C19 (1979) 268.

(2) Amena Begum and R.B. Galloway, Phys. Rev. C20 (1979) 1711.

7.5 The Polarisation and Differential Cross Section for the Elastic Scattering of 2.9 MeV Neutrons (J. Annanu, Amena Begum and R.B. Galloway)

The simultaneous measurements of the angular dependence of polarisation due to elastic scattering and of the elastic differential cross section for 2.9 MeV neutrons scattered by Fe, Cu, I, Hg and Pb referred to last year (UKNDC(79)P94, p.111) have been used to test the results of combining many different optical model and Hauser-Feshbach calculations, and optimum optical model parameter sets have been found. The real potential volume integral per nucleon is generally consistent with values reported for 8 MeV and 11 MeV neutrons and in the case of Pb with the value reported for 30 MeV and 40 MeV protons. The volume integral per nucleon of the imaginary potential follows the trend with A discussed by Kailas and Gupta⁽¹⁾. The spin orbit term volume integral

per nucleon is similar for all except Cu. Even when the optimum parameters are employed the fits to the polarisation data for the heavier nuclei Pb, Hg and I are much poorer than the fits to the Cu and Fe polarisation data. Only for Pb does the level width fluctuation correction⁽²⁾ give a better fit. This work has recently been reported in detail⁽³⁾. In view of the poorer fit to the polarisation data on the heavier nuclei, measurements and calculations are in progress on W, Tl, Pb, Bi and U.

-
- (1) S. Kailas and S.K. Gupta, Phys. Lett. 71B (1977) 271.
(2) P.A. Moldauer, Phys. Rev. 135B (1964) 642.
(3) R.B. Galloway and A. Waheed, Nucl. Phys. A318 (1979) 173.

7.6 Neutron Polarisation in the ${}^7\text{Li}(d,n){}^8\text{Be}$ Reaction (R.B. Galloway and A.M. Ghazarian)

Since preliminary measurements of neutron polarisation indicated that the ${}^7\text{Li}(d,n){}^8\text{Be}$ reaction induced by 450 keV deuterons may be a useful source of polarised 14 MeV neutrons (UKNDC(79)P94, p111), detailed measurements of the angular dependence of the neutron polarisation are being made. DWBA analysis of the data is also in progress.

7.7 The Polarisation of Neutrons from the ${}^2\text{H}(d,n){}^3\text{He}$ Reaction (R.B. Galloway and A.S. Hall)

The angular dependence of the polarisation of the neutrons from the reaction ${}^2\text{H}(d,n){}^3\text{He}$ has been determined for 290 keV and 460 keV deuterons using a ${}^4\text{He}$ scattering polarimeter. The low energy S- and P-wave only description of the reaction found to be acceptable up to 275 keV deuteron energy⁽¹⁾ can be seen to fail at 290 keV. Previous⁽²⁾ neutron energy polarisation values for 350 keV deuterons are 10-15% too small. The present data can be accommodated along with higher energy data⁽³⁾ within the approach cross section description of the reaction.

-
- (1) A.M. Alscraya and R.B. Galloway, Nucl. Phys. A280 (1977) 61.
(2) H.J. Boersma, C.C. Jonker, J.G. Nijenhuis and P.J. van Hall, Nucl. Phys. 46 (1963) 660.
(3) R.B. Galloway, A.S. Hall, R.M.A. Maayouf and D.G. Vass, Nucl. Phys. A242 (1975) 122.

8. BIRMINGHAM RADIATION CENTRE, UNIVERSITY OF BIRMINGHAM

(Director: Professor J. Walker)

8.1 Delayed Neutron Energy Spectra (J. Walker, D.R. Weaver and J.G. Owen)
(Relevant to request number 1221)

The programme of delayed neutron spectrometry in fast fission has been continued with measurements at energies of 490 keV and approximately 7.0 MeV for the neutrons producing fission in ^{235}U . For the former energy, the 104g metallic cylinder, enriched to 96.54% ^{235}U , which was used last year (UKNDC(79)P94, p.102) has again been used with the Birmingham Dynamitron accelerator as the neutron generator; for the latter, a 214g cylinder has been used with the Tandem accelerator at AERE, Harwell.

The delayed neutron spectrum for the 490 keV case is shown in Fig. 8.1 where the histogram has energy steps of 15 keV. These measurements have again involved the gridded ^3He ionisation chamber with rise-time analysis, and the accelerator beam was pulsed on for 0.8s and off for 1s in a repeating cycle; counting occurred for 0.8s during the beam-off period.

Since last year's report, two steps have been taken to improve the extraction of spectra from the raw counts in the spectrometer: firstly, direct measurements of counter efficiency have been made over the extended range of 30 to 2000 keV (previously 100-1300 keV) and, secondly, the actual pulse-height distribution from a ^{252}Cf spontaneous fission source has been used in the correction for the small contributions from prompt fission produced by delayed neutrons in the actual experiment. The modified analysis has also been applied to the earlier data quoted last year at primary neutron energies of 940, 1440, 1760 and 6000 keV, and the new spectra are presented here in Figs. 8.2(a), (b), (c) and (d). The primary neutron energies are now quoted as mean values (1020, 1500, 1770, 5960 keV) instead of the approximate modal values given earlier, and the 15 keV energy groups are also incorporated in the plots. The new treatment has resulted in a reduction of the part of the spectrum below about 200 keV relative to the rest. A full analysis of errors including correlation effects is being undertaken, but, meanwhile, guide values are: $\pm 15\%$ below 100 keV, $\pm 7\%$ up to approximately 1000 keV, $\pm 15\%$ for approximately 1000-1500 keV, $\pm 25\%$ above 1500 keV.

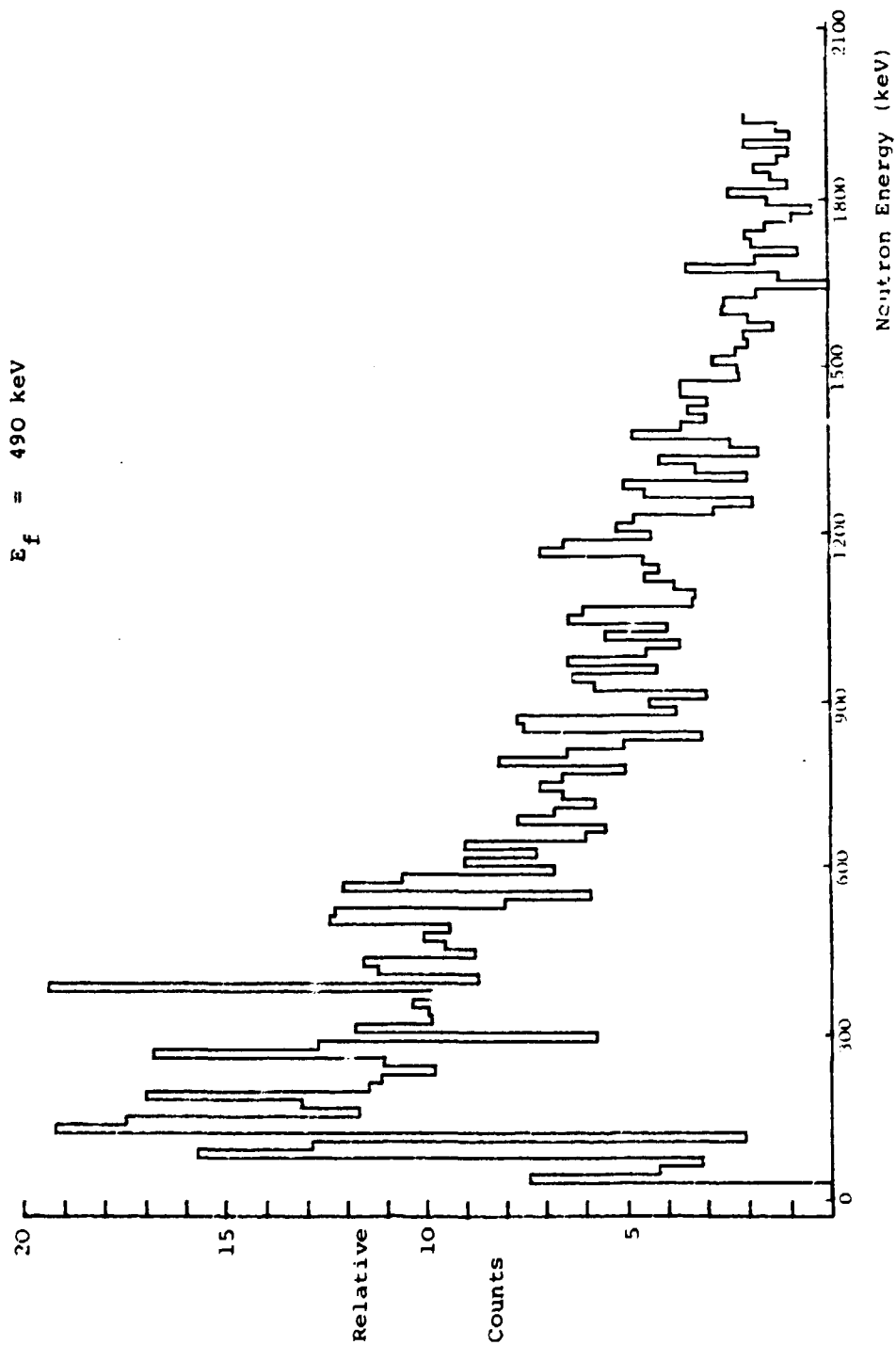


Fig. 8.1. The delayed neutron spectrum from ^{235}U following fission at a mean primary neutron energy of 490 keV

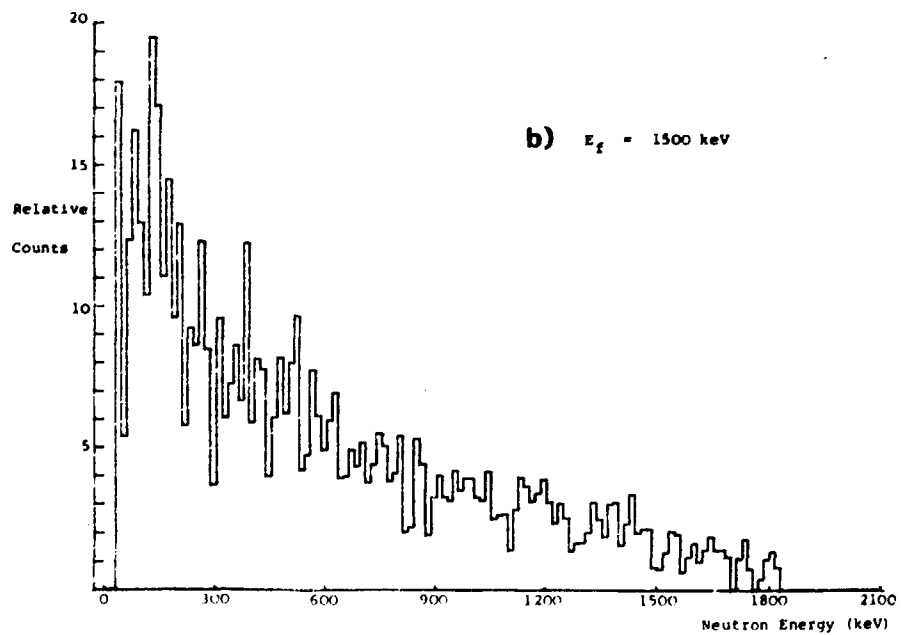
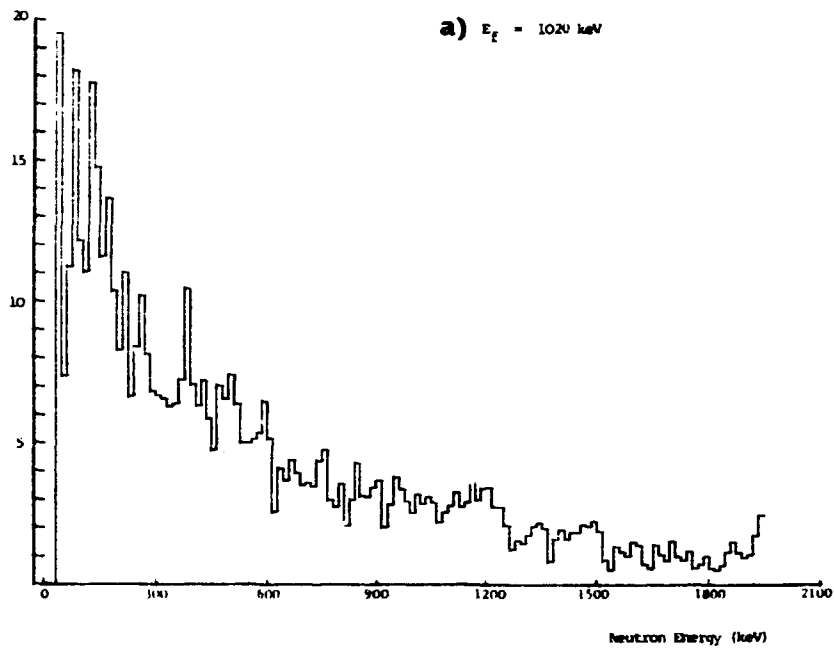


Fig. 8.2. Delayed neutron spectra from ^{235}U fission at mean primary neutron energies of (a) 1020 keV and (b) 1500 keV

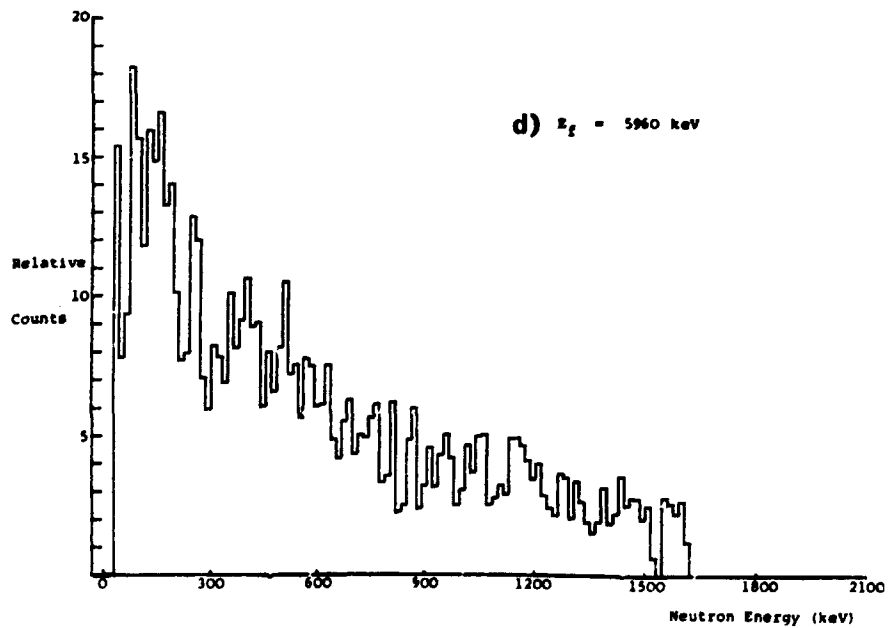
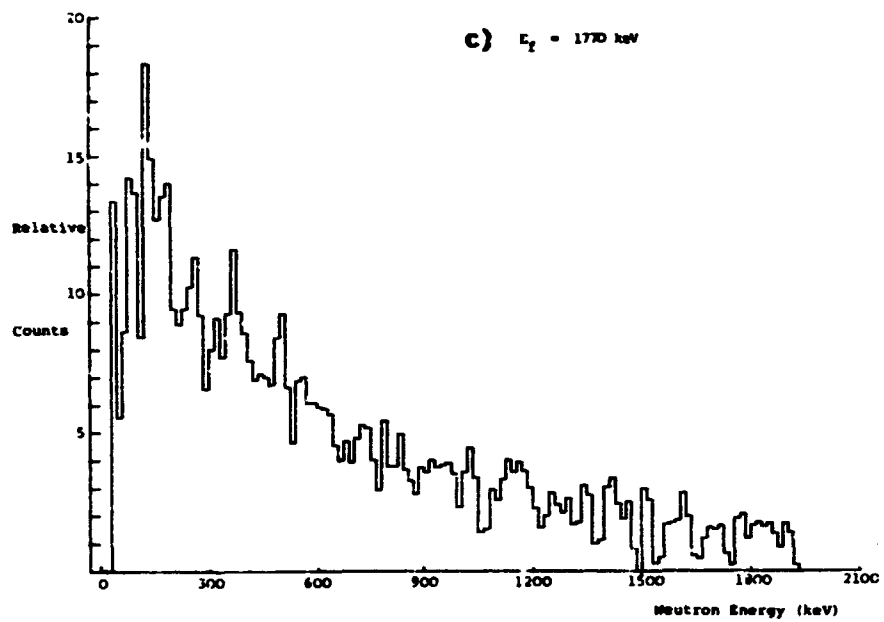


Fig. 8.2. Delayed neutron spectra from ^{235}U fission at mean primary neutron energies of (c) 1770 keV and (d) 5960 keV

8.2 The Neutron Spectrum from an Am/Li Source (J.G. Owen, J. Walker and D.R. Weaver)
(Relevant to request numbers 16, 17)

There exist currently significant discrepancies between delayed neutron spectra measured in various laboratories using different spectrometers (principally ^3He and proton recoil counters). In an attempt to resolve the variations, a recent IAEA Consultants' Meeting⁽¹⁾ recommended that all groups should measure the neutron spectrum from an Am/Li source, which is known to be similar to that of delayed neutrons. In Birmingham we have recently completed a measurement of a 100 mCi source kindly loaned to us by AERE, Harwell. The purity of such a source is of primary importance; in particular any Be contamination would enhance the high energy component of the spectrum. Lees has estimated that of the $4 \cdot 10^3 \text{ n}\cdot\text{s}^{-1}$ emitted from this particular source only 28 ± 9 are attributable to Be⁽²⁾. This low value was supported by measurements made in Birmingham.

The present measurement was made using a ^3He spectrometer of the Shalev type employing pulse rise-time analysis⁽¹⁾ and as far as possible the experimental arrangement, including thermal neutron and gamma-ray shielding, was identical to that used in the delayed neutron work. Unfortunately the low source activity necessitated a counting period of approximately two weeks, which led to a significant contribution to the pulse-height distribution from background counts, particularly at high energies. Corrections for this background distribution were made before unfolding the spectrum.

The unfolded spectrum is shown in Fig. 8.3 together with the measurement of a similar source made by Werle⁽³⁾ using a proton recoil counter. Although there is moderate agreement between the two spectra, variations do exist both at low and high energies, but they may well be due to source construction.

In assessing the errors on the unfolded spectrum an attempt has been made to include not only errors in the measured pulse-height distribution, but also errors inherent in the determination of the spectrometer response function. This analysis has led to the development of a full covariance matrix for the unfolded spectrum, from which we are able to assign errors of $\pm 10\%$ on the data below about 100 keV, and between $\pm 4\%$ and $\pm 7\%$ in the mid-energy range (100 keV - 800 keV). At higher energies the error begins to increase gradually owing to the increased background contribution and reaches $\pm 100\%$ by 1500 keV.

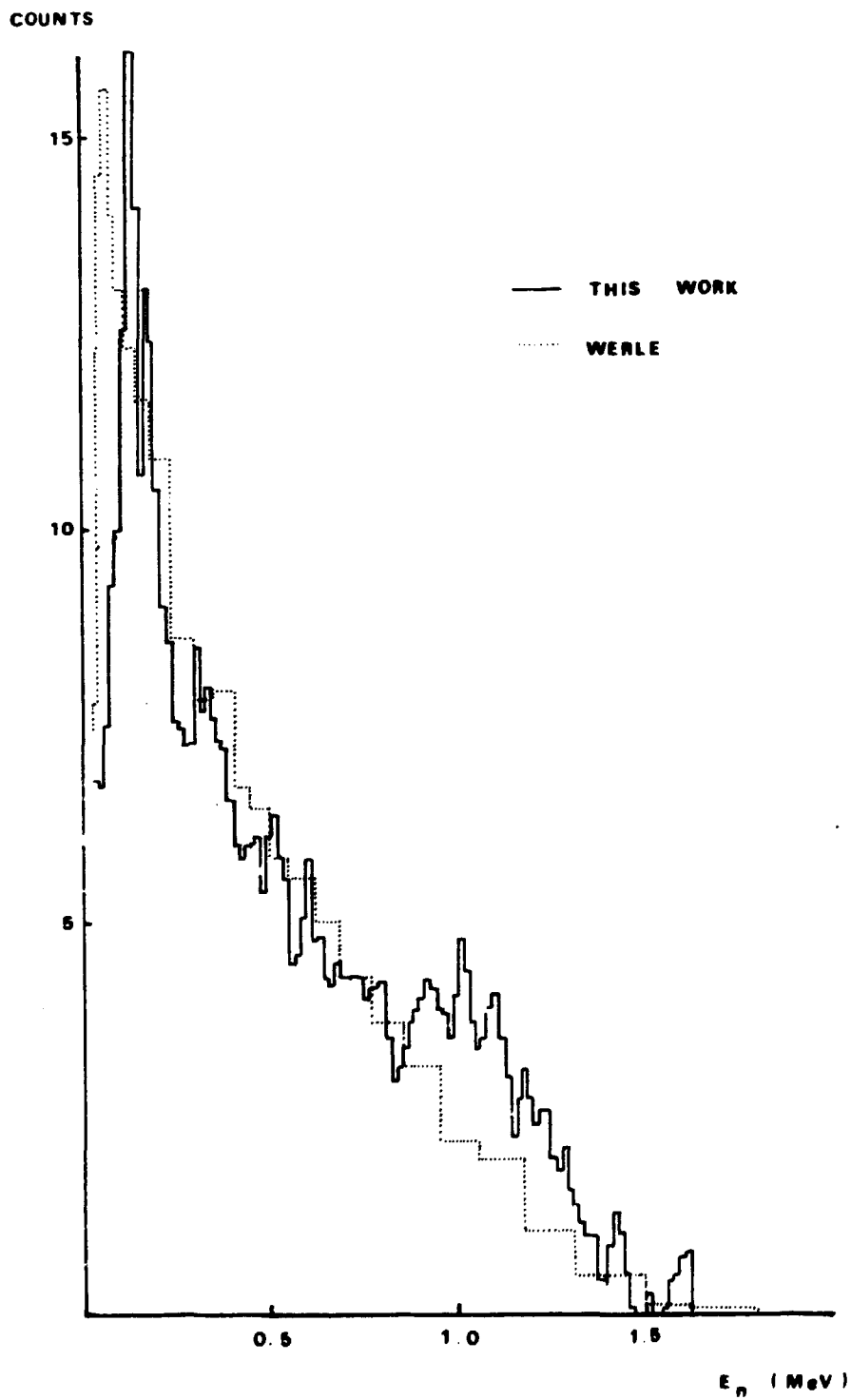


Fig. 8.3. The Am/Li neutron spectrum

The possibility of a slight contamination to the pulse-height distribution from recoil protons within this low pressure spectrometer has recently become apparent, but we estimate that this will result in only about a 4% change in the unfolded spectrum. In a higher pressure counter the effect would of course be greater.

- (1) Consultants' Meeting on Delayed Neutron Properties, Vienna, March 1979.
INDC(NDS)-107/G + Special.
- (2) E.W. Lees, AERE, Harwell. Private communication.
- (3) H. Werle. Oak Ridge National Lab. Report INR-41/70-25 (1970).

9. THE UNIVERSITY OF LONDON REACTOR CENTRE

(Director: Mr. M. Kerridge)

9.1 Decay Scheme Studies (J.B. Olomo and T.D. MacMahon)

(i) Half-Lives: The half-lives of ^{46}Sc and ^{140}La have been determined as 83.79 ± 0.06 days and 40.295 ± 0.005 hours, respectively. For each isotope the decay rate of several thin sources was measured as a function of time using a $4\pi \beta - \gamma$ coincidence technique. The results of this work are compared with earlier values in reference (1).

(ii) Gamma-Ray Emission Rates: Absolute gamma-ray emission rates in the fission product pairs $^{144}\text{Ce}/^{144}\text{Pr}$ and $^{140}\text{Ba}/^{140}\text{La}$ have been determined by means of a combination of $4\pi \beta - \gamma$ coincidence techniques and Ge(Li) gamma-ray spectroscopy. The results are as follows:

	keV	%
^{144}Ce	133.5	10.69 ± 0.12
^{144}Pr	696.5	1.484 ± 0.012
	1489.2	0.276 ± 0.002
	2185.7	0.768 ± 0.009
^{140}Ba	162.9	6.18 ± 0.08
	537.4	23.96 ± 0.22
^{140}La	328.8	20.48 ± 0.21
	487.0	45.52 ± 0.37
	815.8	23.02 ± 0.18
	867.8	5.62 ± 0.05
	925.2	7.08 ± 0.06
	1596.5	95.52 ± 0.48

Details of the measurements and emission rates for several other weaker lines in $^{140}\text{Ba}/^{140}\text{La}$ can be found in reference (2).

-
- (1) J.B. Olomo and T.D. MacMahon, "Half-lives of ^{46}Sc and ^{140}La ", J. Phys. G. (in press).
 - (2) J.B. Olomo, Ph.D. Thesis, "Precise measurement of gamma-ray emission probabilities of nuclear fuel monitor nuclides". University of London, September 1979.